RESEARCH ARTICLE

New and little known Isotomidae (Collembola) from the shore of Lake Baikal and saline lakes of continental Asia

Mikhail Potapov[1,2], Cheng-Wang Huang[3], Ayuna Gulgenova[4], Yun-Xia Luan[5]

1 *Senckenberg Museum of Natural History Görlitz, Am Museum 1, 02826 Görlitz, Germany* **2** *Moscow Pedagogical State University, Moscow, 129164, Kibalchicha St. 6 b. 5, Russia* **3** *Key Laboratory of Insect Developmental and Evolutionary Biology, CAS Center for Excellence in Molecular Plant Sciences, Chinese Academy of Sciences, Shanghai, 200032, China* **4** *Banzarov Buryat State University, Ulan-Ude, 670000, Smolina St. 24a, Russia* **5** *Guangdong Provincial Key Laboratory of Insect Developmental Biology and Applied Technology, Institute of Insect Science and Technology, School of Life Sciences, South China Normal University, Guangzhou, 510631, China*

Corresponding author: Cheng-Wang Huang (cwhuang@cemps.ac.cn)

Citation: Potapov M, Huang C-W, Gulgenova A, Luan Y-X (2020) New and little known Isotomidae (Collembola) from the shore of Lake Baikal and saline lakes of continental Asia. ZooKeys 935: 1–24. https://doi.org/10.3897/zookeys.935.49363

Abstract

Collembola of the family Isotomidae from the shores of Lake Baikal and from six saline lake catenas of the Buryat Republic (Russia) and Inner Mongolia Province (China) were studied. *Pseudanurophorus barathrum* Potapov & Gulgenova, **sp. nov.** and *Parisotoma baicalica* Potapov & Gulgenova, **sp. nov.** from Baikal and *Ephemerotoma buryatica* Potapov, Huang & Gulgenova, **sp. nov.** and *Folsomia mongolica* Huang & Potapov, **sp. nov.** from saline lakes are described here. A morphological description of epitokous males of *Scutisotoma acorrelata* Potapov, Babenko & Fjellberg, 2006 is given. A list of 23 species of the family Isotomidae found in the shores of studied lakes is provided based on literature sources and newly collected material.

Keywords

arid zone, endemism, fauna, sexual dimorphism, shingly beach, springtails

Introduction

The springtail fauna of lake shores in Asia is poorly known. Some data is available from lakes of western Siberia (Stebaeva 1981, 2006; Berezina 2006) where changes in species composition along forest-steppe lakesides were studied. Basing on those materials several specialised species have been discovered at saline lakes (Stebaeva 1978). In 2014 and 2015 a Chinese-Russian team of researchers investigated the Collembola of more eastern areas of arid zone of continental Asia. Saline lands associated with six saline lakes of Buryatia (Russia) and Inner Mongolia (China) were studied resulting in the discovery of two new species.

Approximately 10–20 million years old Lake Baikal, a huge ancient reservoir of fresh water at the centrum of Asia, has exceptionally high faunal diversity and endemism (Martens 1997). Several new species of Collembola have been described from the lake shore (Potapov 1991; Babenko et al. 1994, 2011; Potapov et al. 2006; Huang and Potapov 2012; Potapov and Gulgenova 2013). Recent collecting on shingly beaches revealed two new species of the specialised littoral fauna of the lake.

Earlier, Sokolovskaya (1989) investigated the collembolan communities in the lower and sandy part of delta of Selenga River flowing into Baikal. Five species of Isotomidae were identified from several open and forest sites. Two were widely distributed species, *Isotoma viridis* Bourlet, 1839 and *Desoria olivacea* (Tullberg, 1871) and are not confirmed by us; *Proisotoma buddenbrocki* (Strenzke, 1954) (*Strenzketoma* Potapov, Babenko & Fjellberg, 2006 now) probably refers to *Scutisotoma acorrelata* Potapov, Babenko & Fjellberg, 2006 (see Table of Appendix 1).

In the present paper we describe four new species, two from saline lakes and two from Baikal, and provide a list of springtails of the family Isotomidae recorded from the surveyed lakes.

Materials and methods

Collembola were sampled in catenas of six saline lakes in 2014 and 2015. Shores of the following lakes were studied: Alginskoye (53.633°N, 109.936°E), Nukhe-Nuur (54.027°N, 110.277°E) (Barguzin Valley, N Buryatia: Russia), Verkhneye Beloye (50.634°N, 105.720°E), Selenginskoye (51.356°N, 106.558°E) (Selenga Valley, SW Buryatia: Russia), Bayin Chagan Nuori (48.38°N, 118.71°E), and Hujiri Nuo Ergacha (48.30°N, 118.56°E) (E Inner Mongolia Province: China) (Fig. 58). Tullgren/Berlese funnels were used to extract Collembola from 492 soil cores, 125 cm³ each. Samples were collected from four positions at each catena: lowest accumulative part, two transit parts and upper alluvial part (steppe). One of the views of the catena at Lake Verkhneye Beloye is shown in Fig. 59. All parts were saline and covered with halophytes. On Lake Baikal shore, the springtails were collected in 2008–2017 by floatation in water of shingle and sand.

Abbreviations

A, B, C, D, E	papillae of labial palp;
Abd.	abdominal segments;
alt	altitude;
Ant	antennal segments;
AO	antennal organ;
bms	basal ms on antennal segments;
BSU	Banzarov Buryat State University;
e-guards	supplementary setae for E-papilla of labium;
G, H	ocelli G and H;
ms	micro s-seta(e) (= microsensillum(a) auct.);
MSPU	Moscow State Pedagogical University;
p-row of setae	setae of posterior row;
PAO	postantennal organ;
s	in the text and figures macro **s**-seta or **s**-setae (= macrosensillum(a) or sensillum(a) auct.);
SEM	Shanghai Entomological Museum;
SMNG	Senckenberg Museum of Natural History Görlitz;
Th	thoracic segments;
Ti	tibiotarsi;
U3	inner edge of unguis.

Types of new species are deposited in Moscow State Pedagogical University (Russia), Senckenberg Museum of Natural History Görlitz (Germany), Shanghai Entomological Museum (China), Banzarov Buryat State University (Russia). Cavity slides with Gisin's liquid and flat slides with Hoyer's medium were used to mount the specimens.

Notation of elements of labial palp follow Fjellberg (1999), elements of maxillary head follow Fjellberg (1984), labrum follow Yosii (1976), and chaetotaxy of p-row of tergites in *Parisotoma* Bagnall, 1940 follow Potapov (1991).

Description of species

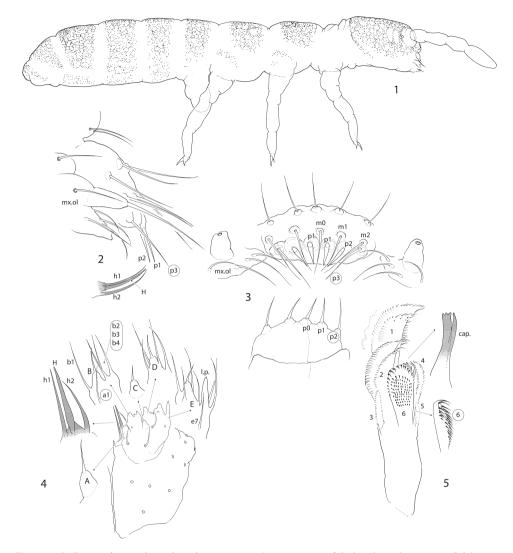***Pseudanurophorus barathrum* Potapov & Gulgenova, sp. nov.**
http://zoobank.org/D3D18099-2978-4569-8E40-29419DA14E20
Figures 1–13

Type material. *Holotype***:** female. Buryat Republic, Severo-Baykalskiy District, ~ 30 km N Severobaykalsk, near Slyudanskoye Lake, 55.4627°N, 109.1698°E, shingly beach of Baikal, 17.VIII.2013, coll. M. Potapov and A. Gulgenova. 5 paratypes from the same place (Holotype and 2 paratypes deposited in MSPU, 3 – in SMNG). 2 para-

types from Russia, East Siberia. Irkutskaya Region, Slyudyanskiy District, Slyudyanka, shore of Lake Baikal, 51.6529°N, 103.7350°E, on moistened big stones (by aspirator), 29.VIII.2008, coll. M. Potapov (deposited in BSU).
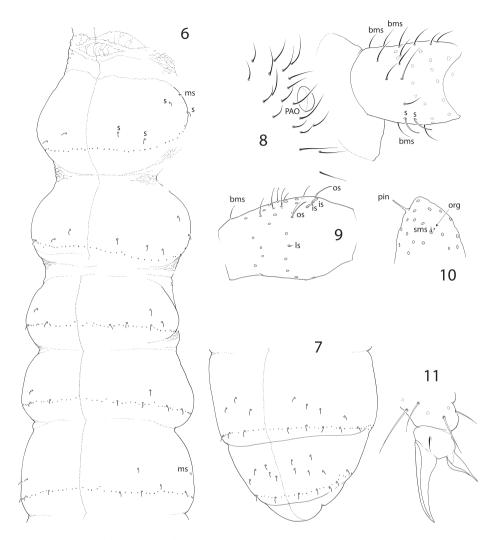
Other material. Irkutskaya Region, Slyudyanskiy District, Angasolskaya, shore of Lake Baikal, 51.7314°N, 103.8280°E, in shingle, 09.VIII.2015, coll. G. Efanov; Irkutskaya Region, Irkutskiy District, shore of Baikal, Primorskiy Range, Pribaikal'skiy Nat. Park, Khargino, 52.320°N, 105.776°E, stony beach, near water edge (by aspirator), 17.VIII.2013, coll. A. Babenko; Irkutskaya Region, Olkhonskiy District, Primorskiy Range, Kuyada, mouth of Talovka River, 52.553°N, 106.136°E, stony beach, under stones, 15.VII.2013, coll. A. Babenko; Buryat Republic, Kabansky District, Posolskiy Sor Bay, near Baykalskiy Priboy, 51.91216°N, 106.13954°E, seaweed debris near water, 23.VII.2011, coll. A. Chimitova and L. Vanyavina; Buryat Republic, Barguzinskiy District, 53.29645°N, 108.6213°E, floatation of shingle at water edge, 03.VIII.2014, coll. M. Potapov and A. Gulgenova. The materials are deposited in MSPU and SEM.

Description. Size 1.0–1.5 mm. Body broad, with long legs (Fig. 1). Pigmentation from almost white to pale grey, forming a diffuse net interrupted by intersegmental areas. Cuticle finely reticulated ("smooth"), size of polygons much smaller than bases of setae. Large specimens sometimes with regularly scattered hardly visible small pits. Lateral parts of intersegmental area with secondary granulation (Fig. 6). Ocelli absent. PAO small, not constricted, ca. 0.3 as long as Ant.1 width and ca. half as long as U3 (Fig. 8). Maxillary outer lobe with simple maxillary palp and four slender sublobal hairs (Figs 2, 3). Labral formula as 3/556 (Fig. 3). Labral edge reduced, apical ridges absent. Apical row (p-row) of labral setae projecting above mouth aperture (Figs 2 and 3), normally with six setae: p1, p2, and p3 on each side, lateral pair (p3) more slender and long. Medial pair p1+p1 is sometimes replaced with one (p0) giving five setae (p0, p1, p2) in apical row and labral formula 3/555 (Fig. 3). Setae of two rows (m, p) of labrum and sublobal hairs form a basket surrounding the mouth. Labium with all papillae (A–E), papillae A without guards (Fig. 4). Guard a1 detached and integrated to papilla B which, in result, supplied with five guards (a1, b1–4). Guards b2, b3, b4 set together, on lateral expansion of papilla B. Papilla C without guards, D with four guards in normal position. E with seven guards, lateral process and two lateral guards enlarged. Terminal setae of all papilla short. All elements of hypostomal group (H, h1, h2) considerably enlarged and bent towards labrum complementing the upper "basket" (Figs 2, 4). Main part of labium with three proximal, four basomedian and five basolateral setae. Maxillary head modified: capitulum slender and formed by fused claws, lamellae enlarged. Lamellae 1 and 2 well beyond capitulum, each supplied with apical and inner rows of cilia. Outer edge of lamella 1 gently ciliated, sometimes wavy. Lamella 3 expanded, with strong teeth (Fig. 5). Ventral side of head with 5-6+5-6 postlabial setae. S-setae and bms-setae of antennae slender and resemble common setae. Ant.1 with two basal, ventral and dorsal, bms, two ventro-lateral s, and ca. 30–40 common setae (Fig. 8). Ant.2 with three bms and one laterodistal s. Ant.3 with one bms, five common s (two outer, two inner, and one lateral spine-like), and a group of additional thin s-setae located on dorsal and inner sides of segment (Fig. 9), inner additional s-setae hardly differ from common setae. S-setae on Ant.4 weakly differentiated, subapical organite rudimental, apex without bulb (Fig. 10).
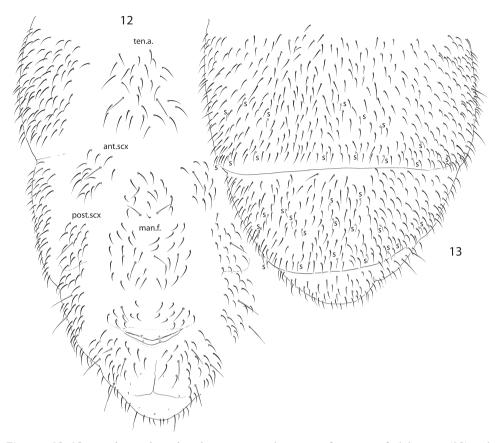
Figures 1–5. *Pseudanurophorus barathrum* sp. nov. **1** appearance of dark coloured specimen **2** labrum, maxillary outer lobe and hypostomal setae, lateral view **3** labrum and maxillary outer lobe, fronto-ventral and ventral views **4** labium, ventral view **5** maxillary head. Abbreviations: A, B, C, D, E-papillae of labial palp, H, h1, h2–hypostomal setae, mo, m1, m2, p1, p2, p3–setae of m – and p-row of labrum, mx.ol-maxillary outer lobe, cap., 1–6–capitulum and lamellae 1–6 of maxillary head, a1, b1, b2, b3, b4, e7–labial guards, l.p.–lateral processes. Characters of greater value encircled.

Body with numerous smooth short setae. Dorsal axial setal pattern asymmetric, can approximately be described as: 12–14,11–14/9–10,9–10,9–10,12–14 (Th.II–Abd. IV). Macrosetae not differentiated. S-setae on tergites weakly differentiated, subequal to common setae (Fig. 13). S-setae varies as 4,4–5/3–5,4–5,4–6, ~9, ~10, number and arrangement asymmetrical. With incomplete set of ms-setae (1,0/0,0,1). Most s-setae on Abd.I–Abd.V in p-row of setae (Figs 6, 7, 13). Th.I, II, and III without ventral setae.

Figures 6–11. *Pseudanurophorus barathrum* sp. nov. **6, 7** s-setae on body in one variant **8** PAO and Ant.1, lateral view **9** Ant.3 (only sockets shown for setae, additional s-setae on inner side of segment not shown), lateral view **10** apex of Ant.4 (pin-seta, organite, and subapical ms shown) **11** apical part of Leg 2. Abbreviations: bms-basal micro s-seta, sms-subapical micro s-seta, org-organite, pin-pin-seta, s-s-seta, ms-micro s-seta, PAO-postantennal organ, is, ls, os-inner, lateral, and outer s-setae of antennal organ.

Unguis rather slender, without teeth (Fig. 11). Empodial appendage with lamellae, without teeth. All tibiotarsi with many additional setae, ca. 40 on Ti.1 and Ti.2 and 50–60 on Ti.3. Adult male often with slightly swollen Ti.3, with stick-like thin spurs (x and B5). Tibiotarsi of all legs with seven setae in apical whorl. Tibiotarsal tenent setae pointed (Fig. 11). Ventral tube with 12–14+12–14 distal and ca. 20 posterior setae, without anterior setae. Distal setae in two groups, anterior (9–11+9–11) and posterior (3+3). Tenaculum and furca entirely absent. Tenacular field with ca. 20–30, manubrial

Figures 12, 13. *Pseudanurophorus barathrum* sp. nov., chaetotaxy of ventrum of Abd.III–VI (**12**) and dorsum of Abd.IV–VI (**13**) Abbreviations: ten.a.–tenacular area, man.f.–manubrial field, ant.scx, post. scx-anterior and posterior subcoxae, s-s-seta.

field with ca. 40–50 setae (Fig. 12). Manubrial setae in anterior and posterior groups. Anterior furcal subcoxae with 13–16 setae, posterior subcoxae with 18–20 setae. Posterior subcoxa weakly separated from setaceous part of segment. Males present.

Affinity. This remarkable species is characterised by two (more rarely one) additional setae on labrum that is so far unknown in *Pseudanurophorus* Stach, 1922 and other Collembola as well. Labral formula 5,5,4 (vs. 5,5,5–6 in *P. barathrum* sp. nov.) is invariable in Isotomidae and it is clear that the character is often omitted although being implied in the descriptions. Other mouth parts are also strongly modified: labral edge is reduced; two anterior setal rows and the sublobal hairs form a basket surrounding the mouth; hypostomal setae and lateral process are enlarged; guard a1 is integrated with papilla B; guards b2, b3, b4 set on lateral expansion of B; maxillary head has slender capitulum and expanded lamella. Unusually high number of setae on tibiotarsi and ventral tube and the dense and short abdominal hair cover is an apparent adaptation to live in close contact with water, as in many other littoral species.

The new species belongs to the "*boerneri*" group due to three prelabral, 4+4 or more postlabial setae, simple maxillary palp and other characters (for details see Potapov 1997). It most resembles two species with short macrosetae *P. arcticus* Christiansen, 1952 and *P. montanus* Martynova, 1971 (1971a), for which labral formula is unknown. Following the first description and Fjellberg's comments (1975) on *P. arcticus* paratypes, these two species have much fewer setae in axial group of tergites and yet have macrosetae on last abdominal segments (vs. absent in *P. barathrum* sp. nov.). *Pseudanurophorus arcticus* is described and subsequently recorded in the Arctic and *P. montanus* in the mountains of Middle Asia.

Distribution and ecology. Several records from the littoral zone of the shore of Lake Baikal, none found inland. It is one of the common species in shingly beaches.
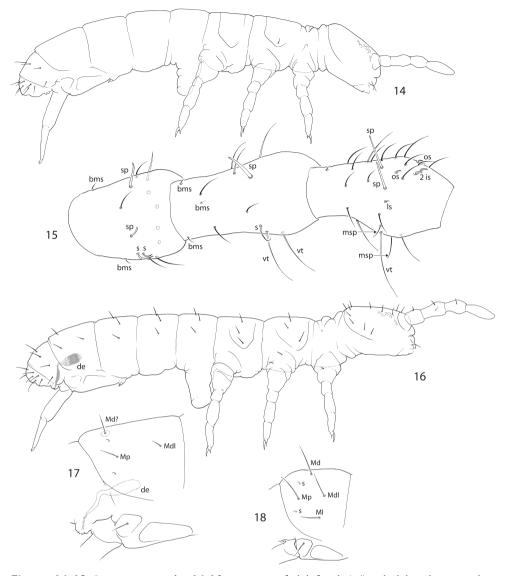
Name derivation. It is named after the specific mouth parts (*barathrum* – a glutton in Latin, among other translations).

Scutisotoma acorrelata **Potapov, Babenko & Fjellberg, 2006**
Sexual dimorphism
Figs 14–17

Material. 37 specimens. Russia, Buryat Republic, Eravninsky District, coast of Bolshaya Eravna Lake, 06.VI.2008, coll. A. Gulgenova; Buryat Republic, Kabansky District, shore of Lake Baikal, Posolskiy Sor Bay, near Baykalskiy Priboy, 51.91216°N, 106.13954°E, seaweed debris near water, 23.VIII.2011, coll. A. Chimitova and L. Vanyavina; Buryat Republic, Barguzin Valley, Alginskoye Lake, floatation of wet coarse sand and shingle at water edge, 03.VIII.2014, coll. M. Potapov, C.W. Huang, and A. Gulgenova.

Description of epitokous males with fully developed ejaculatory duct in shore of Lake Baikal. Size ca. 1.2 mm, subequal to adult females. Macrosetae erect, slightly serrated, well developed on all body tergites and head. Three first segments of antennae with thickened setae (Fig. 16). In females, subadult males and juveniles macrosetae are only developed on thoracic (only lateral pair) and two last abdominal segments (Fig. 14). Number of macrosetae 3,3/3,3,3,3, their arrangement as common for Anurophorinae (in position Md, Mdl and Ml), apart from Abd.IV on which Mp and Mdl are in common position while macrosetae Ml is absent and Md shifted backwards and set in posterior row of setae. Common arrangement of macrosetae on Abd.IV for Anurophorinae shown in Fig. 18. Ventral side of Abd.VI with two thin curved macrosetae (vs. of normal shape in females). Head with macrosetae at posterior edge, in ocellar field, and between antennae. Front of head slightly swollen (vary). Antennae bent downwards. Three first segments of antennae thickened. In fully developed variant Ant.1 with three spiny setae (sp), Ant.2 with one sp and two ventral trichobothria, Ant.3 with two sp, one ventral trichobothrium and few (two or three) male "spurs" (Fig. 15). Thicknesses of sp vary. Tibiotarsus 3 with setae X and B5 insignificantly modified, set in wider sockets than in female.

Figures 14–18. *Scutisotoma acorrelata* **14, 16** appearance of adult female (14) and adult male in reproductive stage (16) (pigmentation not shown) **15** Ant.1–3 in adult male in reproductive stage, lateral view **17** macrosetae on Abd.IV in adult male of *S. acorrelata* **18** common arrangement of macrosetae on Abd.IV in Anurophorinae. Abbreviations: bms-basal micro s-seta, de-ductus ejaculatorius, s-s-seta, is, ls, os-inner, lateral, and outer s-setae of antennal organ, sp-spiny setae, vt-ventral trichobothrium, msp-male spurs, Md, Mdl, Mp, Ml-macrosetae of Abd.IV.

Remarks. Considering the dimorphic species *S. muriphila* (Grinbergs, 1968) and *S. stepposa* (Martynova, 1975) (for details see Grinbergs (1968), Chimitova and Potapov (2011)), *S. acorrelata* is the third member for the genus *Scutisotoma* Bagnall, 1948 which shows well developed sexual dimorphism. Males of *S. acorrelata* are less

modified than in the two other species and polymorphism was not evident in our material. In taxonomical terms, the presence of epitokous males is a character of low value at generic level. It is probably optional in several genera. At species level, the diagnostic value of epitokous males is questionable. In many genera of the family Isotomidae the epitokous males are probably more frequent than usually considered. The short duration of the reproductive instar may have left many epitokous forms undetected.

Distribution and ecology. The species was described from shore of Lake Baikal (Potapov et al., 2006) and was further recorded at saline Alginskoye Lake and freshwater Bolshaya Eravna Lake. It lives in seaweed debris and in coarse sand.

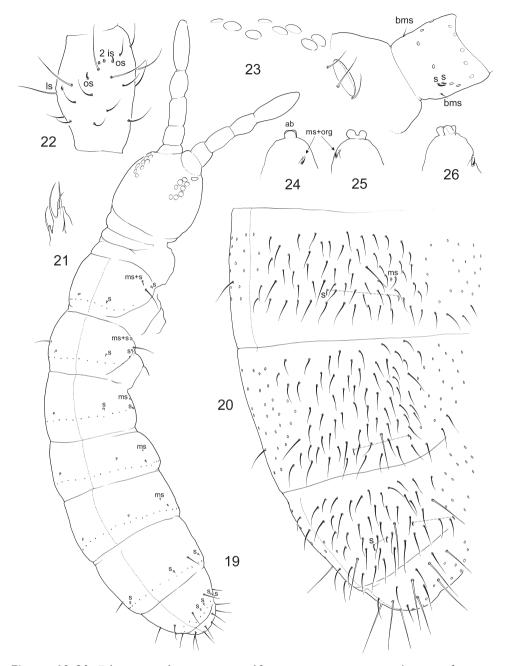## *Ephemerotoma buryatica* Potapov, Huang & Gulgenova, sp. nov.
http://zoobank.org/01C359C5-F519-4B0A-9B06-8445933FD6E0
Figures 19–31

Type material. *Holotype*: female. Russia, south-western part of Buryat Republic, Gusinoozerskaya Basin, 0.5 km SW from Tokhoy, 51.356417°N, 106.558733°E, 590 m alt., southern shore of Sul'phatnoye (= Selenginskoye) Lake, grassland with *Caragana* sp., *Achnatherum splendens*, *Atriplex* sp., *Leymus* sp., 18.X.2015, coll. M. Potapov and A. Gulgenova. 24 paratypes (sub-adult and adult males and females) from the same place. Holotype and 10 paratypes deposited in MSPU, 4 in BSU, 5 in SMNG, 5 in SEM.
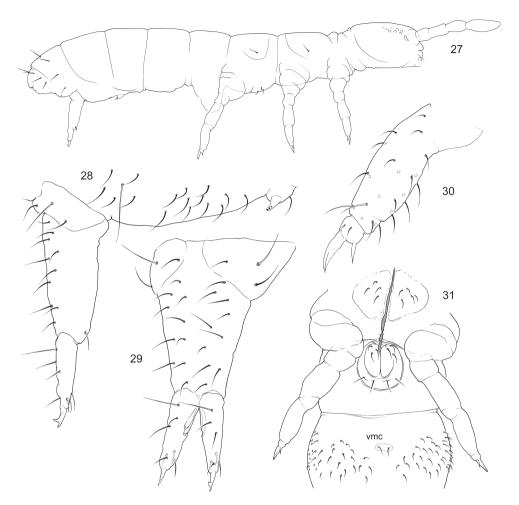
Other material. From the type locality dated 02.V.2015 and 25.VII.2015.

Description. Size 0.6–0.9 mm. Body as common for Anurophorinae with short furca (Fig. 27). Pigmentation grey, as in *Proisotoma minuta* (Tullberg, 1871). Cuticle finely reticulated, size of largest polygons smaller than bases of setae. Ocelli 8+8, G and H smaller (Fig. 23), all ocelli usually look subequal by pigmentation. PAO with three guard setae along posterior margin, elliptical, not constricted, as long as 0.4–0.6 of Ant.1 width and 0.7–1.1 as long as U3 (Fig. 23). Maxillary outer lobe with simple maxillary palp and four sublobal hairs. Labral formula as 2/554. Labium with all papillae (A–E), papillae A–D with normal number of guards (1,4,0,4), E with four guards (Fig. 21). Main part of labium with three proximal, four basomedian and five basolateral setae. Ventral side of head with 4+4 postlabial setae. Ant.1 with two basal, ventral and dorsal, bms, two ventro-lateral s, and eleven setae, without p-setae (Fig. 23). Ant.2 with three bms and one laterodistal s. Ant.3 without bms and with five distal s (including one lateral spine-like), inner s of AO small (Fig. 22). All s-setae on Ant.1–3 very short. S-setae on Ant.4 weakly differentiated, subapical organite small. Apex of Ant.4 with bilobed bulb (Figs 24–26), well visible in dorsal view (Fig. 25). In fully grown animals the bulb can look trilobed due to slight secondary division of one of the lobes (Fig. 26).

Body with smooth and rather short setae. Dorsal axial setal pattern of Th.II–Abd. IV: 7–8,6–7/5,5,5,7–8. Th.I and II without ventral setae, Th.III with 3–5+3–5 (usually 4+4) ventral axial setae (Fig. 31). Abd.II with a pair of mid-ventral setae (Fig. 31). Macrosetae weakly differentiated, medial macrosetae on Abd.V as long as 0.25–0.35 of tergal

Figures 19–26. *Ephemerotoma buryatica* sp. nov. **19** s-, ms-setae, macrosetae, and p-rows of setae on body tergites **20** chaetotaxy of Abd.III–VI **21** labial papilla E **22** Ant.3, dorso-lateral view **23** ommatidia and Ant.1 **24–26** apex of Ant.4, lateral (**24**), dorsal (**25**), and ventro-lateral (**26**) views. Abbreviations: bms-basal micro s-seta, ab-apical bulb, ms-micro s-seta, org-organite, s-s-seta, is, ls, os-inner, lateral, and outer s-setae of antennal organ.

Figures 27–31. *Ephemerotoma buryatica* sp. nov. **27** appearance **28** furcal area, lateral view **29** furca, posterior view **30** tibiotarsus of Leg 3, outer view **31** ventral side of Th.II and Abd.I and II. Abbreviations: vmc-ventro-medial setae.

midline (Fig. 20). S-setae on tergites very short (Fig. 20). S-formula as 3,3/2,2,2,2,4 (s) and 1,1/1,1,1 (ms). In al-group of Th.II and III front s-seta and ms-seta set close to each other (notated as 'ms+s' in Fig. 21). S-setae on Th.II–Abd.V set in front of p-row of setae (Fig. 1). On Abd.V s-setae arranged in one transverse row, lateral pair very short (Fig. 2).

Unguis of unusual shape, expanded at the middle, without teeth. Empodial appendage slender, without lamellae. Ti.1 and Ti.2 without additional setae (21), Ti.3 usually with 25 setae. B-row of setae on Ti.1–2 complete (B4 and B5 present). Male spurs (x and B5 on Ti.3) in adult males thin, stick-like. Tibiotarsal tenent setae pointed (Fig. 30). Ventral tube with 4+4 distal and four posterior setae arranged in one transversal row (Fig. 31). Tenaculum with 3+3 teeth and one seta. Anterior furcal subcoxae with 10–13 setae, posterior subcoxae with five or six setae (Fig. 28). Anterior side of manubrium with a pair of distal setae (Fig. 28), posterior side with 9–10+9–10 setae

on main part, lateral edges without setae (Fig. 29), laterobasal lobes with 3+3 setae. Dens short, about half as along as Ti.3. Anterior side of dens with three setae in sub-apical position (Figs 28, 29). Posterior side of dens usually with large subapical hump, more proximal part without clear modifications. Dens with four posterior setae, three in basal half, one subapical. Mucro with two teeth, subapical tooth largest. Ratio of manubrium : dens : mucro = 5.5–6.5 : 2.4–3.3 : 1.0. Males present.

Affinity. The species belongs to recently described genus *Ephemerotoma* Potapov, Kahrarian, Deharveng & Shayanmehr, 2015 due to simple maxillary palp, reduced number (four) of guards on labial papilla E, two prelabral setae, complete set of ms-setae on tergites (11/111), and tergal s-setae on abdomen set in front of p-row. *Ephemerotoma buryatica* sp. nov. does not share a significant character of the genus, the "two trans-verse rows" pattern of s-setae on Abd.V. The sexual dimorphism common for the genus *Ephemerotoma* [*E. porcella* (Ellis, 1976), *E. skarzynskii* Potapov, Kahrarian, Deharveng & Shayanmehr, 2015, *E. huadongensis* (Chen, 1985)] is not observed in the new spe-cies. Small and rather slender body, short furca, shape of unguis, and absence of sexual dimorphism indicate a preference for deeper edaphic habitat than in its congeners.

Regarding all genera of the *Proisotoma* complex, a peculiarity of the new species is the bilobed apical bulb on Ant.4, which is otherwise known only in *Proisotoma bulba* Chris-tiansen & Bellinger, 1980 (California, U.S.A.). The generic position of *P. bulba* is obscure because of lack of information on mouth parts and s-setae on body. In other characters, *E. buryatica* sp. nov. differs from *P. bulba* by fewer setae on dens (3/4 vs. 4–5/5–6), shorter dens (dens : mucro = 9 : 1 in *bulba*), teeth on tenaculum (3+3 vs. 4+4) and characters of unguis and tibiotarsi (*bulba* has inner tooth on unguis and a clavate tenent hair). In *Proisotoma* complex, a similar furca is shown, for example, for *Weberacantha echinodermata* Potapov, Babenko & Fjellberg, 2006 and *Scutisotoma robustodens* Huang & Potapov, 2012, which belong to other genera. Mouth parts (two prelabral setae, simple maxillary palp and reduced number of e-guards) of *E. buryatica* sp. nov. resemble the "*asiatica*" group of the genus *Subisotoma* but several other characters of great value are different (e.g., presence/absence of anterior setae on manubrium).

Distribution and ecology. Known only from one locality in SW Buryatia where it inhabits soil of dry steppe at upper part of a salt-lake catena. The species probably oc-curs in all seasons since it was recorded in May, July and October in the type locality. It was highly aggregated in October which that suggests a resemblance to the "ephemeral" species of the genus *Ephemerotoma*.

Name derivation. It is named after the type locality.

Folsomia mongolica Huang & Potapov, sp. nov.
http://zoobank.org/F2435043-7D30-4D2D-911C-18F53B719173
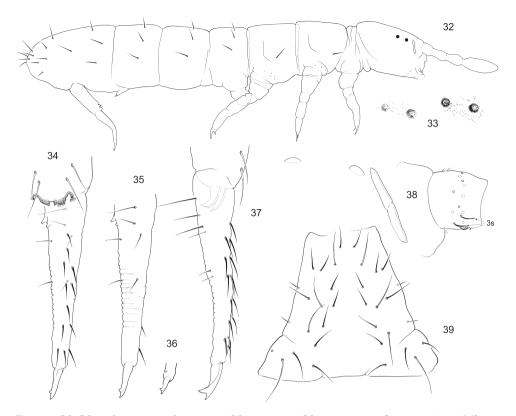Figures 32–42

Type material. *Holotype*: female. NE China, E Inner Mongolia Autonomous Region, Hulun Buir, New Barag Zuoqi, Xinbaoligexi Sumu, Bayin Chagan Nuori Lake, at shore of the saline lake, 48.38°N, 118.71°E, 669 m alt., 09.VIII.2014, coll. C.W.

Huang and M. Potapov. 20 paratypes from the same place. Holotype and 10 paratypes deposited in SEM, 5 – in MSPU, 5 – in SMNG.

Other material. NW China, E Inner Mongolia Autonomous Region, Hulun Buir, New Barag Zuoqi, Xinbaoligexi Sumu, Hujiri Nuo Ergacha Lake, at shore of the saline lake, 48.30°N, 118.56°E, 649 m alt., 09.VIII.2014, coll. C.W. Huang and M. Potapov. China, W Inner Mongolia Autonomous Region, Helan Mts., near Halawu, mixed sample from broadleaved bush and coniferous trees, 2325 m alt., 08.VIII.2010, coll. C.W. Huang and Y. Bu.

Description. Size 1.0–1.3 mm. Body of normal shape (Fig. 32). Usually without pigmentation apart from two contrasting black ommatidia on each side of head (Figs 32, 33). Darker specimens with diffuse black grains also on head and trunk. Specimens with weak eye pigmentation sometimes occur among normal ones, while cornea of ocelli are still distinct. Juveniles almost unpigmented. Cuticle with weak hexagonal primary granulation ("smooth"), thin belts of courser granulations at posterior edge of head, between Abd.IV and V and on medial line of thorax. Two widely separated large subequal ocelli on each side of head, like in *F. quadrioculata* (Tullberg, 1871) (Fig. 38). PAO narrow, well constricted, 1.1–1.4 as long as width of Ant.1 and 1.6–1.9 as long as inner unguis length. Maxillary outer lobe with four sublobal hairs, maxillary palp simple. Labral formula as 4/554. Labium with five papillae (A–E) and full set of guard setae (e7 present), with three proximal and four basomedian setae. Ventral side of a head with 4–5+4–5 postlabial setae. Ant.1 with three ventral s-setae and three short basal ms-setae (bms), two dorsal and one ventral (Fig. 38), Ant.2 with three bms and one latero-distal s, Ant.3 with one bms and with five distal s (including one lateral), without additional s-setae. S-setae on Ant.4 weakly differentiated. Organite small.

Macrosetae smooth and short, 1,1/3,3,3 in number (Fig. 40), medial ones on Abd.V 0.4–0.5 as long as dens and 2.0–3.1 as long as mucro. No foil setae at the tip of abdomen. Axial chaetotaxy as 8–10,7–8 /5,5,4–6 for Th.II–Abd.III. Thorax without ventral setae. S-formula as 4,3/2,2,2,3,5 (s), 1,0/1,0,0 (ms) (Fig. 40). Tergal s-setae as long and wide as common setae and hard to observe. Medial s-setae on Th.II–Abd.III situated in mid-tergal position, on Abd.I between Mac1 and Mac2, on Abd.II and III behind Mac2 (Fig. 40). Abd.V with five s-setae arranged as three dorsal ones (al, accp1, accp2), middle-sized and slender and one lateral (accp3) 2/3 as long as dorsal, and one ventral (the shortest, Fig. 41).
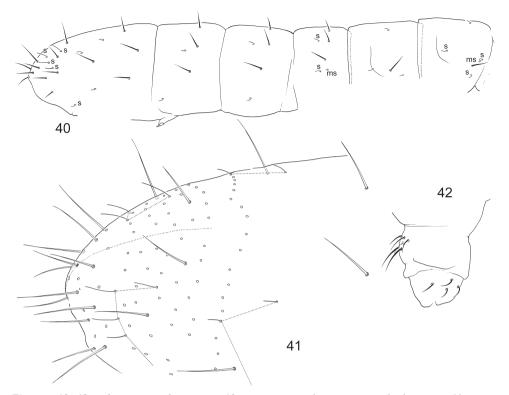
Unguis of normal shape, without lateral and inner teeth. Empodial appendage about half as long as unguis. Tibiotarsi with few additional setae on Legs 1 and 2 (23–25 setae), Leg 3 more polychaetotic. Tibiotarsal tenent setae pointed. VT with 4+4 (3+3 in small juveniles) laterodistal and six posterior setae, no anterior setae (Fig. 42). Tenaculum with 4+4 teeth and one seta. Anterior furcal subcoxae with 12–20 setae, posterior one with 4–6. Anterior side of manubrium with 2+2 setae (Figs 34, 37). Posterior side of manubrium with 4+4 laterobasal, two apical setae (ap), 3+3 setae in distal transversal row (M1, m1, L1), and 6–7+6–7 in central part (Fig. 39). Two pairs of lateral setae present. Dens with 12–14 (rarely 11 or 15) anterior setae (Figs 34, 37). Posterior side of dens crenulated, with seven setae: four setae

Figures 32–39. *Folsomia mongolica* sp. nov. **32** appearance **33** pigmention of eye areas (two different specimens) **34** dens and distal part of manubrium, anterior view **35, 37** dens, posterior (**35**) and lateral (**37**) views **36** distal part of dens and mucro, another specimen, posterior view **38** ommatidia, PAO, and Ant.1 **39** manubrium, posterior view. Abbreviations: s-s-seta.

at base one of which larger, two at middle part, and one rudimentary subapical seta which is often absent or hardly seen (Figs 35, 36). Mucro bidentate. Manubrium a little shorter than dens. Ratio of manubrium : dens : mucro = 3,9–5,4 : 4,7–6,2 : 1. Males present.

Affinity. The species belongs to "*heterocellata*" group due to simple maxillary palp. *F. mongolica* sp. nov. is very similar to two other species inhabiting arid landscapes of continental Asia: *F. pseudodecemoculata* Stebaeva, 1971 and *F. heterocellata* Stebaeva & Potapov, 1997. All three forms have no body pigmentation and share several important characters: structure of furca, body chaetotaxy, number of s-setae on antennae. The only sharp difference is number of ocelli on each side of the head: two in *F. mongolica* sp. nov., four in *F. heterocellata*, and five in *F. pseudodecemoculata*. The last species has shorter PAO than in the new species. *F. montana* Martynova, 1971 (1971b) (high mountains plateaus of Kirghisia) also belongs to "*heterocellata*" group and has 2+2 ocelli, but differs by three basal setae on posterior side of dens (vs. four in *F. mongolica* sp. nov.), 3+3 (vs. 4+4) laterobasal setae on posterior side of manubrium, and shorter PAO.

Figures 40–42. *Folsomia mongolica* sp. nov. **40** s-, ms-setae, and macrosetae on body tergites **41** s-setae and macrosetae of Abd.IV–VI (common setae shown as sockets, only p-row of setae presented on Abd.IV) **42** ventral tube, lateral view. Abbreviations: s-s-seta, ms-micro s-seta.

Distribution and ecology. The species is probably distributed in Inner Mongolia (China). This halophilic species is abundant on saline lands but also inhabits dry forest slopes.

Name derivation. It is named after the location of type place (Inner Mongolia Autonomous Region).

Parisotoma baicalica Potapov & Gulgenova, sp. nov.
http://zoobank.org/34334075-2F6C-48F6-BC8E-3D15FCAF5222
Figures 43–57

Type material. *Holotype*: female. Russia, East Siberia, Irkutskaya Region, Slyudyanka District, Angasolskaya, shore of Lake Baikal, 51.7314°N, 103.8280°E, in shingle, 09.VIII.2015, coll. G. Efanov (deposited in MSPU). 3 paratypes from the same place (deposited in MSPU), 4 paratypes from Russia, Buryat Republic, Barguzinskiy District, 53.29645°N, 108.6213°E, floatation of shingle at water edge, 03.VIII.2014, coll. M. Potapov and A. Gulgenova (2 paratypes deposited in SMNG, 2 – in BSU).
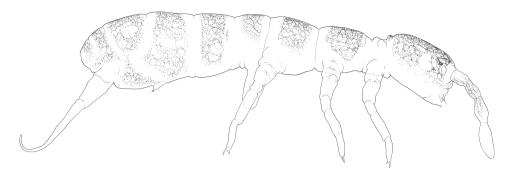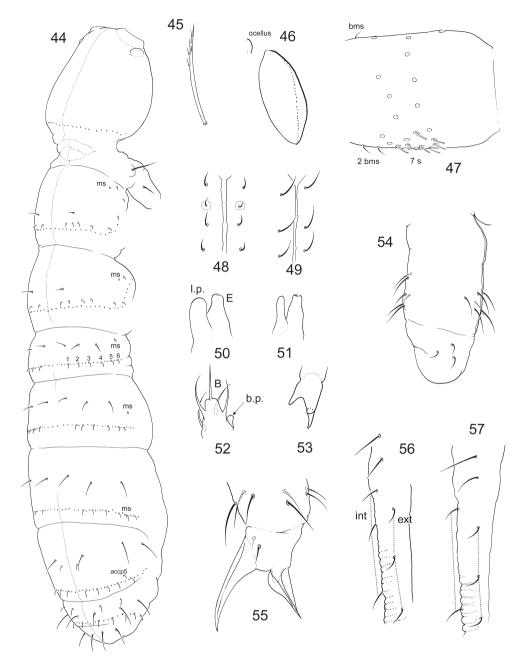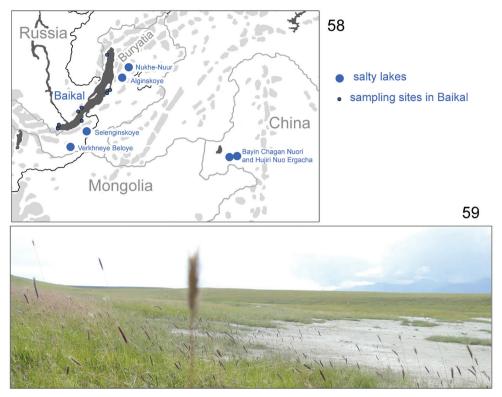
Figure 43. Appearance of *Parisotoma baicalica* sp. nov.

Description. Body length from 0,7 to 0,9 mm. Pale with diffuse greyish pigment on body, eye spot less marked than in most species of *Parisotoma* with one ocellus (Fig. 43). Ant.1 with 5–7 short s-setae ventro-laterally, three basal microsetae, two dorsal and one ventral (Fig. 47). Inner s-setae of AO III large. Ant.4 as common for the genus. One small ocellus on each side of head (Fig. 46). PAO wide, 1.4–1.8 as long as internal crest of Claw 3. Labral formula 4/554, apical folds sharp, as in *P. notabilis* (Schäffer, 1896). Maxillary outer lobe with four sublobal hairs and trifurcate apical palp. Labial palp with five papillae (A–E) and full set of guards (16, including e7), lateral process expanded. Papilla B with small basal process on its inner side (Fig. 52) (see the remarks). Labium with five baso-median, five basolateral, and four proximal setae. Number of postlabial setae from 3+3 to 4+4 (Figs 48 and 49), in the latter case an additional pair set between a1 and m1 (marked in Fig. 48). Inner mouthparts as usual for the genus: lamella 1 longer than capitulum with apex fan-shaped expanded, with marginal ciliation and one row of long denticles on inner side, lamella 6 with marginal ciliation and several (>3) irregular rows of denticles. Lower subcoxa of Leg 1 with one outer seta (Fig. 44). Tibiotarsi of all legs with only seven setae in apical whorl. Claw slender, without clear teeth (Fig. 55). Empodial appendage with broad lamella. Ventral tube with 3+3 lateral, 3+3 anterior (rarely two or four), and 4–6 posterior setae (Fig. 54). Retinaculum with 4+4 teeth and 2(3) setae. Furcal subcoxa with 27–35 setae. Manubrial thickening simple. Anterior side of manubrium with numerous setae of which 2+2 shorter medial ones in its apical part. Dens with numerous setae on anterior side and eight setae on posterior side (two basal, three internal and three external) (Fig. 56). Mucro with three teeth (Fig. 53).

Macrosetae differentiated, on last abdominal segments with few cilia (Fig. 45), on Abd.V shorter than length of tergite (ca. 0.6). S-setae thin, well different from common setae, pattern of s-setae complete, s-formula Th.II–Abd.V: 2al+6accp, 1al+6accp / 6 accp, 6 accp, 6accp, 1 am+6 accp, 2 am + 5 accp (Fig. 44). Micro s-setae 1,1/1,1,1 (ms) on Th.II–Abd.III. Micro s-setae of Abd.III shorter than s-setae (Fig. 10). As a rule, two common setae of p-row separate neighbouring accp s-setae. Formula of common setae in p-row between s and ms: 3–4s1–2s2s1s (Abd.I), 3–5s1–2s2s2–3s1–2s1–2s (Abd.II), 3–5s1–3s2–4s2–4s1–2ms0s1–2s (Abd.III), 1–3s2–3s2s1–2s2–4(s)1s (Abd. IV) (Fig. 44). Males present.

Figures 44–57. *Parisotoma baicalica* sp. nov. (**44–50**), (**52–55**) and *P. reducta* (**51, 56**) **44** s-, ms-setae, and macrosetae on body **45** macroseta of Abd.V **46** PAO and ocellus **47** Ant.1, lateral view (s and ms shown) **48, 49** postlabial setae, variation **50, 51** papilla E of labial palp, lateral view **52** papilla B, ventral view **53** mucro **54** ventral tube, lateral view **55** apical part of Leg 3 **56, 57** posterior side of dens. Abbreviations: s-s-seta, ms-micro s-seta, bms-basal micro s-seta, l.p.–lateral processes, b.p.–basal processes, B, E-papillae of labium, int, ext-internal and external setae of posterior side of dens.

Figures 58, 59. Sampling sites (**58**) and shore of Verkhneye Beloye Lake (**59**).

Affinity. Due to posterior position of accp4 s-setae on Abd.IV the species, as expected, belongs to Palearctic branch of species of the genus *Parisotoma* (Potapov et al. 2011). Short macrosetae, many s on Ant.1, and increased number of common setae between s-setae in p-row indicate the similarity to *P. appressopilosa* Potapov, 1991, described also from Baikal shore. They differ in number of laterodistal setae on ventral tube (3+3 in *P. baicalica* sp. nov. vs. 2+2 in *P. appressopilosa*), outer setae on lower subcoxa of Leg 1 (one vs. two), shape of claw (more slender in *P. baicalica* sp. nov.), number of s-setae on body tergites (fewer in *P. appressopilosa*) and number of internal setae (three vs. two) on dens. In appearance, the grey *P. baicalica* sp. nov. is well distinguished from the white *P. appressopilosa* if mixed in one site. The new species occurs along Baikal shore where the third congener, *P. reducta* Rusek, 1984, is very common in the forest litter. Both species are grey and can be mixed together in littoral zone. Less distinct eye pigment and shorter macrosetae readily help to discriminate between them. They also differ in size of lateral process of papilla E (Fig. 50 vs. Fig. 51), number of internal setae on dens (Fig. 56 vs. Fig. 57), outer setae on lower subcoxa of Leg 1 and other characters. *P. terricola* Rusek, 1984 (also described from Baikal) and *P. baicalica* sp. nov. share large inner s-setae of AO on Ant.3. Concerning European species, *P. agrelli* (Delamare Deboutteville, 1950) lives on sea shores and most resembles the new species due to short macrosetae, small ommatidia, and 3+3 laterodistal setae on ventral

tube. They sharply differ in outer setae on lower subcoxa of Leg 1 (absent in *P. baicalica* sp. nov.) and number of s on Ant.1 (only two in *P. agrelli*).

Slender claw, polychaetosis, short macrosetae, and expanded lateral process of papilla E indicate adaptation to live in contact to fresh water. The combination of 3+3 laterodistal setae on ventral tube and only one outer seta on lower subcoxa of Leg 1 indicate the formal similarity with the eurytopic species *P. notabilis* (rare at Lake Baikal) but *P. baicalica* sp. nov. differs by all "littoral" characters mentioned above.

The value of basal process on labial papilla B (Fig. 52) calls for further study. So far it was not mentioned in the descriptions of labium while we have seen it also in *P. reducta* and *P. appressopilosa* that may suggest its diagnostic importance for the genus *Parisotoma*.

Distribution and ecology. Known only from two distant localities on the Baikal shore. A littoral species.

Name derivation. It is named after the location of the type locality.

New species records on the shore of Lake Baikal

Folsomia uniramia Potapov & Gulgenova, 2013: Buryat Republic, SE shore of Lake Baikal, at Ust'-Barguzin, 53.4086°N, 108.9879°E, floatation of sand at 5 m distance from water edge, 05.VIII.2014, coll. M. Potapov and A. Gulgenova.

Scutisotoma baica Potapov, Babenko & Fjellberg, 2006: Buryat Republic, SE shore of Lake Baikal, at Ust'-Barguzin, 53.4086°N, 108.9879°E, floatation of wet sand at water edge, 05.VIII.2014, coll. M. Potapov and A. Gulgenova.

Isotomurus stuxbergi (Tullberg, 1876): Buryat Republic, SE shore of Lake Baikal, 5 km N from Turka, 14.V.2017, coll. A. Gulgenova and S. Gulgenov.

Other new records of species concern shores of saline lakes and therefore are given in the Table of Appendix 1.

Faunistic notes

Three ecological groups can be recognised among the recorded species:

1. Species widely distributed in the Holarctic and living also at sites distant from the lake shore (notated as W in Appendix 1). This group mostly consists of xerophilic and steppe species (e.g., *F. parvulus*, *A. stebayevae*, *A. mongolicus*, *F. mongolica* sp. nov.) which occur also on neighbouring arid landscapes of continental Asia. They often prefer saline lands and penetrate to catenas of saline lakes where they can be numerous. The group also include widely distributed eurytopic (*P. notabilis*, *P. minima*) and ruderal species (*P. minuta*). The latter species can be very abundant in lower part of catenas.

2. Lake species (as L in Appendix 1). This group consists of species found so far only in lake shores. They mostly belong to the fauna of Lake Baikal (*P. barathrum* sp. nov., *S. acorrelata*, *S. baica*, *S. robustodens*, *P. appressopilosa*, *P. baicalica* sp. nov.). *Folsomia uniramia* presumably belongs to the group since it has been recorded only in dunes

at this lake shore. *S. acorrelata* and *P. appressopilosa* also occur in shore of saline Alginskoye Lake which is close to Baikal Lake. Considering salt-lake catenas, *E. buryatica* sp. nov. is only species which belongs to this group.

3. Hygrophilic widely distributed species (as H in Appendix 1). In our materials, *Isotomurus stuxbergi* (Tullberg, 1876) is the only member belonging to this group. It was found once in the Baikal shore.

Acknowledgements

References

Absolon C (1901) Zwei neue Collembolenformen aus den Höhlen des mahrischen Karstes. Zoologischer Anzeiger Band 24: 32–33.

Babenko AB, Chernova NM, Potapov MB, Stebaeva SK (1994) Collembola of Russia and adjacent countries: Family Hypogastruridae. Nauka, Moscow, 336 pp.

Babenko AB, Chimitova AB, Stebaeva SK (2011) New Palaearctic species of the tribe Thalassaphorurini Pomorski, 1998 (Collembola, Onychiuridae). ZooKeys 126: 1–38. https://doi.org/10.3897/zookeys.126.1229

Bagnall RS (1940) Notes on British Collembola. The Entomologist's Monthly Magazine 76: 163–174.

Bagnall RS (1948) Contributions toward a knowledge of the Isotomidae (Collembola). I–VI. Annals and Magazine of Natural History 8: 529–541. https://doi.org/10.1080/00222934808653930

Berezina OG (2006) The springtails (Hexapoda, Collembola) on the salty lake catenas of the southern forest-steppe of West Siberia. Eurasian Entomological Journal 5: 199–202. [In Russian]

Bourlet C (1839) Mémoire sur les Podures. Mémoires de la Société Royale des Sciences, de l'Agriculture et des Arts, de Lille: 377–418.

Chen BR (1985) Six new species of the family Isotomidae (Collembola). Contributions from Shanghai Institute of Entomology 5: 183–193. [In Chinese]

Chimitova A, Potapov M (2011) Epitoky in *Scutisotoma stepposa* (Collembola; Isotomidae). Soil organisms 83: 367–382.

Christiansen KA (1952) Notes on Alaskan Collembola II. Three new species of Arctic Collembola. Psyche 58[1951]: 125–140. https://doi.org/10.1155/1951/13918

Christiansen K, Bellinger P (1980) The Collembola of North America north of the Rio Grande. A taxonomic analysis. Grinnell College, Grinnell, Iowa, 1322 pp.

Delamare Debouteville C (1950) Notes faunistiques sur les Collemboles de France (Septieme Note 1). Revue Française d'Entomologie 17: 42–47.

Dunger WG (1982) Collembolen (Insecta, Collembola) aus der Mongolischen Volksrepublik, 2. Isotomidae. Annales Historico-Naturales Musei Nationalis Hungarici 74: 35–74.

Ellis WN (1976) Autumn fauna of Collembola from central Crete. Tijdschrift voor Entomologie 119: 221–326.

Fjellberg A (1975) Redescriptions of some little known Collembola of Scandinavia (Insecta: Collembola). Entomologica Scandinavica 6: 81–88. https://doi.org/10.1163/187631275X00154

Fjellberg A (1984) The maxillary outer lobe, an important systematic tool in Isotomidae (Collembola). Annales de la Société Royale Zoologique de Belgique 114: 83–88.

Fjellberg A (1999) The labial palp in Collembola. Zoologischer Anzeiger 237: 309–330.

Grinbergs A (1962) Über die Collembolen der Sowjetunion. II. Neue Collembolen aus der Tuevischen ASSR. Latvijas Entomologs 5: 59–67.

Grinbergs A (1968) Über die Collembolen der Sowjetunion. III. *Proisotoma* (*Dimorphiella*) *muriphila* n. subgen., n. sp., aus Novosibirsk. Opuscula Entomologica 33: 139–142.

Huang C-W, Potapov M (2012) Taxonomy of the *Proisotoma* complex. IV. Notes on chaetotaxy of femur and description of new species of *Scutisotoma* and *Weberacantha* from Asia. Zootaxa 3333: 38–49. https://doi.org/10.11646/zootaxa.3333.1.3

Martens K (1997) Speciation in the ancient lakes. Trends in Ecology & Evolution 12(5): 177–182. https://doi.org/10.1016/S0169-5347(97)01039-2

Martynova EF (1971a) The subfamily Anurophorinae (Collembola, Isotomidae) in the fauna of the USSR. Zoologicheskii Zhurnal 50: 1639–1657. [In Russian]

Martynova EF (1971b) New species of springtails (Collembola) from mountain and steppe regions of the USSR. Entomological Review 50: 598-611. [In Russian]

Martynova EF (1975) On the fauna of Collembola of the Mongolian People's Republic. l. New and little-known species of Collembola from Mongolia and adjacent regions of the USSR. Nasekomye Mongolii 6(3): 10–25. [In Russian]

Potapov MB (1991) Species of the genus *Isotoma* subgenus *Parisotoma* Bagnall, 1940 and *Sericeotoma* subgen. nov. (Collembola, Isotomidae) of USSR fauna. Acta Zoologica Cracoviensia 34: 267–301.

Potapov M (1997) Towards a new systematics of Isotomidae (Collembola). Examples from *Pseudanurophorus* Stach, 1922 with description of a new furcate species from NE Asia. Pedobiologia 41: 29–34.

Potapov M, Babenko A, Fjellberg A (2006) Taxonomy of the *Proisotoma* complex. Redefinition of genera and description of new species of *Scutisotoma* and *Weberacantha* (Collembola, Isotomidae). Zootaxa 1382: 3–74. https://doi.org/10.11646/zootaxa.1382.1.1

Potapov M, Gulgenova A (2013) Isotomidae (Collembola) of Buryat Republic. II. A Revision of the genus *Folsomia*. Zootaxa 3682: 305–330. https://doi.org/10.11646/zootaxa.3682.2.6

Potapov M, Stebaeva S (1997) Four new species of families Onychiuridae and Isotomidae (Hexapoda, Collembola) from Ubsunur Hollow (Tuva, Russia). Miscellania Zoologica (Barcelona) 20 (2): 119–131.

Potapov M, Janion C, Deharveng L (2011) Two new species of *Parisotoma* (Collembola: Isotomidae) from the Western Cape, South Africa. Zootaxa 2771: 17–24. https://doi.org/10.11646/zootaxa.2771.1.2

Potapov M, Kahrarian M, Deharveng L, Shayanmehr M (2015) Taxonomy of the *Proisotoma* complex. V. Sexually dimorphic *Ephemerotoma* gen. nov. (Collembola: Isotomidae). Zootaxa 4052: 345–358. https://doi.org/10.11646/zootaxa.4052.3.4

Rusek J (1984) New species and review of the *Isotoma notabilis* species-group (Collembola, Isotomidae). Acta Entomologica Bohemoslovaca 81(5): 343–369.

Schäffer C (1896) Die Collembola der Umgebung von Hamburg und benachbarter Gebiete. Mittheilungen aus dem Naturhistorischen Museum in Hamburg 13: 149-216.

Sokolovskaya EA (1989) Springtails of lower part of delta of Selenga River. In: Shilenkov VG (Ed.) Nasekomyye i paukoobraznyye Sibiri. Irkutsk National University, Irkutsk, 33–40. [In Russian]

Stach J (1922) Apterygoten aus dem nordwestlichen Ungarn. Annales Musei nationalis Hungarici 19: 1–75.

Stebaeva SK (1971) New species of Collembola from the Tuva and South-East Altai. In: Cherepanov AI (Ed.) Novye i maloizvestnye vidy fauny Sibiri. Nauka, Novosibirsk: 129–136. [In Russian]

Stebaeva SK (1978) A new species of springtail of the genus *Folsomia* Willem (Collembola, Isotomidae) from forest-steppe region of West Siberia. In: Cherepanov AI (Ed.) Novye i maloizvestnye vidy fauny Sibiri. Nauka, Novosibirsk, 65–69. [In Russian]

Stebaeva SK (1981) Population of springtails (Collembola) of shore zones of fresh and saline lakes of southern forest-steppe of West Siberia. In: Cherepanov AI (Ed.) Fauna i ekologiya chlenistonogikh Sibiri. Thesis of V Meeting of entomologists of Siberia, Novosibirsk (Russia), December 1979. Nauka, Novosibirsk, 96–99. [In Russian]

Stebaeva SK (2006) The distribution of springtails (Hexapoda, Collembola) along catenas of fresh and salt lakes in Tuva. In: Entomological Investigations in northern Asia. Thesis of VII Interregional Meeting of entomologists of Siberia and Far East in the frame of Siberian Zoological Conference, Novosibirsk (Russia), September 2006. Taler-Press, Novosibirsk, 291–293. [In Russian]

Stebaeva SK, Potapov MB (1997) New *Folsomia* species (Hexapoda, Collembola, Isotomidae) from Siberia. Russian Entomological Journal 6(1-2): 3-9.

Strenzke K (1954) Verbreitung und Systematik der Collembolen der deutschen Nordund Ostseeküste. Veröffentlichungen des Instituts für Meeresforschung in Bremerhaven 3: 46–65.

Tullberg T (1871) Förteckning öfver Svenska Podurider. Öfversigt af Kongliga Vetenskaps Akademiens Förhandlingar 28: 143–155.

Tullberg T (1876) Collembola borealia (Nordiska Collembola). Öfversigt af Kongliga Vetenskaps Akademiens Förhandlingar 5: 23–42.

Yosii R (1976) Structure and chaetotaxy of labrum as the taxonomic character of Collembola. Revue d'Écologie et de Biologie du Sol 13: 233–239.

Appendix 1

List of species of Isotomidae found at Lake Baikal shore and catenas of saline lakes of Buryatia and Inner Mongolia (Russia and China), based on literature data and new records.

Species*	Lake Baikal	saline lakes of Buryatia				Saline lakes of Inner Mongolia		Source
		1	2	3	4	5	6	
Anurophorus mongolicus Dunger, 1982 (W)			+		+			p.p.
Pseudanurophorus barathrum sp. nov. (L)	+							p.p.
Proisotoma minima (Absolon, 1901) (W)				+				p.p.
Proisotoma minuta (Tullberg, 1871) (W)					+		+	p.p.
Scutisotoma acorrelata Potapov, Babenko & Fjellberg, 2006 (L)	+	+						Sokolovskaya 1989[P.b.], Potapov et al. 2006; p.p.
Scutisotoma baica Potapov, Babenko & Fjellberg, 2006 (L)	+							Potapov et al. 2006; p.p.
Scutisotoma fjellbergi (Dunger, 1982) (W)					+			p.p.
Scutisotoma robustodens Huang & Potapov, 2012 (L)	+							Huang and Potapov 2012
Scutisotoma stepposa (Martynova, 1975) (W)	+							p.p.
Ephemerotoma buryatica sp. nov. (L)					+			p.p.
Appendisotoma stebayevae (Grinbergs, 1962) (W)	+				+	+	+	Sokolovskaya 1989, p.p.
Folsomides parvulus Stach, 1922 (W)				+		+	+	p.p.
Folsomides aridoviator Potapov & Stebaeva, 1997 (W)				+				p.p.
Folsomia mongolica sp. nov. (W)						+	+	p.p.
Folsomia pseudodecemoculata Stebaeva, 1971 (W)		+		+	+		+	p.p.
Folsomia paoinflata Potapov & Stebaeva, 2006 (W)	+							Potapov and Gulgenova 2013
Folsomia quadrioculata (Tullberg, 1871) (W)	+			+				Sokolovskaya 1989, p.p.
Folsomia uniramia Potapov & Gulgenova, 2013 (L)	+							Potapov and Gulgenova 2013, p.p.
Isotomurus stuxbergi (Tullberg, 1876) (H)	+					+	+	p.p.
Parisotoma appressopilosa Potapov, 1991 (L)	+	+						Potapov 1991, p.p.
Parisotoma baicalica sp. nov. (L)	+							p.p.
Parisotoma reducta Rusek, 1984 (W)	+				+			p.p.
Parisotoma notabilis (Schäffer, 1896) (W)						+		p.p.

Key: * – species identified only to generic level are not given, p.p. – data of present paper, Lakes: 1 – Alginskoye, 2 – Verkhneye Beloye, 3 – Nukhe-Nuur, 4 – Selenginskoye (= Sulfatnoye), 5 – Bayin Chagan Nuori, 6 – Hujiri Nuo Ergacha, (W) – widely distributed species, (L) – lake species (see the Faunistic notes), (H) – hygrophilic species, P.b. – as *Proisotoma buddenbrocki* and *P.* cf. *buddenbrocki*.

RESEARCH ARTICLE

A new species of squat lobster of the genus *Hendersonida* (Crustacea, Decapoda, Munididae) from Papua New Guinea

Paula C. Rodríguez-Flores[1,2], Enrique Macpherson[1], Annie Machordom[2]

1 *Centre d'Estudis Avançats de Blanes (CEAB-CSIC), C. acc. Cala Sant Francesc 14 17300 Blanes, Girona, Spain* **2** *Museo Nacional de Ciencias Naturales (MNCN-CSIC), José Gutiérrez Abascal, 2, 28006 Madrid, Spain*

Corresponding author: Paula C. Rodríguez-Flores (paularodriguezflores@gmail.com)

Citation: Rodríguez-Flores PC, Macpherson E, Machordom A (2020) A new species of squat lobster of the genus *Hendersonida* (Crustacea, Decapoda, Munididae) from Papua New Guinea. ZooKeys 935: 25–35. https://doi.org/10.3897/zookeys.935.51931

Abstract

Hendersonida parvirostris **sp. nov.** is described from Papua New Guinea. The new species can be distinguished from the only other species of the genus, *H. granulata* (Henderson, 1885), by the fewer spines on the dorsal carapace surface, the shape of the rostrum and supraocular spines, the antennal peduncles, and the length of the walking legs. Pairwise genetic distances estimated using the 16S rRNA and COI DNA gene fragments indicated high levels of sequence divergence between the new species and *H. granulata*. Phylogenetic analyses, however, recovered both species as sister species, supporting monophyly of the genus.

Keywords

Anomura, mitochondrial genes, morphology, West Pacific

Introduction

Squat lobsters of the family Munididae Ahyong, Baba, Macpherson & Poore, 2010 are recognised by the trispinose or trilobate front, usually composed of a slender rostrum flanked by supraorbital spines (Ahyong et al. 2010; Macpherson and Baba 2011). The family is one of the most diverse of the anomuran decapods, containing 21 genera and

more than 400 species distributed in the Atlantic, Indian, and Pacific oceans, from the coastal area to the abyssal plain (Baba et al. 2008; Schnabel et al. 2011). Among these genera, the genus *Paramunida* Baba, 1988 was proposed based on the presence of spinules or granules densely covering the carapace dorsally (rather than transverse ridges), the short undeveloped rostrum, the antennal peduncle with a well-developed anterior prolongation of article 1, and the absence of the first pair of male gonopods (Baba 1988). *Hendersonida* Cabezas & Macpherson, 2014 was proposed for one species, *Paramunida granulata* (Henderson, 1885), widely distributed from the Philippines to Polynesia. *Hendersonida* is closely related to a clade corresponding to the genus *Paramunida* Baba, 1988 (Cabezas et al. 2012; Cabezas and Macpherson 2014). The two genera show genetic divergences values higher than expected between species, and within the range observed between other genera of munidid squat lobsters (Cabezas et al. 2011; Cabezas and Macpherson 2014). They can also be morphologically differentiated by differences in the spinulation of the carapace and the length of the distomesial spine of the antennal article 2 (Cabezas and Macpherson 2014).

During a recent expedition to Papua New Guinea in August-October 2010 (BIOPAPUA) (Macpherson et al. in press), two specimens of a species of squat lobster of *Hendersonida* were collected. The morphological and molecular analyses of these specimens indicated that they differ from the type species of *Hendersonida*. Therefore, the specimens are described and illustrated here as a second species of the genus.

Materials and methods

Sampling and identification

Specimens were collected using beam trawls in August-October 2010 (BIOPAPUA) expedition to Papua New Guinea. The types are deposited in the collections of the Muséum national d'Histoire naturelle, Paris (**MNHN**). The terminology employed in the description largely follows Baba et al. (2009) and Macpherson and Baba (2011). The size of the carapace indicates the postorbital carapace length measured along the dorsal midline from the posterior margin of the orbit to the posterior margin of the carapace. The length of each pereopod article is measured in lateral view along its extensor margin (excluding distal spine), the breadth is measured at its widest portion.

Molecular analysis

Tissue of each specimen was isolated from the muscle of pereopod 5 and homogenised overnight with 20 µl proteinase K in 180 µl of buffer ATL (QIAGEN). The extraction was performed using DNeasy Blood and Tissue Kit following manufacturer instructions (QIAGEN). Two molecular markers were amplified: a fragment from the mitochondrial cytochrome oxidase subunit I (COI) using primers LCO1490 (Folmer et al.

1994) and COI-H (Machordom et al. 2003), and a 16S rRNA (16S) fragment, using 16SAR-16SBR from Palumbi et al. (2002) pair of primers.
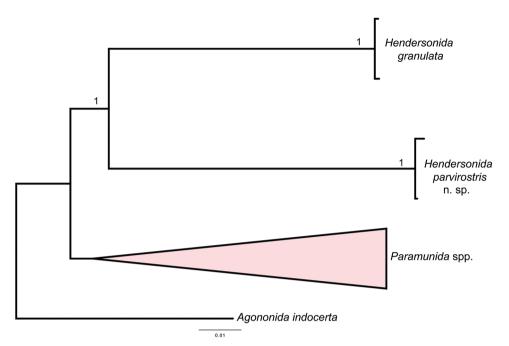
The pre-mixing of the PCR reagents was built in 25 μl total volume, which included 2 μl of DNA extracted, 0.2 mM of each deoxyribonucleotide triphosphate (dNTP), 0.2 μM of each primer forward and reverse, 2U of MyTaq polymerase (Bioline), 5 μl of 5× buffer solution with $MgCl_2$ and sterilised H_2O. PCR amplification was performed with a thermal cycle including an initial denaturation of 94–95 °C for 1–4 min and 40 cycles with 95 °C for 1 min, annealing in 42–45 °C for 1 min followed by an extension set on 72 °C for 1 min. A final extension cycle at 72 °C was set for 10 min. The amplicons were visualised in agarose 1% gels and purified using ExoSAP-IT™ PCR Product Cleanup Reagent (Thermo Fischer) before sequencing. The purified products were sent to Secugen S.L. (Madrid) for DNA Sanger sequencing.

The nucleotide sequences of both forward and reverse were visualised and assembled with Sequencher 4.10.1 software package (Gene Codes Corp.). Multiple sequence alignment for the 16S genes was carried out in MAFFT (Katoh et al. 2002) and the revised in AliView (Larsson 2014). Uncorrected-p pairwise distances between species were calculated in PAUP (Swofford 2002), using the sequences from Cabezas et al. (2012) and McCallum et al. (2016). All the obtained sequences were submitted to GenBank. To test the monophyly of *Hendersonida*, we included all genetic data available from *Paramunida* species included in Cabezas et al. (2012) and McCallum et al. (2016). We collapsed the *Paramunida* node to facilitate the comparison between genera. Sequences of *Paramunida* spp., *Hendersonida granulata* and *Agononida indocerta* were obtained from GeneBank.

Bayesian phylogenetic analysis was performed in MrBayes v3. 2. 1 (Huelsenbeck and Ronquist 2001) using a matrix with the concatenated COI and 16S partial genes. *Agononida indocerta* was selected as the outgroup (GenBank accessions: KM281837.1, KM281818.1). The run was performed in CIPRES portal (Miller et al. 2010). To estimate the posterior probabilities, four Markov Chains Monte Carlo (MCMC) were run for 2×10^7 generations sampling trees and parameters every 20000 generations. The initial 25 % of the generations were discarded as burn-in. The phylogenetic tree was visualised and edited in FigTree v1. 4. 2 (Rambaut 2014); nodes posterior probabilities from the Bayesian Inference were included.

Results

Our results demonstrated the existence of two species of *Hendersonida* supported both by molecular and morphological characters. Both species formed a clade with high Bayesian posterior probability (Fig. 1) and with high genetic distances (11% and 16% for the 16S and COI, respectively). The uncorrected-p distance values between the species of *Hendersonida* and the species of *Paramunida* obtained a range from 9% to 13% for the 16S and from 14% to 19% for the COI.

Figure 1. Phylogenetic hypothesis based on mitochondrial molecular data (COI and 16S) represented by a tree obtained by Bayesian inference, including Bayesian posterior probabilities. To test the monophyly of *Hendersonida*, we have included all genetic data available from species of *Paramunida* included in Cabezas et al. (2012) and McCallum et al. (2016) (38 species). We have collapsed the *Paramunida* node to facilitate comparison between genera.
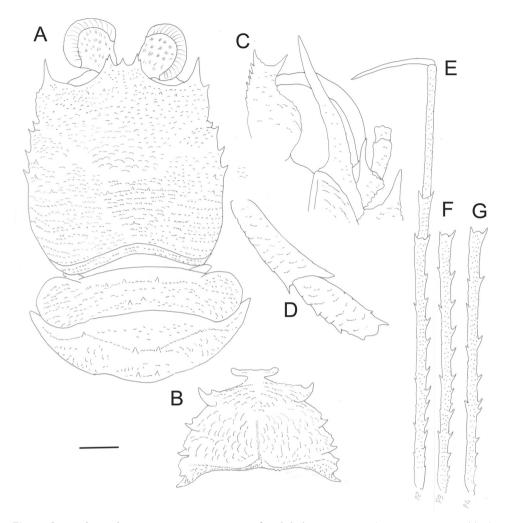
Systematic account

Superfamily Galatheoidea Samouelle, 1819
Family Munididae Ahyong, Baba, Macpherson & Poore, 2010
Genus *Hendersonida* Cabezas & Macpherson, 2014

***Hendersonida parvirostris* sp. nov.**
http://zoobank.org/603BB920-7558-4FA4-BB27-8058768F3668
Figures 2, 3

Material. ***Holotype*:** Biopapua stn CP3645, 24/8/2010, 06°46.394'S, 147°50.605'E, 403–418 m: ovigerous female, 8.9 mm (MNHN-IU-2011-4498). ***Paratype*:** Biopapua. Stn CP3633, 22/8/2010, 06°51.841'S, 147°04.672'E, 395–406 m: 1 ovigerous female, 12.2 mm (MNHN-IU-2011-3379).
　　Diagnosis. Rostrum shorter than supraocular spines, each supraocular spine with small lateral spine. Carapace dorsal surface granulated with few scattered minute spines. Thoracic sternites with numerous arcuate striae, sternite 4 narrowly contiguous

Figure 2. *Hendersonida parvirostris* sp. nov. ovigerous female holotype, 8.9 mm (MNHN-IU-2011-4498), Papua New Guinea. **A** Carapace and abdomen, dorsal view **B** sternum **C** left antennule and antenna, ventral view **D** right maxilliped 3, lateral view **E** left pereopod 2, lateral view **F** left pereopod 3 merus, lateral view **G** left pereopod 4 merus, lateral view. Scale bars: 4 mm (**A, B, E, F, G**); 8 mm (**C, D**).

to sternite 3. Abdominal somites 2 and 3 spinose. Distomesial spine of antennal article 2 reaching end of article 3. Extensor distal margin of maxilliped 3 armed. Pereopods 2–4 long and slender, merus ca. 25 times as long as wide.

Description. *Carapace*: Slightly broader than long; dorsal surface covered with numerous granules and few scattered minute spines, with few short simple setae; epigastric region with row of 6 minute spines; mesogastric region slightly convex, unarmed; cervical groove distinct; cardiac and anterior branchial regions slightly circumscribed; cardiac region with anterior transverse row of four minute spines, and two

minute spines posterior to it; each branchial region with 2–4 small spines near lateral borders; frontal margin slightly concave; lateral margins convex; anterolateral spine reaching sinus between rostral and supraocular spines. Rostrum very short; supraocular spines longer than rostrum, each spine with additional small lateral spine; margin between rostral and supraocular spines concave.

Sternum: Thoracic sternites with numerous arcuate striae; sternite 3 width less than half width of sternite 4, anterior margin nearly straight; sternite 4 with anterior margin moderately elongate, narrowly contiguous to sternite 3; sternite 7 with numerous granules.

Abdomen: Somites 2 and 3 each with some small or moderate–sized spines on anterior and posterior ridges, two median spines larger than others; posterior ridge of somite 4 without distinct single median spine.

Eyes: Large, cornea dilated, much wider than eyestalk.

Antennule: Article 1 barely exceeding corneae, with distomesial spine slightly shorter than distolateral; ca. twice as long as wide; lateral margin without fringe of long setae, with distal slender portion ca. half as long as proximal inflated portion.

Antenna: Anterior prolongation of article 1 overreaching antennular article 1 by ca. one-fourth of its length; article 2 shorter than article 3 and slightly longer than wide, ventral surface with small scales; distomesial spine well developed, reaching end of article 3, and clearly not reaching midlength of anterior prolongation of article 1, distolateral angle unarmed; article 3 twice longer than wide, unarmed.

Maxilliped 3: Ischium 1.5 times length of merus measured along dorsal margin, distoventrally bearing one spine; merus with two or three small spines on flexor margin, extensor margin with distal spine.

Pereopod 1: Lost in holotype, only merus preserved in paratype. Merus 2.5 times carapace length, ca. 15 times longer than high, with row of spines along mesial margin.

Pereopods 2–4: Similar, long and slender, with minute granules and short scales on ventrolateral sides of meri, carpi and propodi; scales with short setae; extensor and flexor margins with numerous long plumose setae; pereopod 2 6.0 times carapace length, merus 3.0 times longer than carapace, ca. 25 times as long as wide, 1.8 times as long as propodus; propodus 20 times as long as wide, and 1.7 times dactylus length; merus with well-developed spines along extensor border, flexor margin with few spines; carpus with distal spine on extensor and flexor margin; propodus with some small movable spines along flexor margin; dactylus slightly curved, with longitudinal carinae along mesial and lateral sides, ventral border, under flexor margin, unarmed; pereopods 3 and 4 of similar length as pereopod 2, with similar spinulation and segment proportions as pereopod 2.

Colour in life: Base colour of carapace light orange, gastric region reddish; granules and spines orange. Rostrum and supraocular spines reddish. Abdominal somites 1–4 light orange, with scales and granules orange or reddish; somites 5 and 6 and telson whitish. Pereopods 2–4 light orange, spines along flexor margins reddish, spines along flexor margins whitish; distal portion of meri, carpi, and propodi and proximal part of carpi, propodi, and dactyli with reddish band, distal half of dactyli whitish.

Figure 3. *Hendersonida parvirostris* sp. nov. dorsal view of ovigerous female holotype, 8.9 mm (MNHN-IU-2011-4498), Papua New Guinea.

Genetic data. GenBank accession numbers: 16S MT252616–MT252617, and COI MT250542–MT250543 (Fig. 1).

Etymology. From the Latin, *parvus*, little, and *rostrum*, in reference to the small size of the rostral spine.

Remarks. The genus *Hendersonida* was erected for one rare species, *H. granulata* (Henderson, 1885) known from several localities of the western Pacific, clearly differentiable from all species of the genus *Paramunida* Baba, 1988 (Macpherson 1993; Cabezas et al. 2010). The new species, *H. parvirostris*, is the second representative of the genus. Both species are morphologically and genetically separated from all the species of *Paramunida* (Fig. 1).

Two conspicuous diagnostic characteristics differentiate the *Hendersonida* genus from *Paramunida*: the granulated surface of the carapace; and the long distomesial spine of antennal article 2, almost reaching the end of the anterior prolongation of article 1 (Cabezas and Macpherson 2014). The morphology of the new species, however, shows that the long distomesial spine of antennal article 2 is not a valid generic character because this spine is moderately short, only reaching the end of antennal article 3, in *H. parvirostris*. Additionally, in both species the anterior margin of sternite 4 is moderately elongate, narrowly contiguous with sternite 3, whereas this margin is nearly transverse, broadly contiguous with sternite 3, in *Paramunida*.

The two species of *Hendersonida* can be differentiated by the following characters:

- The dorsal carapace surface has numerous well-developed spines in *H. granulata*, whereas these spines are minute and nearly absent in *H. parvirostris*.
- The supraocular spines slightly exceed the rostral spine in the new species, whereas the rostral spine clearly overreaches the supraocular spines in *H. granulata*. Furthermore, each supraocular spine has one additional small lateral spine in the new species, which are absent in *H. granulata*.
- The distomesial spine of the antennal article 2 reaches the end of the article 3 in the new species, whereas this spine almost reaches the end of the anterior prolongation of the article 1 in *H. granulata*.
- The extensor margin of maxilliped 3 merus has a distal spine in the new species, whereas this spine is absent in *H. granulata*.
- Pereopods 2–4 are much longer and slender in the new species: propodus 20 times as long as wide in *H. parvirostris* and 7–8 times as long as wide in *H. granulata* (Cabezas et al. 2010).

Distribution. Papua New Guinea, between 395 and 418 m.

Discussion

Here, we demonstrate the existence of a new species of the formerly monotypic genus *Hendersonida*, based on morphology, molecular characters, and phylogenetic information.

The genetic distances observed between the new species and *H. granulata* were 11% for 16S and 16% for COI. These values imply high levels of genetic divergence, even exceeding the mean divergence reported for other munidid species in previous studies (Machordom and Macpherson 2004; Cabezas et al. 2011; Rodríguez-Flores et al. 2019). The phylogenetic tree, however, supported the existence of a common ancestor and a close relationship of *H. granulata* and *H. parvirostris* with respect to other genera, for instance *Paramunida* or *Agononida* (Fig. 1). Moreover, high genetic distances between closely related species of squat lobsters have been already recorded, for instance, in the genus *Phylladiorhynchus* Baba, 1969, where the values can even be higher than 25% for the COI marker (Schnabel and Ahyong 2019). Alternatively, we cannot discard the possibility of a higher rate of extinction in this lineage than in their *Paramunida* relatives, that might account for the scarcity of the taxa and the long branch lengths (Fig. 1). Indeed, given the general values of nucleotide substitution rate for the COI marker, the age of divergence of these two species of *Hendersonida* would be placed by the Early Miocene, at the time when most munidids suffered a notably burst of speciation (Cabezas et al. 2012). Moreover, the granulated surface of the carapace is constant in both species, and seems to be a diagnostic synapomorphy of the genus, in addition to the shape of the sternum, specifically the anterior margin of the sternite 4 (Cabezas and Macpherson 2014).

Acknowledgments

References

Ahyong ST, Baba K, Macpherson E, Poore GCB (2010) A new classification of the Galatheoidea (Crustacea: Decapoda: Anomura). Zootaxa 2676: 57–68. https://doi.org/10.11646/zootaxa.2676.1.4

Baba K (1969) Four new genera with their representatives and six new species of the Galatheidae in the collection of the Zoological Laboratory, Kyushu University, with redefinition of the genus *Galathea*. Ohmu 2: 1–32.

Baba K (1988) Chirostylid and galatheid crustaceans (Decapoda: Anomura) of the "Albatross" Philippine Expedition, 1907–1910. Researches on Crustacea, Special Number 2: 1–203. https://doi.org/10.18353/rcrustaceasn.2.0_1

Baba K, Macpherson E, Poore GCB, Ahyong ST, Bermudez A, Cabezas P, Lin C-W, Nizinski M, Rodrigues C, Schnabel K (2008) Catalogue of squat lobsters of the world (Crustacea: Decapoda: Anomura – families Chirostylidae, Galatheidae and Kiwaidae). Zootaxa 1905: 1–220. https://doi.org/10.11646/zootaxa.1905.1.1

Baba K, Macpherson E, Lin CW, Chan T-Y (2009) Crustacean Fauna of Taiwan: squat lobsters (Chirostylidae and Galatheidae). Taipei: National Science Council, Taiwan, R.O.C, ix + 312 pp.

Cabezas P, Macpherson E (2014) A new species of *Paramunida* Baba, 1988 from the Central Pacific Ocean and a new genus to accommodate *P. granulata* (Henderson, 1885). ZooKeys 425: 15–32. https://doi.org/10.3897/zookeys.425.7882

Cabezas P, Macpherson E, Machordom A (2010) Taxonomic revision of the genus *Paramunida* Baba, 1988 (Crustacea: Decapoda: Galatheidae): a morphological and molecular approach. Zootaxa 2712: 1–60. https://doi.org/10.11646/zootaxa.2712.1.1

Cabezas P, Lin CW, Chan TY (2011) Two new species of the deep-sea squat lobster genus *Munida* Leach, 1820 (Crustacea: Decapoda: Munididae) from Taiwan: morphological and molecular evidence. Zootaxa 3036: 26–38. https://doi.org/10.11646/zootaxa.3036.1.2

Cabezas P, Sanmartín I, Paulay G, Macpherson E, Machordom A. (2012) Deep under the sea: unraveling the evolutionary history of the deep-sea squat lobster *Paramunida* (Decapoda, Munididae). Evolution 66: 1878–1896. https://doi.org/10.1111/j.1558-5646.2011.01560.x

Folmer O, Black M, Hoeh W, Lutz R, Vrijenhoek R (1994) DNA primers for amplification of mitochondrial cytochrome c oxidase subunit I from diverse metazoan invertebrates. Molecular Marine Biology and Biotechnology 3: 294–299.

Henderson JR (1885) Diagnoses of new species of Galatheidae collected during the "Challenger" expedition. Annals and Magazine of Natural History (ser. 5) 16: 407–421. https://doi.org/10.1080/00222938509459908

Huelsenbeck JP, Ronquist F (2001) MRBAYES: Bayesian inference of phylogenetic trees. Bioinformatics 17: 754–755. https://doi.org/10.1093/bioinformatics/17.8.754

Katoh K, Misawa K, Kuma KI, Miyata T (2002) MAFFT: a novel method for rapid multiple sequence alignment based on fast Fourier transform. Nucleic Acids Research 30: 3059–3066. https://doi.org/10.1093/nar/gkf436

Larsson A (2014) AliView: a fast and lightweight alignment viewer and editor for large datasets. Bioinformatics 30: 3276–3278. https://doi.org/10.1093/bioinformatics/btu531

Machordom A, Araujo R, Erpenbeck D, Ramos MA (2003) Phylogeography and conservation genetics of endangered European Margaritiferidae (Bivalvia: Unionoidea). Biological Journal of the Linnean Society 78: 235–252. https://doi.org/10.1046/j.1095-8312.2003.00158.x

Machordom A, Macpherson E (2004) Rapid radiation and cryptic speciation in galatheid crabs of the genus *Munida* and related genera in the South West Pacific: molecular and morphological evidence. Molecular Phylogenetics and Evolution 33: 259–279. https://doi.org/10.1016/j.ympev.2004.06.001

Macpherson E (1993) Crustacea Decapoda: species of the genus *Paramunida* Baba, 1988 (Galatheidae) from the Philippines, Indonesia and New Caledonia. In: Crosnier A (Ed.) Résultats des Campagnes MUSORSTOM, volume 10. Mémoires du Muséum National d'Histoire Naturelle, Paris 156: 443–473.

Macpherson E, Baba K (2011) Chapter 2. Taxonomy of squat lobsters. In: Poore GCB, Ahyong ST, Taylor J (Eds) The biology of squat lobsters. CSIRO Publishing, Melbourne and CRC Press, Boca Raton, 39–71.

Macpherson E, Rodríguez-Flores PC, Machordom A (in press) Squat lobsters of the families Munididae and Munidopsidae from Papua New Guinea. In: Ahyong ST, Chan T-Y, Corbari L (Eds) Tropical Deep-Sea Benthos 31, Papua New Guinea. Muséum national d'Histoire naturelle, Paris: 00-00 (Mémoires du Muséum national d'Histoire naturelle, 213).

McCallum AW, Cabezas P, Andreakis N (2016) Deep-sea squat lobsters of the genus *Paramunida* Baba, 1988 (Crustacea: Decapoda: Munididae) from north-western Australia: new records and description of three new species. Zootaxa 4173: 201–224. https://doi.org/10.11646/zootaxa.4173.3.1

Miller MA, Pfeiffer W, Schwartz T (2010) Creating the CIPRES Science Gateway for inference of large phylogenetic trees. Proceedings of the Gateway Computing Environments Workshop (GCE), 14 Nov. 2010, New Orleans, LA, 1–8. https://doi.org/10.1109/GCE.2010.5676129

Palumbi S, Martin A, Romano S, McMillan WO, Stice L, Grabowski G (2002) The simple fool's guide to PCR. University of Hawaii, Honolulu, 45 pp.

Rambaut A (2014) FigTree 1.4. 2 software. Institute of Evolutionary Biology, Univ. Edinburgh.

Rodríguez-Flores PC, Machordom A, Abelló P, Cuesta JA, Macpherson E (2019) Species delimitation and multi-locus species tree solve an old taxonomic problem for European squat lobsters of the genus *Munida* Leach, 1820. Marine Biodiversity 49: 1751–1773. https://doi.org/10.1007/s12526-019-00941-3

Samouelle G (1819) The entomologists' useful compendium; or an introduction to the knowledge of British Insects, comprising the best means of obtaining and preserving them, and a description of the apparatus generally used; together with the genera of Linné, and modern methods of arranging the Classes Crustacea, Myriapoda, spiders, mites and insects, from their affinities and structure, according to the views of Dr. Leach. Also an explanation of the terms used in entomology; a calendar of the times of appearance and usual situations of near 3,000 species of British Insects; with instructions for collecting and fitting up objects for the microscope. Thomas Boys, London, 496 pp. [412 pls.] https://doi.org/10.5962/bhl.title.120094

Schnabel KE, Ahyong ST (2019) The squat lobster genus *Phylladiorhynchus* Baba, 1969 in New Zealand and eastern Australia, with description of six new species. Zootaxa 4688: 301–347. https://doi.org/10.11646/zootaxa.4688.3.1

Schnabel KE, Cabezas P, McCallum A, Macpherson E, Ahyong ST, Baba K (2011) Chapter 5. World-wide distribution patterns of squat lobsters. In: Poore GCB, Ahyong ST, Taylor J (Eds) The biology of squat lobsters. CSIRO Publishing: Melbourne and CRC Press, Boca Raton, 149–182.

Swofford DL (2002) PAUP*: phylogenetic analysis using parsimony, version 4.0 b10.

RESEARCH ARTICLE

ZooKeys
A peer-reviewed open-access journal
Launched to accelerate biodiversity research

Two new cyclophoroid species from Hubei, China, with proposal of a new genus (Gastropoda, Caenogastropoda, Diplommatinidae and Alycaeidae)

Zhe-Yu Chen[1,2], Min Wu[2]

1 *College of food science and engineering, Wuhan Polytechnic University, Wuhan 430023, China* **2** *School of Life Sciences, Nanjing University, Xianlindadao 163, Nanjing 210023, China*

Corresponding author: Min Wu (minwu1969@aliyun.com)

Citation: Chen Z-Y, Wu M (2020) Two new cyclophoroid species from Hubei, China, with proposal of a new genus (Gastropoda, Caenogastropoda, Diplommatinidae and Alycaeidae). ZooKeys 935: 37–46. https://doi.org/10.3897/zookeys.935.51414

Abstract

Two new species, *Sinoarinia feii* Chen, **gen. et sp. nov.** and *Pincerna vallis* Chen & Wu, **sp. nov.**, are described from western Hubei, China. The new genus *Sinoarinia* Chen & Wu, **gen. nov.** is established based on the strongly constricted penultimate whorl and the ascending last whorl. The Vietnamese species *Pincerna costulosa* (Bavay & Dautzenberg) is newly reported from Yunnan, China. For comparison, photographs of the shells of closely related species are provided. A key to the known species of *Sinoarinia* **gen. nov.** is included.

Keywords

new genus, new species, *Pincerna*, *Sinoarinia*

Introduction

The malacofauna of western Hubei has usually been studied at some well-known localities along the Yangtze River, for example in Badong and Changyang (Heude 1882, 1885, 1890; Yen 1939). In the region farther south, which encompasses vast areas of limestone mountains, the land snail fauna is still poorly known. During a short faunal survey in Wufeng (Tujiazu Autonomous County) in summer 2019, we found

two cyclophoroid species new to science, namely *Sinoarinia feii* Chen gen. et sp. nov. (Diplommatinidae) and *Pincerna vallis* Chen & Wu, sp. nov. (Alycaeidae).

Arinia H. Adams & A. Adams, 1856 (Diplommatinidae) is a speciose genus widely distributed in Southeast Asia (Zilch 1953; Vermeulen 1996; Vermeulen et al. 2007; Páll-Gergely and Hunyadi 2018). Only three species of this genus were reported from China so far, namely *Arinia cathaicola* Pilsbry, 1934, *Arinia mirifica* Li, Zhuo & Luo, 2005, and *Arinia maolanensis* Zhang, Chen & Zhuo, 2013 (Pilsbry 1934; Li et al. 2005; Zhang et al. 2013). Based on our morphological studies of shells, we believed that *A. mirifica* and *A. maolanensis*, *Diplommatina aesopus* Bavay & Dautzenberg, 1904 from Vietnam, and *S. feii* sp. nov. belong to a distinct, undescribed genus.

Methods

Photographs of the shells and the habitats were taken using a Canon 5D Mark IV camera. The shells were measured with digital vernier calipers to the nearest 0.1 mm. Whorls were counted as described by Kerney and Cameron (1979). The terminology to describe alycaeid shells (Regions 1–3) follows Páll-Gergely et al. (2017).

Abbreviations: **a.s.l.** – above sea level; **D** – shell breadth; **H** – shell height; **HBUMM** – mollusc collection of the Museum of Hebei University, Baoding, China; **MNHN** – Muséum National d'Histoire Naturelle, Paris, France; **R1** (Region 1) – from the beginning of the teleoconch to the beginning of the differently ribbed region along the suture; **R2** (Region 2) – the differently ribbed area before the constriction; **R3** (Region 3) – from the constriction to the peristome.

Systematics

Diplommatinidae Benson, 1849

Sinoarinia Chen & Wu, gen. nov.
http://zoobank.org/97E91F22-0BD2-4A64-A6A9-2811065ED0F4

Type species. *Sinoarinia feii* Chen, sp. nov.

Diagnosis. Shell minute, dextral, thin, translucent, cylindrical. Penultimate whorl strongly constricted. Last whorl strongly ascending, covering part of penultimate whorl. Protoconch oblique. Apical whorls depressed, with strong or weak ribs. Aperture rounded; peristome double, expanded but not reflected. Columellar lamella not visible from aperture but internally present; one parietal lamella and one palatal plica extending inwards from last whorl to penultimate whorl (in type species). Palatal plica visible through semitransparent parietal wall. Constriction absent or very weak where lamellae and plica terminate. Umbilicus closed, forming a chink.

Etymology. Combination of the Latin prefix sino- (= China) with *Arinia*.

Distribution. Southern China (Hubei, Guizhou), northern Vietnam.

Figure 1. Map of sampling sites and type localities **1** type locality of *Sinoarinia feii* Chen, gen. et sp. nov. and *Pincerna vallis* Chen & Wu, sp. nov. **2** type locality of *Sinoarinia maolanensis* (Zhang, Chen & Zhuo, 2013) comb. nov. **3** type locality of *Sinoarinia mirifica* (Li, Zhuo & Luo, 2005) comb. nov. **4** type locality of *Pincerna costulosa* (Bavay & Dautzenberg, 1912) and *Sinoarinia aesopus* (Bavay & Dautzenberg, 1904) comb. nov., Vietnam **5** Sampling site of *Pincerna costulosa* in Yunnan.

Remarks. The new genus can be distinguished from the sympatric diplommatinid genera (*Arinia*, *Diplommatina* Benson, 1849 and *Gastroptychia* Kobelt & Möllendorff, 1900) by its constricted penultimate whorl and the ascending last whorl (Kobelt 1902; Zilch 1953; Vermeulen 1996; Vermeulen et al. 2007; Páll-Gergely and Hunyadi 2018). In general, *Sinoarinia* gen. nov. has a cylindrical shell, depressed apex, and deeply incised lamellae and plica, which differs from the conical shell with an exposed columellar lamella in *Diplommatina* and *Gastroptychia*. *Arinia* usually lacks internal apertural barriers (Kobelt 1902; Vermeulen 1996; Vermeulen et al. 2007), which are well developed in *Sinoarinia* gen. nov. The constricted structure of the new genus is similar to that found in the non-sympatric diplommatinid genus *Diancta* E. von Martens, 1864, which differs from the new genus by its mostly sinistral coiling and conical

whorls as showed in *Diancta* (s. str.) (Neubert and Bouchet 2015), or by the constricted penultimate whorl which is not partially covered by the last whorl, as showed in *Diancta* (*Paradiancta*) Möllendorff, 1895 (Egorov 2013).

Three species, *Arinia mirifica* Li, Zhuo & Luo, 2005, *A. maolanensis* Zhang, Chen & Zhuo, 2013, and *Diplommatina aesopus* Bavay & Dautzenberg, 1904, which some authors currently assign to *Arinia* (Li et al. 2005; Zhang et al. 2013) and *Diplommatina* (Bavay & Dautzenberg, 1904), are here transferred to *Sinoarinia* gen. nov.

Included species. *Sinoarinia aesopus* (Bavay & Dautzenberg, 1904) comb. nov., *Sinoarinia feii* Chen sp. nov., *Sinoarinia maolanensis* (Zhang et al., 2013) comb. nov., and *Sinoarinia mirifica* (Li et al., 2005) comb. nov.

Vernacular name. 华阿勇螺属

Sinoarinia feii Chen, gen. et sp. nov.
http://zoobank.org/CD2C6088-75C0-430D-92CD-5BEB49BD06E8
Figures 1, 2A, 3, 5B

Type material. *Holotype* (HBUMM 10016-spec. 1), China, Hubei, Wufeng Tujiazu Autonomous County, Chaibuxi National Forest Park, 30.216N, 110.199E, 1220 m a.s.l., leg. Zhe-Yu Chen and Qiao-Zhen Hu, 27 June 2019 (Fig. 5B). *Paratypes*: 4 ex. (HBUMM 10016-spec. 2–5), same data as holotype.

Measurements. Shell width = 1.6–1.7 mm, shell height = 2.4–2.7 mm (*n* = 4).

Diagnosis. Shell minute, cylindrical and apically flat. Penultimate whorl strongly constricted. Columellar lamella, one parietal lamella and one palatal plica present.

Description. Shell minute, dextral, cylindrical, translucent, with 5½ whorls. Shell suture depressed. Protoconch oblique, with no obvious sculpture. Upper whorls depressed. Penultimate whorl so strongly constricted that ½ whorl is invisible. Last whorl strongly ascending, dorsally covering part of penultimate whorl. Ribs strong and sharp, concentrated around umbilical region. Aperture rounded. Peristome double, expanded but not reflected. Angular protrusion weakly present near basal columella. Columellar lamella invisible from aperture, but stronger at penultimate whorl. One parietal lamella and one palatal plica extending from last whorl to penultimate whorl (Fig. 3). Palatal plica visible through semi-transparent parietal wall; obvious constriction absent or very weakly bulged at dorsal side of penultimate whorl. Umbilicus closed, chink-shaped. Operculum unknown.

Etymology. This name honors the herpetologist, Prof. Liang Fei, who encouraged the first author to carry out the research work.

Type locality. China, Hubei, Wufeng Tujiazu Autonomous County, Chaibuxi National Forest Park, 30.216N, 110.199E, 1220 m a.s.l.

Distribution. This species is known only from the type locality.

Remarks. *Sinoarinia maolanensis* (Zhang et al. 2013) is morphologically similar, but differs in having a larger shell with stronger ribs (Fig. 2B). *Sinoarinia mirifica* (Li
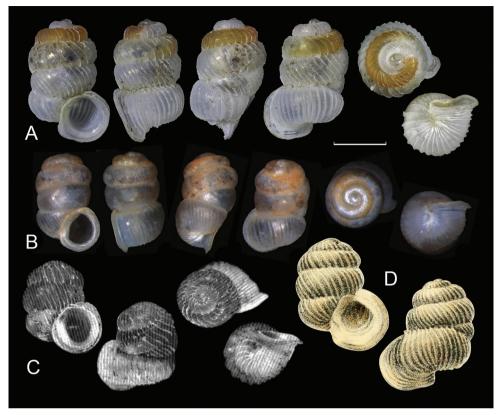
Figure 2. A *Sinoarinia feii* Chen, gen. et sp. nov. (HBUMM 10016-spec. 1, holotype) (Photos: Zhe-Yu Chen) **B** *Sinoarinia maolanensis* (Zhang et al., 2013) comb. nov. (after Zhang et al. 2013) **C** *Sinoarinia mirifica* (Li et al., 2005) comb. nov. (after Li et al. 2005) **D** *Sinoarinia aesopus* (Bavay & Dautzenberg, 1904) comb. nov. (after Bavay & Dautzenberg, 1904). Scale bar: 1 mm, refers to **A** and **B** only.

et al. 2005) can be distinguished by its stout shape of shell, sparser ribs, shorter and fewer whorls, and in that the last whorl covers the penultimate whorl dorso-laterally (Fig. 2C) (in *S. feii* gen. et sp. nov. the last whorl covers penultimate whorl dorsally).

Vernacular name. 费氏华阿勇螺

Key to the species of *Sinoarinia* gen. nov.

1	Shell height greater than 3 mm .... ***S. aesopus* (Bavay & Dautzenberg, 1904) (Fig. 2D)**	
–	Shell height less than 3 mm **2**	
2	Whorls fewer than 5. Shell width / shell height approximately 0.9 ....***S. mirifica* (Li et al. 2005) (Fig. 2C)**	
–	Whorls more than 5. Shell width / shell height approximately 0.5–0.7 ....**3**	

3   Shell height greater than 2 mm. Shell ribs strong ....
           ....*S. feii* **Chen sp. nov. (Fig. 2A)**
–   Shell height less than 2 mm. Shell ribs weak ....
           .... ***S. maolanensis*** **(Zhang et al. 2013) (Fig. 2B)**

Alycaeidae Blanford, 1864

Pincerna **Preston, 1907**
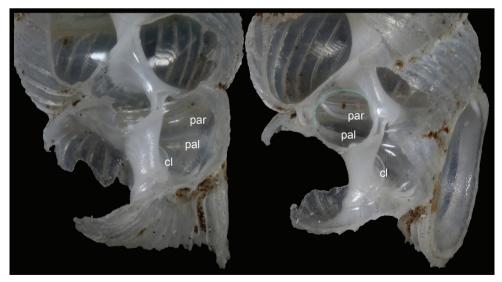
Type species. *Alycaeus* (*Pincerna*) *liratula* Preston, 1907, by monotypy (Páll-Gergely 2017).
    Vernacular name. 平沟螺属

Pincerna vallis **Chen & Wu, sp. nov.**
http://zoobank.org/63A4E519-86E7-453A-9F90-2EAAFE527185
Figures 1, 4A, B, 5A
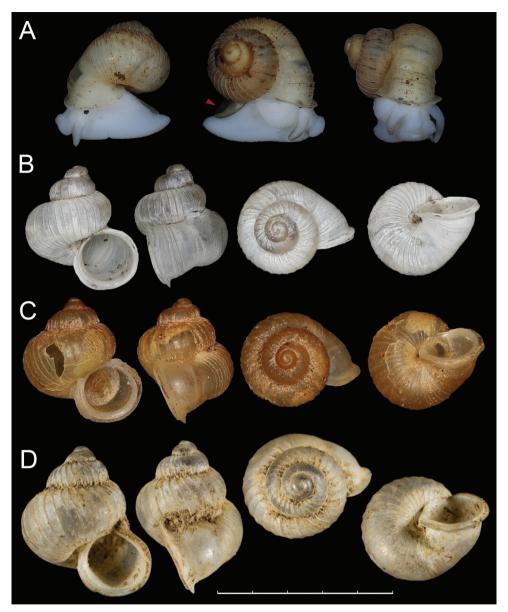
Type material. *Holotype* (HBUMM10017-spec. 1, fully mature animal), China, Hubei, Wufeng Tujiazu Autonomous County, Chaibuxi National Forest Park, 30.216N, 110.199E, 1220 m a.s.l., leg. Zhe-Yu Chen and Qiao-Zhen Hu, 27 June 2019 (Fig. 5A). *Paratype***:** 1 ex. (HBUMM 10017-spec. 2, an empty shell), same data as holotype.
    Measurements. Shell width = 3.3 mm, shell height = 3.5 mm.

Figure 3. Inner structure of *Sinoarinia feii* Chen, gen. et sp. nov. (HBUMM 10016-spec. 5, paratype) (Photos: Zhe-Yu Chen). Abbreviations: par-parietal lamella, pal-palatal plica, cl-columellar lamella, green dotted line-constriction.

Figure 4. A, B *Pincerna vallis* Chen & Wu, sp. nov. **A** HBUMM 10017-spec. 1, holotype, red arrow shows the operculum **B** HBUMM 10017-spec. 2, paratype **C, D** *Pincerna costulosa* (Bavay & Dautzenberg, 1912) **C** HBUMM10018 **D** syntype, MNHN-IM-2000-31786. Scale bar: 5 mm. Photos: Zhe-Yu Chen (**A–C**) and M. Caballer Gutierrez (**D**).

Diagnosis. R3 with some ribs. Ribs on R2 more intensive than those in *P. costulosa*.

Description. Shell conical ovoid, orangish when fresh, with 3¼–3½ convex whorls. Suture deep. Protoconch finely granulate, 1–1¾ whorls. R1 ca 2½ whorls,

Figure 5. A Habitat of *Pincerna vallis* Chen & Wu, sp. nov. (HBUMM 10017-spec. 1, holotype) **B** habitat of *Sinoarinia feii* Chen, gen. et sp. nov. Photos: Zhe-Yu Chen.

with regularly spaced strong ribs. R2 very short (ca 0.5 mm), consisting of ca 15 lighter stripes (= breathing tunnels); constriction between R2 and R3 rather shallow. R3 slightly less than ¼ whorl, smooth near R2 side, with about 5 weak but distinct ribs near aperture. Aperture rounded, nearly vertical, not descending. Peristome expanded but not reflected, internally thickened, protruding; boundary between inner and outer peristomes visible. Umbilicus open, narrow. Operculum (Fig. 4A, arrowed) corneous, translucent, thin, concave.

Etymology. The name *vallis* (Latin: valley) refers to the type locality inside the Chaibuxi Grand Canyon.

Type locality. China, Hubei, Wufeng Tujiazu Autonomous County, Chaibuxi National Forest Park, 30.216N, 110.199E, 1220 m a.s.l.

Distribution. This species is known only from the type locality.

Remarks. Two *Pincerna* species have been recorded in adjacent areas, *P. costulosa* (Bavay & Dautzenberg, 1912) from Vietnam (Holotype: MNHN-IM-2000-31786, Tonkin, Phong Tho) (Fig. 4D) and Yunnan, China (HBUMM10018, see below) (Fig. 4C) and *Pincerna maolanensis* Luo, Zhang & Zhuo, 2009 from Guizhou. *Pincerna vallis* sp. nov. can be distinguished from *P. maolanensis* by its smaller and more fragile shell, relatively short R2 (ca 0.5 mm, whereas it is 0.83–1.00 mm in *P. maolanensis*). *Pincerna costulosa* is most similar to the new species in size and shape. However, *P. vallis* sp. nov. has a more convex body whorl. *Pincerna costulosa* has a smooth/ribless R3 while the new species has some ribs near the aperture. In addition, the ribs of *P. vallis* sp. nov. on R2 are stronger than those in *P. costulosa*.

Vernacular name. 峡谷平沟螺

Pincerna costulosa **(Bavay & Dautzenberg, 1912)**
Figures 1, 4C, D

Alycaeus costulosus Bavay & Dautzenberg, 1912: 49–50, pl. 4, figs 1–4.
Pincerna costulosa-Páll-Gergely et al. 2017: 10, fig. 3F.

Materials examined. HBUMM10018 (Fig. 4C), Yunnan, Xishuangbanna, Menglun Botanical Garden, Lvshilin (21.911N, 101.283E), leg. Xiao-Ran Zнu, 6 August 2018.
Type locality. "Phong-Tho, Tonkin".
Distribution in China. Yunnan.
Vernacular name. 弱肋平沟螺

Acknowledgements

References

Bavay A, Dautzenberg P (1904 [«1903»]) Description de coquilles nouvelles de l'Indo-Chine (3e suite). Journal de Conchyliologie 51(3): 201–236.

Bavay A, Dautzenberg P (1912) Description de coquilles nouvelles de l'Indo-Chine. Journal de Conchyliologie 60(1): 1–54.

Egorov R (2013) A review of the genera of the terrestrial pectinibranch molluscs (synopsis mainly based on published data). Littoriniformes: Liareidae, Pupinidae, Diplommatinidae, Alycaeidae, Cochlostomidae. Treasure of Russian Shells, Supplement 3(3): 1–62.

Heude PM (1882) Notes sur les mollusques terrestres de la vallée du fleuve Bleu. Mémoires Concernant l'Histoire Naturelle de l'Empire Chinois 1: 1–84. https://doi.org/10.5962/bhl.title.50365

Heude PM (1885) Notes sur les mollusques terrestres de la vallée du fleuve Bleu. Mémoires Concernant l'Histoire Naturelle de l'Empire Chinois 3: 89–132.

Heude PM (1890) Notes sur les mollusques terrestres de la vallée du fleuve Bleu. Mémoires Concernant l'Histoire Naturelle de l'Empire Chinois 4: 125–188.

Kerney MP, Cameron RAD (1979) A field guide to the land snails of Britain and North-West Europe. Collins, London, 288 pp.

Kobelt W (1902) Das Tierreich. Eine Zusammenstellung und Kennzeichnung der rezenten Tierformen. Verbindung mit der Deutschen Zoologischen Gesellschaft herausgegeben von

der Königlich Preussischen Akademie der Wissenschaften zu Berlin. Mollusca: Cyclophoridae. R. Friedländer und Sohn, Berlin, 662 pp.

Li Y, Zhou W, Luo T (2005) A new species of Cyclophoridae from Guizhou Province, China, (Prosobranchia: Mesogastropoda: Cyclophoridae). Acta Zootaxonomica Sinica 30(1): 67–69.

Luo TC, Zhang WH, Zhuo WC (2009) A new species of the genus *Dioryx* Benson from China (Prosobranchia, Mesogastropoda, Cyclophoridae). Acta Zootaxonomica Sinica 34 (4): 862–864.

Neubert E, Bouchet P (2015) The Diplommatinidae of Fiji–a hotspot of Pacific land snail biodiversity (Caenogastropoda, Cyclophoroidea). ZooKeys 487: 1–85. https://doi.org/10.3897/zookeys.487.8463

Páll-Gergely B (2017) A new species of Alycaeidae, *Pincerna yanseni* sp. nov. from Sumatra, with the resurrection of the genus *Pincerna* Preston, 1907 (Gastropoda: Cyclophoroidea). Raffles Bulletin of Zoology 65: 213–219.

Páll-Gergely B, Hunyadi A (2018) Four new cyclophoroid species from Thailand and Laos (Gastropoda: Caenogastropoda: Alycaeidae, Diplommatinidae, Pupinidae). Zoosystema 40(3): 59–66. https://doi.org/10.5252/zoosystema2018v40a3

Páll-Gergely B, Hunyadi A, Đỗ ĐS, Naggs F, Asami T (2017) Revision of the Alycaeidae of China, Laos and Vietnam (Gastropoda: Cyclophoroidea) I: the genera *Dicharax* and *Metalycaeus*. Zootaxa 4331(1): 1–124. https://doi.org/10.11646/zootaxa.4331.1.1

Pilsbry HA (1934) Zoological results of the Dolan West China Expedition of 1931, part II, mollusks. Proceedings of the Academy of Natural Science of Philadelphia 86: 5–28.

Vermeulen JJ (1996) Notes on the non-marine molluscs of the island of Borneo 8, the genus *Arinia*; additions to the genera *Diplommatina* and *Opisthostoma* (Gastropoda Prosobranchia: Diplommatinidae). Basteria 60(4–6): 87–138.

Vermeulen JJ, Phung LC, Truong QT (2007) New species of terrestrial molluscs (Caenogastropoda, Pupinidae and Pulmonata, Vertiginidae) of the Hon Chong-Ha Tien limestone hills, Southern Vietnam. Basteria 71(1–3): 81–92.

Yen TC (1939) Die chinesischen Land- und Süßwasser-Gastropoden des Natur-Museums Senckenberg. Abhandlungen der Senckenbergischen Naturforschenden Gesellschaft 444: 1–234. [16 pls.]

Zhang W, Chen D, Zhou W (2013) A new species of the genus *Arinia* H. and A. Adams from China (Prosobranchia: Caenogastropoda: Diplommatinidae). Acta Zootaxonomica Sinica 38(4): 773–775.

Zilch A (1953) Die Typen und Typoide des Natur-Museums Senckenberg, 9: Mollusca, Cyclophoridae, Diplommatininae. Archiv für Molluskenkunde 82(1/3): 1–47.

RESEARCH ARTICLE

ZooKeys
A peer-reviewed open-access journal
Launched to accelerate biodiversity research

Description of a new *Tegenaria* Latreille, 1804 from southern Turkey with remarks on the *Tegenaria ariadnae* species-complex (Arachnida, Araneae)

Dragomir Dimitrov[1]

I *National Museum of Natural History, Bulgarian Academy of Sciences, 1 Tsar Osvoboditel Blvd, 1000 Sofia, Bulgaria*

Corresponding author: Dragomir Dimitrov (dimitrov@nmnhs.com)

Abstract

A new cave-dwelling species of *Tegenaria*, *T. lazarovi* **sp. nov.**, is described from southern Turkey, based on both sexes. The new species belongs to the *T. ariadnae* species-complex which is distributed in the Eastern Mediterranean (Crete, northern Libya). The new species is compared to its morphologically closest congeners. New taxonomically relevant pictures are given for two of them. The distribution of the *Tegenaria ariadnae* species-complex is summarized and discussed.

Keywords

Cave fauna, endemic, funnel weaver spiders, new species, taxonomy

Introduction

With 112 valid species (WSC 2020), *Tegenaria* Latreille, 1804 is one of the largest genera in the spider family Agelenidae. The genus is very species-rich in Turkey. Demir and Seyyar (2017) listed 31 species, Özkütük et al. (2017) and Topçu and Demircan (2018) added two more, increasing the number of known species from the country to 33. Many of these species are known by one sex only. Especially high is the number of species where only the female is known (12 spp.), while in just one species only the male is known. The

remaining 20 species are known by both sexes. The species known only by females are described mostly from caves by Brignoli (1972b, 1977, 1978a, 1978b) and the absence of the male sex is a cause of certain difficulties in the taxonomy of the genus.

While processing unidentified material collected in 2006 by my colleagues Stoyan Lazarov and Pavel Stoev in Turkish caves, I discovered an unknown *Tegenaria* species captured in an unnamed cave situated between Anamur and Silifke, southern Turkey. The species is described below and its possible relationships, as well as the distribution of the *T. ariadnae* species-complex, are discussed.

Material and methods

The material was preserved in vials with 80% ethanol in the field. The specimens were examined and measured using a Wild M5A stereomicroscope; all measurements are in mm. Pictures were taken with a Canon EOS 1100D digital camera attached to a Carl Zeiss Amplival microscope. The drawings were executed on a Wacom tablet and using Adobe Illustrator graphic design software. The map was generated with the SimpleMappr API. Colour was described from specimens preserved in ethanol. The male palp and epigyne were dissected in order to be studied and illustrated. The epigyne was cleared in lactic acid. Leg measurements formula: total length (coxa + trochanter, femur, patella, tibia, metatarsus, tarsus). Tarsus length includes claws.

Abbreviations: Morphology. **ALE** – anterior lateral eyes, **AME** – anterior median eyes, **C** – conductor, **CO** – copulatory openings, **DBTA** – dorsal branch of the tibial apophysis, **DPC** – dorsal part of terminal end of the conductor, **LBTA** – lateral branch of the tibial apophysis, **MA** – median apophysis, **MPE** – median plate of epigyne, **PLE** – posterior lateral eyes, **PME** – posterior median eyes, **R** – receptacles, **VPC** – ventral part of terminal end of the conductor.
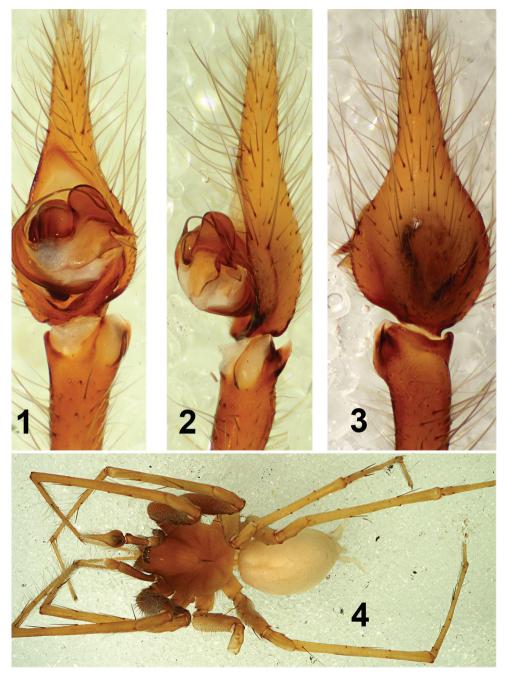
Institutions. MBCG – Museo Civico Scienze Naturali Enrico Caffi, Bergamo, Italy; **MCSN** – Museo Civico di Storia Naturale, Verona, Italy; **NMNHS** – National Museum of Natural History, Sofia, Bulgaria; **SMF** – Senckenberg Research Institute, Frankfurt, Germany.

Taxonomy

Family Agelenidae C. L. Koch, 1837
Genus *Tegenaria* Latreille, 1804

Tegenaria lazarovi **sp. nov.**
http://zoobank.org/CADBD8E5-2299-4BC4-AFF6-9CFCAA55D011
Figs 1–6

Type material. ♂ holotype, 2 ♀ paratypes, Turkey, Silifke distr., Karatepe village, unnamed cave on the left side of the road Anamur-Silifke, Akçalı Dağları Mts. 36;

Figures 1–4. *Tegenaria lazarovi* sp. nov. male holotype. Palp ventral (**1**), palp retrolateral (**2**), palp dorsal (**3**), habitus (**4**).

36°10'55"N, 33°26'41"E, altitude 182 m, wet sand; 16.07.2006; P. Stoev and S. Lazarov leg. (NMNHS); 1 ♀ paratype, the same data as holotype (SMF).
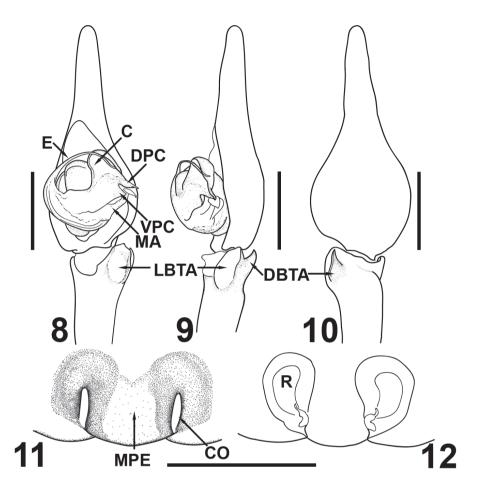
Figures 5–7. *Tegenaria lazarovi* sp. nov. female paratype. Epigyne ventral (**5**), vulva dorsal (**6**), habitus (**7**).

Other material. 3 ♀ juveniles, the same data as holotype (NMNHS).

Comparative material examined. *Tegenaria vallei* Brignoli, 1972. ♂ holotype, Libya, Cyrenaica, Lete Cave, Benghasi, 06.04.1966, Valle and Bianchi leg., 1 ♂ paratype, the same locality as holotype, 31.12.1967, Valle leg. (MBCG); 1 ♀ paratype, the same locality as holotype, 31.12.1967, Valle leg. (MCSN); *Tegenaria pieperi* Brignoli, 1979. ♀ holotype, Crete, Sitia, Agios Georgios, Megalo Katafigi Cave, 21.05.1977, H. Pieper leg. (MCSN).

Etymology. The species is dedicated to my colleague, Bulgarian arachnologist Stoyan Lazarov who provided me with the type material. He was chosen over Pavel Stoev by tossing a coin.
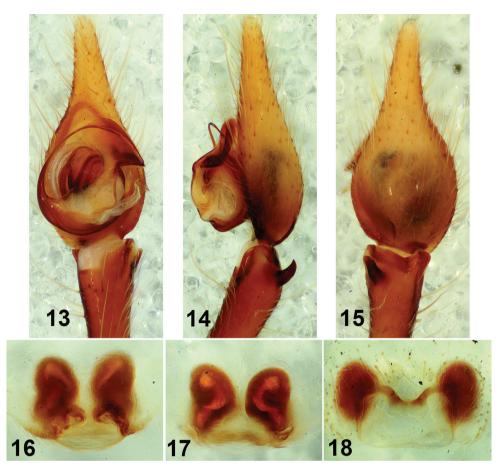
Diagnosis. The new species fits well in the genus *Tegenaria* as defined by Bolzern, Burckhardt and Hänggi (2013) according to its straight trochanters, the absence of dorsal spines on the patellae and the shape of the conductor. It appears closest to *Tegenaria ariadnae* Brignoli, 1984. The males can be separated by the following characters:(1) The DBTA of *Tegenaria lazarovi* sp. nov. is claw-shaped, with a sharp tip (Figs 2, 3, 9, 10), while in *T. ariadnae* it is more massive and with a blunt tip (Bolzern, Burckhardt and Hänggi 2013: 769, fig 14R); (2) A lighter, less sclerotized LBTA (Figs 1, 2, 8, 9), more sclerotized in *T. ariadnae* (Bolzern, Burckhardt and Hänggi 2013: 769, fig 14R, 16M); (3) A pointed, triangular VPC (Figs 1, 8), trapezoid in *T. ariadnae*

Figures 8–12. *Tegenaria lazarovi* sp. nov. Male holotype (**8–10**). Palp ventral (**8**), palp retrolateral (**9**), palp dorsal (**10**). Female paratype (**11, 12**). Epigyne ventral (**11**), vulva dorsal (**12**) Scale bars: 1.0 mm.

(Bolzern, Burckhardt and Hänggi 2013:769, fig 14Q); the females of the two species can be separated by (4) the trapezoid epigynal median plate (MPE) with a broader distal part in *Tegenaria lazarovi* sp. nov. (Figs 5, 11), which in *T. ariadnae* is broader in the basal part (Bolzern, Burckhardt and Hänggi 2013:769, fig 14S); (5) The copulatory openings are perpendicular to the MPE and positioned to its distal part (Figs 5, 11) while in *T. ariadnae* they are horizontal, positioned much higher (Bolzern, Burckhardt and Hänggi 2013: 769, fig 14S); (6) The receptacles are larger, kidney-shaped (Figs 6, 12) while being smaller and more oval in *T. ariadnae* (Bolzern, Burckhardt and Hänggi 2013: 769, fig 14T, 16D).

Description. Male. Measurements. Total length (including spinnerets) 7.66; carapace length 3.23, width 2.50; chelicerae length 1.43; clypaeus height 0.22; eye diam-

Figures 13–18. *Tegenaria vallei* Brignoli, 1972 (**13–17**) Male holotype (**13–15**) palp ventral (**13**) palp retrolateral (**14**) palp dorsal (**15**) Female paratype (**16, 17**) epigyne ventral (**16**) vulva dorsal (**17**) *Tegenaria pieperi* Brignoli, 1979 female holotype, epigyne ventral (**18**).

eters AME 0.075, ALE 0.090, PME 0.090, PLE 0.090; AE separated from each other by 0.020, ALE almost touching PLE, PME separated from each other by 0.14 and from PLE by 0.080; abdomen length 4.43 (including spinnerets), width 2.05; Leg measurements I 20.71 (1.65, 5.55, 1.13, 4.80, 4.80, 2.40), II 16.96 (1.50, 4.13, 1.25, 3.75, 4.15, 2.18), III 15.79 (1.45, 3.75, 1.13, 3.45, 3.90, 2.10); IV 22.55 (1.58, 4.88, 1.13, 4.60, 5.40, 2.48). Leg spination typical for the genus. Coloration (Fig. 4). Carapace light brown to yellow, darker in the anterior half, gradually lightening posteriorly. Chelicerae light brown. Legs I, II light brown, legs III, IV yellow. Sternum without pattern, yellow in the center, gradually darkening to light brown at the edges. Palpal femur light brown, other segments gradually lightening, yellowish. Abdomen white, without pattern. Other somatic characters. Chelicerae with 2–3 promarginal and 5 retromarginal teeth. All trochanters straight. Colulus is a single trapezoid plate, slightly notched in the middle of the distal part. Palp (Figs 1–3, 8–10). Femur length 1.80; pa-

tella length 0.60; tibia length 2.03; cymbium length 2.93. Tibia with short retrolateral apophysis with dorsal and lateral branches. Dorsal branch (DBTA) claw-shaped with sharp end. Lateral one (LBTA) rounded, less chitinized, whitish, surrounded by a light brown more sclerotized strip (Figs 2, 3, 9, 10). Cymbium long and narrow with a slight depression dorsally (Figs 2, 9). Embolus comparatively long and thin, originating at 9 o'clock and ending at 2 o'clock position. Conductor short and broad, distal portion rounded, both dorsal and ventral part of terminal end sharp. MA membranous, long and narrow, ending in a more chitinized plate, situated between the dorsal and ventral part of the conductor's terminal end (Figs 1, 8).

Female. Measurements. Total length (including spinnerets) 8.30; carapace length 3.80, width 2.50; chelicerae length 0.88; clypaeus height 0.29; eye diameters and arrangement as in male; abdomen length 4.50 (including spinnerets) width 2.25; Leg measurements I 19.14 (1.58, 4.50, 1.13, 5.63, 4.50, 1.80), II 16.71 (1.58, 4.05, 1.13, 3.90, 3.90, 2.15), III 15.41 (1.50, 3.60, 1.13, 3.38, 3.90, 1.90); IV 22.81 (1.73, 4.80, 1.13, 4.65, 5.25, 2.25). Leg spination typical for the genus. Female palpal tibia with 2 dorsal and 2 prolateral spines. Coloration (Fig 7). Carapace, chelicerae and sternum as in male. All legs yellow. Palpal femur, patella and tibia yellow, tarsus light brown. Abdomen whitish to light gray, darker than in male, without pattern. Median plate of epigyne light brown, framed laterally by dark brown spots. Other somatic characters. Chelicerae with 3 promarginal and 5 retromarginal teeth. All trochanters straight. Colulus is a single trapezoid plate, slightly notched in the middle of the distal part. Epigyne and vulva (Figs 5, 6, 11, 12). Width 0.98. Epigynal median plate trapezoid, with M-shaped base, broader in the distal part. Copulatory openings vertical, situated on both sides of the median plate (Figs 5, 11). Posterior sclerite absent. Receptacles large and oval (Figs 6, 12).

Distribution. Known only from the type locality in southern Turkey.

Remarks. Two *Tegenaria* species known from Crete, namely *Tegenaria pieperi* Brignoli, 1979 and *Tegenaria schmalfussi* Brignoli,1976 are also similar to *T. ariadnae* and *T. lazarovi* sp. nov. *Tegenaria pieperi* Brignoli, 1979 is known only by the female which differs from *T. lazarovi* sp. nov. by the rectangular MPE and the smaller and much higher positioned receptacles (Fig 18). The male of *T. schmalfussi* differs from *T. lazarovi* sp. nov. by the lack of VPC and the smaller DBTA and LBTA (Bosmans et al. 2013, figs 50–52); the female can be distinguished by the smaller MPE and different shape of the receptacles (Bosmans et al. 2013, figs 53–54). I would include in this species complex also *Tegenaria vallei* Brignoli, 1972, known from a cave near Benghazi, Libya. Its male can be distinguished by having conductor with entirely missing VPC (Fig. 13) and different DBTA and LBTA (Figs 14, 15). The female differs by the oval MPE (Fig. 16) and the longer receptacles (Fig. 17). The *T. ariadnae* species-complex has a typical Eastern Mediterranean distribution with three species known from Crete, one from northern Libya and one from southern Turkey (Fig 19). It is interesting that *T. lazarovi* sp. nov. appears more closely related to species inhabiting Crete and northern Libya than to any of the *Tegenaria* species known from the Turkish mainland. However, the current knowledge of the spider fauna of the easternmost Mediterranean (especially in north-eastern Africa) is insufficient to provide an explanation for this observation.

Figure 19. Distribution of the *Tegenaria ariadnae* species-complex.

Acknowledgements

References

Bolzern A, Burckhardt D, Hänggi A (2013) Phylogeny and taxonomy of European funnel-web spiders of the *Tegenaria-Malthonica* complex (Araneae: Agelenidae) based upon morphological and molecular data. Zoological Journal of the Linnean Society 168: 723–848. https://doi.org/10.1111/zoj.12040

Bosmans R, Van Keer J, Russell-Smith A, Kronestedt T, Alderweireldt M, Bosselaers J, De Koninck H (2013) Spiders of Crete (Araneae). A catalogue of all currently known species

from the Greek island of Crete. Nieuwsbrief van de Belgische Arachnologische Vereniging 28(1): 1–147.

Brignoli PM (1972a) Una nuova *Tegenaria* cavernicola della Cirenaica (Araneae, Agelenidae). Fragmenta Entomologica 8(3): 157–160.

Brignoli PM (1972b) Terzo contributo alla conoscenza dei ragni cavernicoli di Turchia (Araneae). Fragmenta Entomologica 8: 161–190.

Brignoli PM (1976) Ragni di Grecia IX. Specie nuove o interessanti delle famiglie Leptonetidae, Dysderidae, Pholcidae ed Agelenidae (Araneae). Revue Suisse de Zoologie 83(3): 539–578. https://doi.org/10.5962/bhl.part.91452

Brignoli PM (1977) Ragni di Grecia X. Nuovi dati sulla Grecia continentale ed insulare (Araneae). Revue Suisse de Zoologie 84: 937–954. https://doi.org/10.5962/bhl.part.91369

Brignoli PM (1978a) Ragni di Turchia IV. Leptonetidae, Dysderidae ed Agelenidae nuovi o interessanti di grotte della Turchia meridionale (Araneae). Quaderni di Speleologia, Circolo Speleologico Romano 3: 37–54.

Brignoli PM (1978b). Ragni di Turchia V. Specie nuove o interessanti, cavernicole ed epigee, di varie famiglie (Araneae). Revue Suisse de Zoologie 85(3): 461–541. https://doi.org/10.5962/bhl.part.82243

Brignoli PM (1979) Ragni di Grecia XI. Specie nuove o interessanti, cavernicole ed epigee. Revue Suisse de Zoologie 86(1): 181–202. https://doi.org/10.5962/bhl.part.82285

Brignoli PM (1984) Ragni di Grecia XII. Nuovi dati su varie famiglie (Araneae). Revue Suisse de Zoologie 91(2): 281–321. https://doi.org/10.5962/bhl.part.81881

Demir H, Seyyar O (2017) Annotated Checklist of the Spiders of Turkey. Munis Entomology and Zoology 12(2): 433–469.

Koch CL (1837) Übersicht des Arachnidensystems. C. H. Zeh'sche Buchhandlung, Nürnberg, Heft 1, 1–39. https://doi.org/10.5962/bhl.title.39561

Latreille PA (1804) Tableau methodique des Insectes. Nouveau Dictionnaire d'Histoire Naturelle, Paris 24: 129–295.

Özkütük RS, Elverici M, Kunt KB, Kiliç G (2017) First faunistic record of *Tegenaria vankeerorum* Bolzern, Burckhardt & Hänggi, 2013 (Araneae: Agelenidae) from Turkey with description of unknown female. Biological Diversity and Conservation 10(3): 178–183.

Topçu A, Demircan N (2018) New records of family Agelenidae for the spider fauna of Turkey (Araneae: Agelenidae). Indian Journal of Arachnology 6(2017): 20–22.

WSC (2020) World Spider Catalog. Version 21.0. Natural History Museum Bern. http://wsc.nmbe.ch [accessed on 08 March 2020]

RESEARCH ARTICLE

A peer-reviewed open-access journal
ZooKeys
Launched to accelerate biodiversity research

Seven new species of spider-attacking *Hymenoepimecis* Viereck (Hymenoptera, Ichneumonidae, Pimplinae) from Ecuador, French Guiana, and Peru, with an identification key to the world species

Diego Galvão de Pádua[1], Ilari Eerikki Sääksjärvi[2],
Ricardo Ferreira Monteiro[3], Marcio Luiz de Oliveira[1]

1 *Programa de Pós-Graduação em Entomologia, Instituto Nacional de Pesquisas da Amazônia, Av. André Araújo, 2936, Petrópolis, 69067-375, Manaus, Amazonas, Brazil* **2** *Biodiversity Unit, Zoological Museum, University of Turku, FIN-20014, Turku, Finland* **3** *Laboratório de Ecologia de Insetos, Depto. de Ecologia, Universidade Federal do Rio de Janeiro, Av. Carlos Chagas Filho, 373, Cidade Universitária, Ilha do Fundão, 21941-971, Rio de Janeiro, Rio de Janeiro, Brazil*

Corresponding author: Diego Galvão de Pádua (paduadg@gmail.com)

Citation: Pádua DG, Sääksjärvi IE, Monteiro RF, Oliveira ML (2020) Seven new species of spider-attacking *Hymenoepimecis* Viereck (Hymenoptera, Ichneumonidae, Pimplinae) from Ecuador, French Guiana, and Peru, with an identification key to the world species. ZooKeys 935: 57–92. https://doi.org/10.3897/zookeys.935.50492

Abstract

Seven new species of *Hymenoepimecis* Viereck are described from Peruvian Andes and Amazonia, French Guiana and Ecuador: *H. andina* Pádua & Sääksjärvi, **sp. nov.**, *H. castilloi* Pádua & Sääksjärvi, **sp. nov.**, *H. dolichocarinata* Pádua & Sääksjärvi, **sp. nov.**, *H. ecuatoriana* Pádua & Sääksjärvi, **sp. nov.**, *H. longilobus* Pádua & Sääksjärvi, **sp. nov.**, *H. pucallpina* Pádua & Sääksjärvi, **sp. nov.**, and *H. rafaelmartinezi* Pádua & Sääksjärvi, **sp. nov.** In addition, the male of the *Hymenoepimecis kleini* Pádua & Sobczak, 2015 is described, new faunistic records for the genus provided, as well as an illustrated identification key to all known species of the genus.

Introduction

Hymenoepimecis Viereck, 1912 is a moderately large genus of spider-attacking Darwin wasps. It is confined to the New World where it occurs from Mexico and Central America to Southern Brazil (Gauld 1991; Kumagai and Graf 2002; Yu et al. 2012; Pádua et al. 2015).

The species of *Hymenoepimecis* are known to be koinobiont ectoparasitoids attacking sub-adult and adult orb-web-spinning spiders belonging to the families Araneidae and Tetragnathidae (summarised in Pádua et al. 2016). *Hymenoepimecis* is closely related to *Acrotaphus* Townes and *Ticapimpla* Gauld and it can be easily separated from these two genera by possessing a pocket-like structure on the mediodorsal part of the pronotum (Gauld 1991).

Currently, there are 20 described species in the genus (Yu et al. 2012; Pádua et al. 2015) and the majority of them have been discovered from Brazil (Brullé 1846; Kriechbaumer 1890; Loffredo and Penteado-Dias 2009; Sobczak et al. 2009; Pádua et al. 2015) and Central America (see Cresson 1865; Brues and Richardson 1913; Townes and Townes 1966; Gauld 1991, 2000). Very little is known about the occurrence of the genus in other Latin American countries. The main aim of this work is to describe seven new species of *Hymenoepimecis* from Peru, French Guiana and Ecuador. In addition, we provide new faunistic records for the genus and an illustrated identification key to all species.

Materials and methods

The specimens studied in this work are deposited at the Florida State Collection of Arthropods (**FSCA**), Gainesville, USA, The Natural History Museum, University of San Marcos (**MUSM**), Lima, Peru, The Natural History Museum, London, UK (**NHM**), and the Biodiversity Unit, Zoological Museum, University of Turku (**ZMUT**), Turku, Finland. The specimens of MUSM are currently on loan in ZMUT.

Specimens were examined with an Olympus SZ61 and SZX10 stereomicroscopes and measurements were made through a millimetre ocular. Digital layer images were taken using a Canon DS126461 digital camera attached to an Olympus SZX16 stereomicroscope and combined by using the software Zerene Stacker (Version 1.04 Build T201706041920). Drawings were vectorized digitally using Adobe Illustrator.

The morphological terminology and style of descriptions follow those of Pádua et al. (2015). In this study, the measures and proportions between the structures are given as the value of the holotype [in brackets], followed by the minimum and maximum number of variations. The new country records of the genus are marked with a double asterisk and new country records of the species were marked with a single asterisk. The maps were produced through the website Simplemappr (https://www.simplemappr.net).

Key to the world species of Hymenoepimecis

[The female of the *H. cameroni* and males of *H. amazonensis*, *H. atriceps*, *H. castilloi* sp. nov., *H. heidyae*, *H. heteropus*, *H. jordanensis*, *H. neotropica*, *H. pucallpina* sp. nov., *H. silvanae*, and *H. sooretama* are unknown].

1 Female; ovipositor projecting conspicuously beyond the apex of metasoma.....**2**
– Male **27**
2 Face sculptured below the insertion of antennae, with a longitudinal carina in the middle (Figs 7, 12, 15); head with occipital carina projected, not curved upwards, with a dorsal concavity in the apex (Figs 22, 27, 30); pronotum with a pocket-like structure reduced longitudinally (Figs 22, 27, 30); sternite I with a spine-like ventral projection posteriorly (Figs 52, 57, 60)................
....(**H. jordanensis** species group) **3**
– Face not sculptured below the insertion of antennae, without a longitudinal carina in the middle (Figs 1–6, 8–11, 13, 14); head with occipital carina projected and curved upwards, without a dorsal concavity in the apex (Figs 16–21, 23–26, 28, 29); pronotum with the pocket-like structure not reduced longitudinally (Figs 31–36, 38–41, 43, 44); sternite I with a low, rounded swelling posteriorly (Figs 31–36, 38–41, 43, 44) or with a high, laterally compressed, nasute ventral protuberance (Fig. 47) **7**
3 Wing bicoloured (blackish, with one yellowish hyaline band) (Fig. 75) or fore wing yellowish, with two blackish bands (Fig. 72) **4**
– Wing monocoloured (hyaline, without band(s)) (Fig. 67) **5**
4 Fore wing blackish, with a yellowish hyaline preapical band; hind leg black, with base of coxa orange (Fig. 75) ....**H. uberensis** Pádua & Onody, 2015
– Fore wing hyaline yellowish, with apex blackish and with a blackish preapical band; hind leg orange with femur, tibia and tarsus blackish brown (Fig. 72)...
....**H. rafaelmartinezi** sp. nov.
5 Metasoma darkish brown, with whitish lateral marks on anterior margins of tergites II–V (e.g., Fig. 61) ....**H. jordanensis** Loffredo & Penteado-Dias, 2009
– Metasoma orange, with blackish marks on posterior margins in some tergites (Fig. 67)..**6**
6 Tarsal claw with a flat preapical tooth, apex of claw 3.0 times the length of the tooth (Fig. 82) .... **H. kleini** Pádua & Sobczak, 2015
– Tarsal claw with a short basal lobe vertically, more or less square, apex of claw clearly overtaking the lobe (Fig. 95) ....
.... **H. amazonensis** Pádua & Oliveira, 2015
7 Epicnemial carina present (Figs 34, 44, 96A) **8**
– Epicnemial carina absent (Figs 31–33, 35–43, 45)...................................**10**
8 Fore wing black (Fig. 92); submetapleural carina present (Fig. 96B) ....
....**H. argyraphaga** Gauld, 2000
– Fore wing hyaline (Figs 61, 63, 64, 69, 74); submetapleural carina absent.... **9**

9   Mesosoma entirely orange (Fig. 34); metasoma orange, with posterior margins of tergites II–IV narrowly black, tergites V+ black (Fig. 64)...................
         ....***H. dolichocarinata* sp. nov.**
–   Mesosoma orange, with propleuron, pronotum, dorsal half of metapleuron and propodeum blackish; metasoma entirely blackish (Fig. 74)....................
         ....***H. tedfordi* Gauld, 1991**
10   Sternite with a high, nasute ventral protuberance (Fig. 47) **11**
–   Sternite I with a low, rounded swelling posteriorly (Figs 46, 48–51, 53–56, 58, 59)..**13**
11   Fore wing yellowish hyaline, with black apex (Fig. 62)....................................
         ....***H. bicolor* (Brullé, 1846)**
–   Fore wing hyaline (sometimes with apex slightly blackish) (Figs 61, 63, 64, 69, 74)..**12**
12   Hind leg black, except base of coxa orange.............***H. heidyae* Gauld, 1991**
–   Hind leg orange, with distal 0.5 of tibia and tarsus blackish (Fig. 93) ....
         ....***H. robertsae* Gauld, 1991**
13   Wing monocoloured (hyaline or yellowish hyaline or blackish) (Figs 61, 63, 64, 69, 74, 91, 92)...**14**
–   Wing bicoloured (with one band or two bands) (Figs 65, 66, 68, 70, 71) ....
         .... **20**
14   Metasoma reddish brown..**15**
–   Metasoma mainly darkish brown to black or orange (Figs 61–75) **16**
15   Fore wing hyaline (e.g., Fig. 92)....................... ***H. atriceps* (Cresson, 1865)**
–   Fore wing blackish, with pterostigma yellow (Fig. 91)....................................
         ....***H. veranii* Loffredo & Penteado-Dias, 2009**
16   Metasoma entirely black, tergites without whitish anterior margin (Fig. 63)....
         .... ***H. castilloi* sp. nov.**
–   Metasoma blackish or darkish brown, some tergites with whitish anterior margin (e.g., Fig. 61) or metasoma orange, some tergites with posterior margin blackish (Fig. 69) **17**
17   Metasoma blackish or blackish brown, some tergites with anterior margin whitish (e.g., Figs 61)..**18**
–   Metasoma orange, some tergites with posterior margin blackish (Fig. 69)....**19**
18   Occipital carina only slightly projected (Figs 31, 33); ovipositor < 1.2 times as long as hind tibia ....***H. andina* sp. nov.**
–   Occipital carina clearly projected (e.g., Figs 32, 38); ovipositor > 1.4 times as long as hind tibia ....***H. sooretama* Sobczak et al., 2009**
19   Posterior ocelli separated from eyes by 0.4 times its own maximum diameter, in dorsal view; fore wing fuscous (see Sobczak et al. 2009); ovipositor 0.9 times as long as hind tibia; hind leg brownish, except base of coxa orange ....
         ....***H. japi* Sobczak et al., 2009**
–   Posterior ocelli separated from eyes by 0.6–0.8 times its own maximum diameter, in dorsal view; fore wing hyaline; ovipositor 1.1–1.3 times as long as

hind tibia; hind leg orange, with femur, tibia and tarsus blackish (Figs 69) ...
....***H. manauara* Pádua & Oliveira, 2015**

20   Fore wing blackish, with a yellowish band more or less in median region
(Fig. 71)...**21**

–   Fore wing yellowish hyaline, with two black bands (Figs 65, 66, 68).........**22**

21   Occipital carina reduced in dorsal part (Fig. 43); metasoma orange, with ter-
gites VI+ black (Fig. 73)......................***H. ribeiroi* Pádua & Sobczak, 2015**

–   Occipital carina not reduced in dorsal part (Fig. 41); metasoma entirely black
(Fig. 71)... ***H. pucallpina* sp. nov.**

22   Tarsal claw with a preapical tooth (Fig. 85)...
.... ***H. neotropica* (Brues & Richardson, 1913)**

–   Tarsal claw with a longitudinally elongated lobe or with a square lobe
(Figs 76–81, 83, 84, 86–90) **23**

23   Tarsal claw with a longitudinally elongated lobe (Fig. 83) ....
....***H. longilobus* sp. nov.**

–   Tarsal claw with a more or less square lobe (Figs 76–81, 84, 86–90) **24**

24   Metasoma black, with tergite I orange (Fig. 94) ....
....***H. heteropus* (Kriechbaumer, 1890)**

–   Metasoma entirely brownish orange or orange, with posterior tergites black-
ish (Figs 65, 66, 68, 70)...**25**

25   Metasoma brownish orange or ferruginous (see Loffredo & Penteado-Dias
2009)....................................***H. silvanae* Loffredo & Penteado-Dias, 2009**

–   Metasoma orange, with posterior tergites blackish (Figs 65, 66, 68, 70)....**26**

26   Ovipositor > 1.5 times as long as hind tibia; pronotum black (in general)
(Fig. 35)...***H. duckensis* Pádua & Onody, 2015**

–   Ovipositor < 1.3 times as long as hind tibia; pronotum orange (Fig. 36).......
....***H. ecuatoriana* sp. nov.**

27   Face sculptured below the insertion of antennae, with a longitudinal carina
in the middle part (Figs 7, 12, 15); head with occipital carina projected,
not curved upwards, with a concavity dorsally in the apex (Figs 22, 27, 30);
pronotum with the pocket-like structure reduced longitudinally (Figs 22, 27,
30); sternite I with a spine-like ventral projection posteriorly (Figs 52, 57,
60)...(***H. jordanensis* species group) 28**

–   Face not sculptured below the insertion of antennae, without a longitudinal
carina in the middle part (Figs 1–6, 8–11, 13, 14); head with occipital ca-
rina projected and curved upwards, without a concavity in the apex dorsal
(Figs 16–21, 23–26, 28, 29); pronotum with the pocket-like structure not
reduced longitudinally (Figs 31–36, 38–41, 43, 44); sternite I with a low,
rounded swelling posteriorly (Figs 31–36, 38–41, 43, 44) or with a high,
laterally compressed, nasute ventral protuberance (Fig. 47) **30**

28   Fore wing hyaline (Fig. 103) .... ***H. kleini* Pádua & Sobczak, 2015**

–   Fore wing blackish, with one yellowish hyaline band (Fig. 106) or fore wing
yellowish, with two blackish bands (Figs 100, 102, 104)............................**29**

29   Fore wing blackish, with yellowish hyaline band between junction of vein R1 up to pterostigma until half vein M; hind leg black, with base of coxa orange (Fig. 106)..***H. uberensis* Pádua & Onody, 2015**
–   Fore wing hyaline yellowish, with apex distal to 2rs-m blackish, and with a blackish median band extending backwards from anterior margin, to veins Rs+M and junction of pterostigma with vein R1; hind leg orange with femur, tibia and tarsus blackish brown (Fig. 104) ....
....***H. rafaelmartinezi* sp. nov.**
30   Epicnemial carina present (Figs 34, 44, 96) **1**
–   Epicnemial carina absent (Figs 31–33, 35–43, 45).....................................**34**
31   Fore wing hyaline (Figs 97, 99, 101, 103)...**32**
–   Fore wing blackish (Fig. 92)..**33**
32   Mesosoma entirely orange; metasoma orange, with posterior margins of tergites II–IV narrowly black, tergites V+ black (Fig. 99); margin of the gena flat behind the eyes (Fig. 19)....................................***H. dolichocarinata* sp. nov.**
–   Mesosoma orange, with pronotum, metapleuron and propodeum blackish; metasoma entirely black (Fig. 74); margin of gena strongly narrowed behind eyes (see female in Fig. 29).....................................***H. tedfordi* Gauld, 1991**
33   Submetapleural carina present (Fig. 96B).......***H. argyraphaga* Gauld, 2000**
–   Submetapleural carina absent............................ ***H. cameroni* Townes, 1966**
34   Sternite I with a high, laterally compressed ventral protuberance (Fig. 47) **35**
–   Sternite I with a low, rounded swelling posteriorly (Figs 46, 48–51, 53–56, 58, 59)..**36**
35   Fore wing yellowish hyaline, with black apex; hind leg orange, with femur, tibia and tarsus black (Fig. 98) .... ***H. bicolor* (Brullé, 1846)**
–   Fore wing hyaline (sometimes with apex slightly blackish) (e.g., Figs 99, 101); hind leg orange, with 0.5 distal of tibia and tarsus blackish (Fig. 93) ....
....***H. robertsae* Gauld, 1991**
36   Wing bicoloured (with one band or two bands) (Figs 100, 102, 104).......**37**
–   Wing monocoloured (hyaline or yellowish hyaline or fuscous or blackish) (Figs 91, 97, 99) **39**
37   Fore wing blackish, with one yellowish band in median region (sometimes fore wing with base yellowish) (Fig. 105); occipital carina reduced in dorsal part (Fig. 43) ....***H. ribeiroi* Pádua & Sobczak, 2015**
–   Fore wing yellowish, with two black bands (Figs 100, 102, 104); occipital carina not reduced in dorsal part (Figs 35, 38, 40); metasoma blackish (Fig. 97)..**38**
38   Pronotum entirely black or orange, with anterior region black (Fig. 100) .....
....***H. duckensis* Pádua & Onody, 2015**
–   Pronotum entirely orange (the Peruvian specimens have anterior margin of pronotum blackish) (Fig. 102) ....***H. longilobus* sp. nov.**
39   Fore wing blackish, with pterostigma yellow (Fig. 91)...................................
....***H. veranii* Loffredo & Penteado-Dias, 2009**
–   Fore wing hyaline (Figs 99, 101, 103)...**40**

40   Occipital carina only slightly projected and not curved upwards dorsally (Figs 16, 31); metasoma darkish brown, with whitish lateral marks on anterior margins of tergites II–V (Fig. 97) ....***H. andina* sp. nov.**
–   Occipital carina clearly projected and curved upwards dorsally (Figs 24, 39); metasoma orange, with some tergites with posterior margins black (Fig. 103)...**41**
41   Posterior ocelli separated from eyes by more or less 0.4 times its own maximum diameter, in dorsal view; fore wing fuscous (see Sobczak et al. 2009); hind leg brownish, except base of coxa orange ....***H. japi* Sobczak et al., 2009**
–   Posterior ocelli separated from eyes by 0.6–0.8 times its own maximum diameter, in dorsal view; fore wing hyaline (Fig. 24); hind leg orange, with femur, tibia and tarsus blackish (there are specimens with femur basal half orange and apical half blackish or femur orange with apex blackish) (Fig. 103).........
        ....***H. manauara* Pádua & Oliveira, 2015**

Faunistics and taxonomy

Hymenoepimecis Viereck, 1912
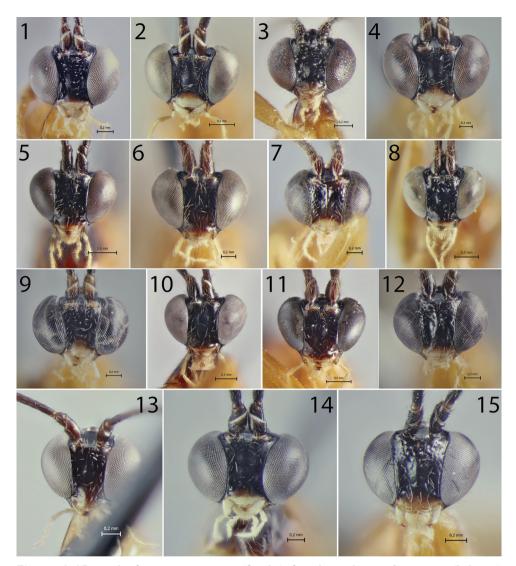
Epimecis Brullé, 1846: 112. Type-species: *Epimecis bicolor* Brullé, by subsequent designation; Ashmead, 1900: 54.
Hymenoepimecis Viereck, 1912: 149. [Replacement name for *Epimecis* Brullé, 1846, junior homonym of *Epimecis* Hübner, 1825]

Comments. According to Gauld (1991, 2000) *Hymenoepimecis* is very similar with the sister genus *Acrotaphus* Townes, 1960. They both have the occipital carina strongly raised (flange-like) and projecting posteriorly to surround the anterior reflexed end of the pronotum; head rounded with the genae strongly narrowed from the eyes to the occipital flange; and the pronotum unusually elongated, with a long horizontal part mediodorsally. It differs from *Acrotaphus* by having a unique forwardly directed pocket-like structure on the pronotum mediodorsally.

Hymenoepimecis andina Pádua & Sääksjärvi, sp. nov.
http://zoobank.org/98DE0A8A-6E2D-4B2C-BD1D-1C0416E067D1
Figures 1, 16, 31, 46, 61, 76, 97

Diagnosis. This species can be distinguished from all other *Hymenoepimecis* by the combination of the following characters: 1) head, in dorsal view, with gena short and slightly convex behind eyes; 2) posterior ocelli separated from eyes by 0.7–0.8 times its own maximum diameter; 3) occipital carina only slightly projected and not curved upwards dorsally; 4) ovipositor 1.1–1.2 times as long as hind tibia; 5) metasoma darkish brown, with whitish lateral marks on anterior margins of tergites II–V.

Figures 1–15. Heads of *Hymenoepimecis* spp. (females), frontal view **1** *H. andina* sp. nov. (holotype) **2** *H. bicolor* **3** *H. castilloi* sp. nov. (holotype) **4** *H. dolichocarinata* sp. nov. (holotype) **5** *H. duckensis* **6** *H. ecuatoriana* sp. nov. (holotype) **7** *H. kleini* **8** *H. longilobus* sp. nov. (holotype) **9** *H. manauara* **10** *H. neotropica* **11** *H. pucallpina* sp. nov. (holotype) **12** *H. rafaelmartinezi* sp. nov. (holotype) **13** *H. ribeiroi* **14** *H. tedfordi* **15** *H. uberensis.*

Description. Female. Body approx. [8.0] 7.0–8.5 mm; face [0.8] times as broad as high, smooth, slightly convex with few spaced bristles laterally; head in dorsal view, with gena short and slightly convex behind eyes; posterior ocelli separated from eyes by approx. [0.7] 0.7–0.8 times its own maximum diameter; occipital carina lit-

tle projected and not curved upwards dorsally. Pronotum more or less long, smooth and polished, with distance from tegula to head greater than [0.5] 0.5–0.6 times distance from tegula to hind margin of propodeum, and in anterior part with opening pocket-like structure not reduced longitudinally; mesoscutum smooth and polished; scutellum, in profile, convex; mesopleuron smooth and polished, with anterodorsal and posterodorsal parts bearing sparse, fine setiferous punctures; metapleuron smooth and polished, with few sparse, fine setiferous punctures; propodeum smooth, polished, with sparse, fine setiferous punctures and with lateral longitudinal carina present only posteriorly. Fore wing approx. [6.0] 6.0–7.0 mm; cu-a more or less interstitial to the base of Rs&M; 2rs-m approx. [0.3] 0.3–0.5 times as long as abscissa of M between 2rs-m and 2m-cu; hind wing with abscissa of Cu1 meet cu-a equidistant between 1A and M. Hind leg with tibia + tarsus [0.6] times fore wing length; tarsal claw with more or less square basal lobe with apex of claw slightly overtaking the lobe. Metasoma slender; tergite I [1.7] 1.6–1.7 times as long as posteriorly width, centrally quite strongly convex with lateral carinae present only at extreme anterior end flanking the anterior concavity; sternite I with a low, rounded swelling posteriorly; tergite II approx. [1.4] 1.3–1.4 times as long as posteriorly width; tergites III and IV approx. [1.2] 1.2–1.3 times as long as posteriorly width; ovipositor [1.1] 1.1–1.2 times as long as hind tibia.

Colour. Head black with apical margin of clypeus and mouthparts (except apex mandible black) yellowish; antenna blackish. Mesosoma orange. Fore and mid leg orange, the hind leg black. Wings hyaline slightly darkish; pterostigma brownish. Metasoma darkish brown, with whitish lateral marks on anterior margins of tergites II–V; ovipositor brownish with base and apex whitish, sheath blackish.

Male. (Fig. 97). Similar to female in structure and colouration, but with body with 6.0–8.0 mm; face approx.1.1 times as width as high; posterior ocelli separated from eyes by 0.7–0.9 times its own maximum diameter. Fore wing 4.5–6.5 mm. Tarsal claw simple. Metasoma slender; tergite I 1.6 times as long as posteriorly width; tergite II approx.1.4 times as long as posteriorly width; tergites III and IV 1.2–1.3 times as long as posteriorly width.

Distribution. Peru (Andes) (Fig. 107).

Biological notes. Host unknown.

Etymology. The specific name refers the locality of the specie type, in the Peruvian Andes, Cusco Peru.

Type material. *Holotype* ♀. Peru, Cusco, San Pedro, 13°02'58"S, 71°32'13"W, 1500 m., 20.ix.2007, Malaise trap (C. Castillo leg.), MUSM. *Paratypes:* idem holotype, 4♂♂ and 2♀♀, MUSM; idem, but 23.vii.2007, 3♂♂, MUSM; idem, but 13°03'22"S, 71°32'55"W, 1520 m., 25.vii.2007, 1♀, MUSM; idem, but Cosñipata valley, 13°03'11"S, 71°32'08"W, 1302 m., 1♀, ZMUT; idem, but 13°03'23"S, 71°32'55"W, 24.x.2007, 1♀, ZMUT.

Comments. *Hymenoepimecis andina* sp. nov. closely resembles *H. tedfordi* Gauld, 1991 and *Hymenoepimecis castilloi* sp. nov., mainly by having hyaline fore wing and

darkish metasoma. It differs from both by having metasoma with whitish lateral marks on anterior margins of tergites II–V and propodeum orange (metasoma without whitish marks and propodeum black in other two species).

Hymenoepimecis bicolor (Brullé, 1846)
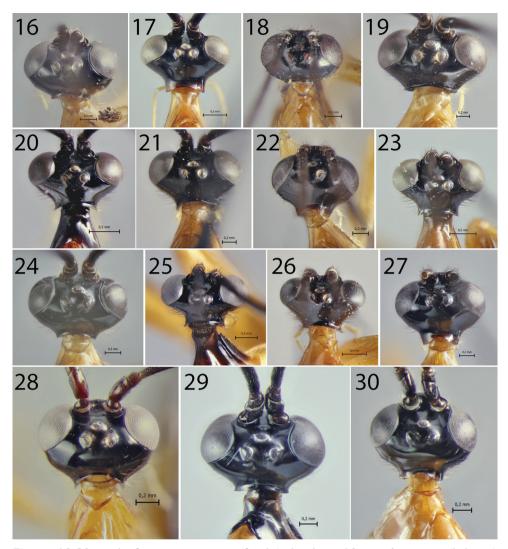Figures 2, 17, 32, 47, 62, 77, 98

Epimecis bicolor Brullé, 1846: 113.
Hymenoepimecis bicolor (Brullé): Viereck, 1912: 149.

Diagnosis. See Pádua et al. (2015).

Distribution. Brazil, Ecuador** and Peru* (Fig. 108).

Biological notes. Parasitoid of *Trichonephila clavipes* (Linnaeus, 1767) (as *Nephila clavipes*) (Araneae: Araneidae) (Gonzaga et al. 2010).

Material examined. Ecuador: Dept. Orellana, Tiputini, 00°37'55"S, 76°08'39"W, a.s.l.: 220–250 m., 5.vii.1998, Fogging (T.L. Erwin et al. leg.), Lot #1894, 1♂, ZMUT; idem, but Onkonegare, 00°39'25"S, 76°27'10,8"W, a.s.l.: 216.3 m., 6.vii.1995, Lot #1129, 1♂, ZMUT. Peru: Dept. of Loreto, Iquitos area, Allpahuayo, 17.x–8.xi.2000, Malaise trap, clay (I.E. Sääksjärvi et al. leg.), APHI, H1/15, 1♀, ZMUT; idem, but 11–29.vi.2000, APHI, H1/8, 1♀, ZMUT; idem, but 14.ix–4.x.2000, APHI, H1/13, 1♀, ZMUT; idem, but 24.iii–16.iv.2000, white sand, APHI, G1/4, 1♀, ZMUT; idem, but 19.ix–4.x.2000, APHI, I1/13, 1♂, ZMUT; idem, but 24.i–20.ii.2000, APHI, G1/1, 1♀, ZMUT; idem, but 8–24.iii.2000, APHI, G2/3, 1♀, ZMUT; idem, but 22.v–11.vi.2000, APHI, 1♀ ZMUT; idem, but 20.ii–8.iii.2000 APHI, 1♀, ZMUT; idem, but iv.2011 (Gómez & Sääksjärvi leg.), 1♀, ZMUT; idem, but 30°57'49"S, 73°24'93"W, 1♀, ZMUT; idem, but 7–13.xi.2011, 1♀, ZMUT; idem, but 11–20.xi.2011, 1♀, ZMUT; idem, but 31.x–6.xi.2011, 1♀, ZMUT; idem, but 14–20.xi.2011, 1♀, ZMUT; 31.x–6.xi.2011, 1♀, ZMUT; idem, but 14–20.xi.2011, 1♀, ZMUT; idem, but 24–30.x.2011, 1♀, ZMUT; idem, but 3–9.x.2011, 1♀, ZMUT; 10–16.x.2011, 1♀, ZMUT; Alto Nanay, Albarenga north, 172 m., 18M 0532618E/ 9645753N, 17.xi.2008 (C. Castillo leg.), 1♂, ZMUT; idem, but Rio Copaluacu, 3°42'59"S, 75°26'0"W, 8.xii.2009, Malaise trap, 165 m. (L. Sulca leg.), 1♀, ZMUT; Dept. Madre de Díos, Los Amigos, 24–31.vii.2008, E: 380792, 164/N: 8610919,14, Malaise trap, a.s.l.: 280.5 (I. Gómez leg.), 1♂, ZMUT; idem, but Tambopata, Explore's inn, 12°50'30"S, 69°17'31"W, 6.vii.2009, Malaise trap, 161 m. (M. Alvarado leg.), 1♀, ZMUT; Cusco, Reserva Comunal Amarakaeri, 12°55'S, 70°51'W, 333–884 m., 17.ix–14.xi.2010, Malaise trap (M. Vilchez & C. leg.), 1♀ and 2♂♂, ZMUT; idem, but La Convención, Echarate, San Martin Norte, 11°45'18.8"S, 72°42'26"W, 430 msnm, 10–14.xi.2010 (B. Medina & Z. Bravo leg.), 1♂, ZMUT; idem, but Pagoreni Camp., 465m., 11°47'05,4"S, 72°42'03"W, 25.ix.1998, Flight intercept trap, Camisea Project, 1♂, ZMUT; idem, but 23.ix.1998, 3♂♂, ZMUT; idem, but 5.v.1998, 2♂♂, ZMUT.
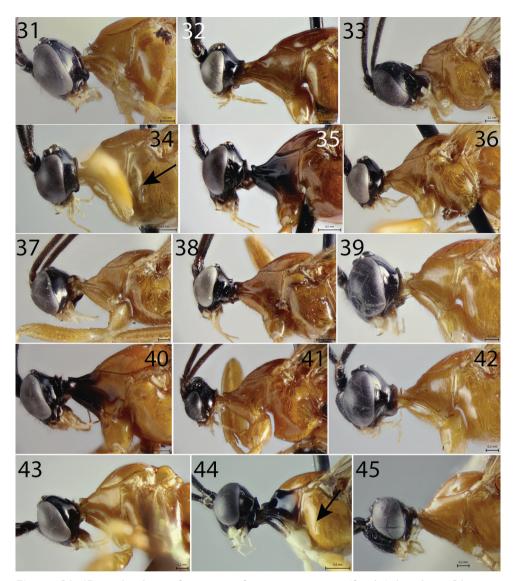
Figures 16–30. Heads of *Hymenoepimecis* spp. (females), dorsal view **16** *H. andina* sp. nov. (holotype) **17** *H. bicolor* **18** *H. castilloi* sp. nov. (holotype) **19** *H. dolichocarinata* sp. nov. (holotype) **20** *H. duckensis* **21** *H. ecuatoriana* sp. nov. (holotype) **22** *H. kleini* **23** *H. longilobus* sp. nov. (holotype) **24** *H. manauara* **25** *H. neotropica* **26** *H. pucallpina* sp. nov. (holotype) **27** *H. rafaelmartinezi* sp. nov. (holotype) **28** *H. ribeiroi* **29** *H. tedfordi* **30** *H. uberensis*.

Hymenoepimecis castilloi **Pádua & Sääksjärvi, sp. nov.**
http://zoobank.org/BE9BBA71-5809-4E5C-AA94-6C59F601E7B0
Figures 3, 18, 33, 48, 63, 78

Diagnosis. This species can be distinguished from all other *Hymenoepimecis* by the combination of the following characters: 1) head in dorsal view with gena short and

Figures 31–45. Head and part of mesosoma of *Hymenoepimecis* spp. (females), lateral view **31** *H. andina* sp. nov. (holotype) **32** *H. bicolor* **33** *H. castilloi* sp. nov. (holotype) **34** *H. dolichocarinata* sp. nov. (holotype), arrow shows the epicnemial carina **35** *H. duckensis* **36** *H. ecuatoriana* sp. nov. (holotype) **37** *H. kleini* **38** *H. longilobus* sp. nov. (holotype) **39** *H. manauara* **40** *H. neotropica* **41** *H. pucallpina* sp. nov. (holotype) **42** *H. rafaelmartinezi* sp. nov. (holotype) **43** *H. ribeiroi* **44** *H. tedfordi*, arrow shows the epicnemial carina **45** *H. uberensis*.

slightly convex behind eyes; 2) posterior ocelli separated from eyes by approx. 0.7 times its own maximum diameter; 3) occipital carina only slightly projected and not curved upwards dorsally; 4) ovipositor 1.1 times as long as hind tibia; 5) mesosoma

orange, with propleuron, metapleuron (except its posterior margin whitish), and propodeum darkish brown; 6) metasoma darkish brown.

Description. Female. Body approx. [6.0] mm; face [0.9] times as broad as high (from supraclypeal suture to base of antenna), smooth, flat with few spaced bristles laterally; head in dorsal view, with gena short and slightly convex behind eyes; posterior ocelli separated from eyes by [0.7] times its own maximum diameter; occipital carina little projected and not curved upwards dorsally. Pronotum as long as high, smooth and polished, with distance from tegula to head greater than approx. [0.7] times distance from tegula to hind margin of propodeum, and in anterior part with opening pocket-like structure not reduced longitudinally; mesoscutum smooth and polished; scutellum, in profile, convex; mesopleuron smooth and polished, with posterodorsal part bearing sparse, fine setiferous punctures; metapleuron smooth and polished, with a few sparse, fine setiferous punctures; propodeum smooth, polished, with sparse, fine setiferous punctures and with lateral longitudinal carina present only posteriorly. Fore wing [5.0] mm; cu-a more or less interstitial to the base of Rs&M; 2rs-m approx. [0.3] times as long as abscissa of M between 2rs-m and 2m-cu; hind wing with abscissa of Cu1 meet cu-a equidistant between 1A and M. Hind leg with tibia + tarsus approx. [0.6] times fore wing length; tarsal claw with more or less square basal lobe with apex of claw slightly overtaking the lobe. Metasoma slender; tergite I [2.0] times as long as posteriorly width, centrally quite strongly convex with lateral carinae present only at extreme anterior end flanking the anterior concavity; sternite I with a low, rounded swelling posteriorly; tergite II approx. [1.4] times as long as posteriorly width; tergites III–IV approx. [1.1] times as long as posteriorly width; ovipositor [1.1] times as long as hind tibia.

Colour. Head black with apical margin of clypeus and mouthparts (except apex of mandible) yellowish; antenna brownish. Mesosoma orange, with propleuron, metapleuron (except its posterior margin whitish), and propodeum darkish brown. Fore and mid leg orange, the hind leg darkish brown. Wings hyaline; pterostigma brownish. Metasoma darkish brown; ovipositor brownish with base and apex whitish, sheath brownish.

Male. Unknown.

Distribution. Peru (Andes) (Fig. 108).

Biological notes. Host unknown.

Etymology. This species is named in honour of Carol Castillo, collector of the type specimen. Carol is a Peruvian entomologist and has studied Darwin wasps in the tropical Andes. She has discovered and/or described a large number of new species.

Type material. *Holotype* ♀. Peru, Cusco, Cosñipata valley, San Pedro, 13°03'23"S, 71°32'55"W, 1520 m., 24.x.2007, Malaise trap (C. Castillo leg.), MUSM.

Comments. *Hymenoepimecis castilloi* sp. nov. closely resembles *H. tedfordi* Gauld, 1991 and *Hymenoepimecis andina* sp. nov., mainly by having fore wing hyaline and metasoma darkish. It differs from *H. tedfordi* by having mesosoma orange, with propleuron, metapleuron (except its posterior margin whitish), and propodeum darkish brown, hind legs entirely brownish and occipital carina short (mesosoma orange, with propleuron, pronotum, dorsal half of metapleuron, and propodeum blackish hind leg with coxa whitish and femur, tibia, and tarsus orange and occipital carina long, in
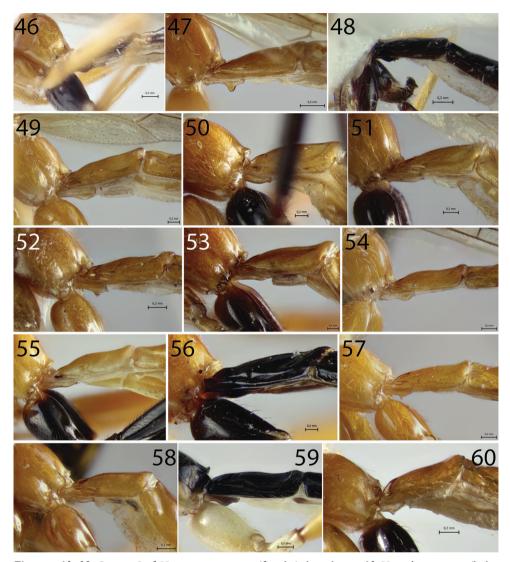
H. tedfordi). It differs from *H. andina* sp. nov. by having mesosoma orange, with propleuron, metapleuron (except its posterior margin whitish) and propodeum darkish brown and metasoma darkish brown without whitish bands anteriorly (propodeum orange and metasoma darkish brown, with whitish lateral marks on anterior margins of tergites II–V in *H. andina* sp. nov.).

Hymenoepimecis dolichocarinata Pádua & Sääksjärvi, sp. nov.
http://zoobank.org/66F48B80-3F42-4EDB-8B3B-DA1D9DB4ABD0
Figures 4, 19, 34, 49, 64, 79, 99

Diagnosis. This species can be distinguished from all other *Hymenoepimecis* by the combination of the following characters: 1) epicnemial carina present ventrally, extending to the level of the lower corner of the pronotum laterally; 2) wings slightly yellowish hyaline; 3) margin of the gena flat behind the eyes; 4) metasoma orange, with posterior margins of tergites II–IV narrowly black, tergites V+ black.

Description. Female. Body approx. [13.0] 11.5–13.0 mm; face [1.0] 0.9–1.0 times as broad as high, smooth, slightly convex with few spaced bristles; head in dorsal view, with margin of gena flat behind eyes; posterior ocelli separated from eyes by approx. [0.6] 0.5–0.6 times its own maximum diameter; occipital carina little projected, slightly curved upwards in the mediodorsal part. Pronotum more or less long, smooth and polished, with distance from tegula to head greater than [0.6] 0.5–0.6 times distance from tegula to hind margin of propodeum, and in anterior part with opening pocket-like structure not reduced longitudinally; mesoscutum smooth and polished; scutellum, in profile, convex; mesopleuron smooth and polished, with anterodorsal and posterodorsal parts bearing sparse, fine setiferous punctures; epicnemial carina present ventrally, extending until reaching the level of lower corner of pronotum laterally; metapleuron smooth and polished, rather uniformly covered with sparse, fine setiferous punctures. Fore wing approx. [10.0] 9.0–11.0 mm; cu-a interstitial to the base Rs&M; 2rs-m approx. [0.6] times as long as abscissa of M between 2rs-m and 2m-cu; hind wing with abscissa of Cu1 meeting cu-a equidistant between M and 1A. Hind leg with tibia + tarsus [0.6] 0.55–0.6 times the fore wing length; tarsal claw with more or less square lobe, with apex slightly overtaking the lobe. Metasoma slender; tergite I [1.6] 1.5–1.6 times as long as posteriorly width, centrally quite strongly convex with lateral carinae present only at extreme anterior end flanking the anterior concavity; sternite I with a low, rounded swelling posteriorly; tergite II [1.4] 1.3–1.4 times as long as posteriorly width; tergites III and IV approx. [1.5] 1.2–1.5 times as long as posteriorly width; ovipositor [1.45] 1.3–1.5 times as long as hind tibia.

Colour. Head black; clypeus yellowish, with base slightly black; mouthparts yellowish, with apex mandible black; antenna brownish. Mesosoma orange. Fore and mid leg orange, the hind leg orange, with femur, tibia, and tarsus brownish. Wings slightly yellowish hyaline; pterostigma brown. Metasoma orange, with tergites II–V with lateral marks on posterior margins black and tergites V+ brownish; ovipositor and sheath brown.

Figures 46–60. Sternite I of *Hymenoepimecis* spp. (females), lateral view **46** *H. andina* sp. nov. (holotype) **47** *H. bicolor* **48** *H. castilloi* sp. nov. (holotype) **49** *H. dolichocarinata* sp. nov. (holotype) **50** *H. duckensis* **51** *H. ecuatoriana* sp. nov. (holotype) **52** *H. kleini* **53** *H. longilobus* sp. nov. (holotype) **54** *H. manauara* **55** *H. neotropica* **56** *H. pucallpina* sp. nov. (holotype) **57** *H. rafaelmartinezi* sp. nov. (holotype) **58** *H. ribeiroi* **59** *H. tedfordi* **60** *H. uberensis*.

Male. (Fig. 99). Similar to female in structure and colouration, but with body with 5.0–7.0 mm; face 0.9–1.1 times as broad as high; head in dorsal view, with margin of gena short, slightly convex behind eyes; posterior ocelli separated from eyes by approx. 0.8 times its own maximum diameter; occipital carina not projected. Fore wing 4.0–6.0 mm; cu-a more or less interstitial to the base Rs&M; 2rs-m 0.3–0.4 times as long as abscissa of M between 2rs-m and 2m-cu. Tarsal claw simple. Metasoma slender;

tergite I 1.6–1.7 times as long as posteriorly width; tergite II approx. 1.3 times as long as posteriorly width; tergites III and IV 1.2 times as long as posteriorly width.

Variation. Tergite V black with anterior margin orange or apical half orange and basal half-black. Three females from French Guiana (Saül city) presented margin of gena slightly convex. We think they are conspecific, but we are not treating them as paratypes.

Distribution. Ecuador**, French Guiana and Peru (Fig. 107).

Biological notes. Host unknown.

Etymology. The specific name refers to the long epicnemial carina, reaching the level of the lower corner of the pronotum laterally.

Type material. *Holotype* ♀. Peru, Dept. of Loreto, Iquitos area, Allpahuayo, APHI, 29.i–20.ii.2000, Malaise trap I1, (I.E. Sääksjärvi et al. leg.), MUSM. *Paratypes*: Peru: idem holotype, 1♀, ZMUT; Dept. of Loreto, Iquitos area, Allpahuayo, 20.ii–8. iii.2000, white sand, Malaise trap (Sääksjärvi et al. leg.), APHI, G2/2, 1♀, MUSM; idem, but 30°57'84"S, 73°25'39"W, 5–11.xii.2011 (Gómez & Sääksjärvi leg.), 1♀, ZMUT; idem, but H2 (16), 21.xii.2000, 1♀, ZMUT; idem, but J1, 1.xii.2000, 1♀, ZMUT. Ecuador: Dept. Orellana, Onkonegare, 00°39'25,7"S, 76°27'10,8"W, a.s.l.: 216 m., 08.ii.1996, Fogging (T.L. Erwin leg.), Lot #1473, 1♂, ZMUT; idem, but 30.ix.1996, Lot #1677, 1♂, ZMUT.

Other material. French Guiana, Saül, 27.xii or viii.2011 [sic], Malaise trap (without collector), 1♀, ZMUT; idem, but 7.v.2012, 1♀, ZMUT; idem, but 13.xii.2011, 1♀, ZMUT.

Comments. *Hymenoepimecis dolichocarinata* sp. nov. closely resembles *H. japi* Sobczak, Loffredo, Penteado-Dias & Gonzaga, 2009, *H. sooretama* Sobczak, Loffredo, Penteado-Dias & Gonzaga, 2009 and *H. manauara* Pádua & Oliveira mainly by having weak black lateral marks on posterior margins of tergites II–V and by having sternite I with a low, rounded swelling posteriorly, but it differs from them mainly by having epicnemial carina present (absent in all other mentioned species).

Hymenoepimecis duckensis Pádua & Onody, 2015
Figures 5, 20, 35, 50, 65, 80, 100
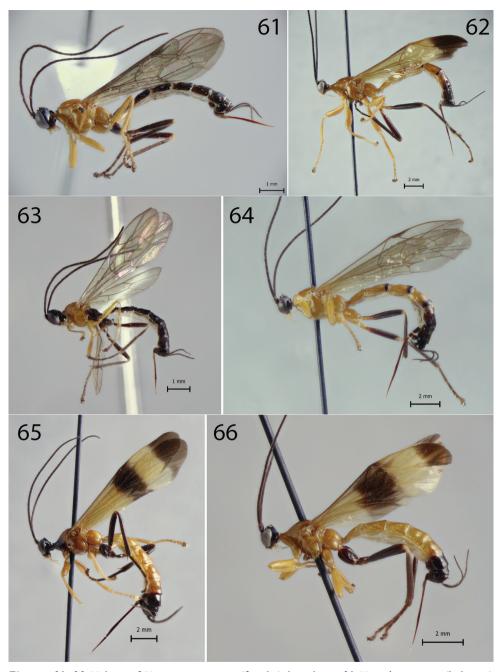
Hymenoepimecis duckensis Pádua & Onody, 2015: 181.

Diagnosis. See Pádua et al. (2015).

Distribution. Brazil, Ecuador**, French Guiana* and Peru* (Fig. 109).

Biological notes. Host unknown.

Material examined. French Guiana: M. de Kaw, Patawa (PM), ii.2003 (O. Morvan leg.), 1♂ and 1♀, ZMUT; idem, but 3.iii.2003, 1♂ and 1♀, ZMUT. Ecuador: Dept. Orellana, Onkonegare, 00°39'25,7"S, 76°27'10,8"W, a.s.l.: 216 m., 4.x.1996, Fogging, Lot #1758 (T.L. Erwin leg.), 1♂, ZMUT; idem, but 6.x.1995, Lot
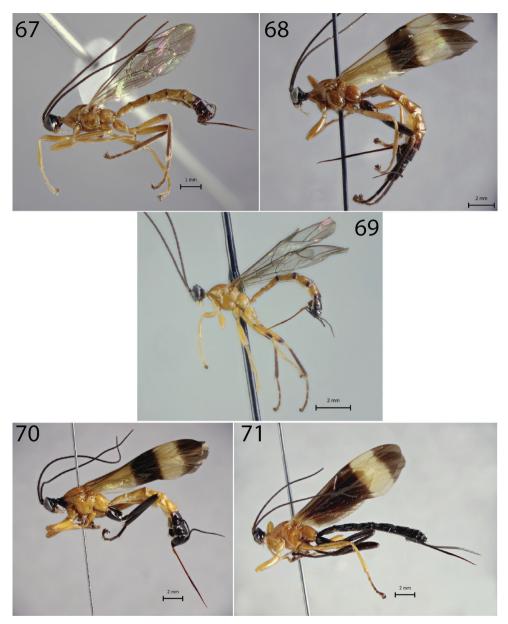
Figures 61–66. Habitus of *Hymenoepimecis* spp (females), lateral view **61** *H. andina* sp. nov. (holotype) **62**, *H. bicolor* **63** *H. castilloi* sp. nov. (holotype) **64** *H. dolichocarinata* sp. nov. (holotype) **65** *H. duckensis* **66** *H. ecuatoriana* sp. nov. (holotype).

#1217, 1♂, ZMUT; idem, but Tiputini, 00°37'55"S, 76°08'39"W, a.s.l.: 220–250 m., 28.x.1998, Lot #1955, 1♀, ZMUT; idem, but 00°39'25,7"S, 76°27'10,8"W, 216.3 m., 5.ii.1996, Lot #1422, 1♂, ZMUT; Napo province, Yasuni National Park, PUCE, 00°38'S, 76°36'W, 20.xi.1998, Malaise trap (T. Pape & B. Viklund leg.), 1♂, ZMUT. Peru: Loreto, Alto Nanay, Albarenga north, 195 m., 18M 05.30961S, 96.46100W, 20.xi.2008 (C. Castillo leg.), 1♂, ZMUT; idem, but Qda. Pucacuro, Bosque de terraza media, 18M 05.01611S,97.26184W, 173 m., 24.x.2008, Malaise trap (M. Vilchez leg.), 1♀, ZMUT; idem, but Iquitos area Allpahuayo, 29.vi–16.vii.2000, Malaise trap, white sand (I.E. Sääksjärvi & et al.), APHI, E1/9, 1♀, ZMUT; idem, but 30°57'49"S, 73°24'93"W, 3–9.x.2011 (Gómez & Sääksjärvi leg.), 1♀, ZMUT; idem, but clay (I.E. Sääksjärvi et al. leg.), 22.v–11.vi.2000, J1 (7), 1♀, ZMUT.

Hymenoepimecis ecuatoriana Pádua & Sääksjärvi, sp. nov.
http://zoobank.org/D27F8C9C-3B30-4690-A01C-79723F7B1A11
Figures 6, 21, 36, 51, 66, 81

Diagnosis. This species can be distinguished from all other *Hymenoepimecis* by the combination of the following characters: 1) fore wing hyaline yellowish, with two blackish bands; 2) pronotum orange; 3) female with tarsal claw with more or less square lobe, and with apex overtaking the lobe; 4) female with ovipositor 1.2 times as long as hind tibia.

Description. Female. Body [9.0] mm; face [1.0] times as broad as high, smooth, slightly convex with few spaced bristles; head in dorsal view, with gena strongly narrowed behind eyes; posterior ocelli separated from eyes by approx. [1.0] times its own maximum diameter; occipital carina projected and weakly reduced and curved upwards dorsally. Pronotum long, smooth and polished, with distance from tegula to head approx. [0.8] times distance from tegula to hind margin of propodeum, and in anterior part with opening pocket-like structure not reduced longitudinally; mesoscutum smooth and polished; scutellum, in profile, convex; mesopleuron smooth and polished, with anterodorsal and posterodorsal parts bearing sparse, fine setiferous punctures; metapleuron smooth and polished, rather uniformly covered with sparse, fine setiferous punctures; propodeum smooth, polished, with sparse, fine setiferous punctures and with lateral longitudinal carina present only posteriorly. Fore wing [7.0] mm; cu-a more or less interstitial to the base of Rs&M; 2rs-m [0.5] times as long as abscissa of M between 2rs-m and 2m-cu; hind wing with abscissa of Cu1 meeting cu-a equidistant between M and 1A. Hind leg with tibia + tarsus [0.6] times the fore wing length; tarsal claw with more or less square lobe, with apex of claw overtaking the lobe. Metasoma slender; tergite I [1.4] times as long as posteriorly width, centrally quite strongly convex with lateral carinae present only at extreme anterior end flanking the anterior concavity; sternite I with a low, rounded swelling posteriorly; tergite II approx. [1.2] times as long as posteriorly width; tergites III and IV approx. [1.1] times as long as posteriorly width; ovipositor [1.2] times as long as hind tibia.

Figures 67–71. Habitus of *Hymenoepimecis* spp. (females), lateral view **67** *H. kleini* **68** *H. longilobus* sp. nov. (holotype) **69** *H. manauara* **70** *H. neotropica* **71** *H. pucallpina* sp. nov. (holotype).

Colour. Head black; clypeus black with apex yellowish; mouthparts yellowish, with apex mandible black; antenna brownish. Mesosoma orange. Fore and mid leg orange, the hind entirely blackish brown. Fore wing hyaline yellowish, with apex blackish and with a blackish preapical band; pterostigma with basal half black and apical half yellow; hind wing with slightly blackish band in median part. Metasoma orange, with tergites VI+ black; ovipositor and sheath brownish.

Male. Unknown.

Distribution. Ecuador** (Fig. 109).

Biological notes. Host unknown.

Etymology. The specific name refers to Ecuador.

Type material. *Holotype* ♀. Ecuador, Dept. Orellana, Yasuni, 00°37'55"S, 76°08'39"W, a.s.l.: 220–250 m., 5.ii.1999, Fogging, Lot #2086 (T.L. Erwin leg.), ZMUT.

Comments. *Hymenoepimecis ecuatoriana* sp. nov. closely resembles *H. neotropica* (Brues & Richardson, 1913), *Hymenoepimecis longilobus* sp. nov. and *H. duckensis* Pádua & Onody, 2015 mainly by having the fore wing yellowish hyaline with two blackish bands, metasoma orange with last tergites black and face without a sculptured, longitudinal carina in the middle part of face. It differs from the first and second congeneric species by having tarsal claw with a more or less square lobe (tarsal claw with a preapical tooth, in *H. neotropica* and lobe longitudinally elongated in *H. longilobus* sp. nov.), and from the last species by having the ovipositor < 1.3 times as long as hind tibia (> 1.5 times as long as hind tibia in *H. duckensis*).

Hymenoepimecis kleini Pádua & Sobczak, 2015
Figures 7, 22, 37, 52, 67, 82, 101

Hymenoepimecis kleini Pádua & Sobczak, 2015: 183.

Diagnosis. See Pádua et al. (2015).

Male. (Fig. 101). Similar to female in structure and colouration, but with hind leg black, except coxa, with basal part orange; body approx. 8.0 mm; face a approx. 1.1 times as broad as high; posterior ocelli separated from eyes by approx. 0.8 times its own maximum diameter. Fore wing approx. 6.0 mm; 2rs-m approx. 0.2 times as long as abscissa of M between 2rs-m and 2m-cu. Tarsal claw simple. Metasoma slender; tergite I approx. 1.6 times as long as posteriorly width; tergite II approx. 1.4 times as long as posteriorly width; tergites III and IV approx. 1.3 times as long as posteriorly width.

Distribution. Brazil, Ecuador** and Peru* (Fig. 107).

Biological notes. Host unknown.

Material examined. Ecuador, Dept. Orellana, Onkonegare, 00°39'25,7"S, 76°27'10,8"W, a.s.l.: 216.3 m., 21.vi.1996, Fogging, Lot # 1543 (T.L. Erwin et al. leg.), 1♂, ZMUT. Peru: Cusco, Cashiariari, 11°52'S, 72°39'W, 24.xi.1997, 690 m. (S. Cordova leg.), 1♀, ZMUT.

Hymenoepimecis longilobus Pádua & Sääksjärvi, sp. nov.
http://zoobank.org/8FFC81FF-D55A-4C66-A274-8EA5EAA3164F
Figures 8, 23, 38, 53, 68, 83, 102

Diagnosis. This species can be distinguished from all other *Hymenoepimecis* by the combination of the following characters: 1) fore wing hyaline yellowish, with two

Figures 72–75. Habitus of *Hymenoepimecis* spp. (females), lateral view **72** *H. rafaelmartinezi* sp. nov. (holotype) **73** *H. ribeiroi* **74** *H. tedfordi* **75** *H. uberensis*.

blackish bands; 2) pronotum orange (Peruvian specimens with anterior margin of the pronotum blackish); 3) female with tarsal claw with a longitudinally elongated lobe, and with apex overtaking the lobe; 4) female with ovipositor 1.5–1.6 times as long as hind tibia.

Description. Female. Body approx. [15.0] 12.0–15.0 mm; face [1.1] 1.0–1.1 times as broad as high, smooth, slightly convex with few spaced bristles; head in dorsal view, with gena strongly narrowed behind eyes; posterior ocelli separated from eyes by approx. [0.9] 0.8–1.0 times its own maximum diameter; occipital carina projected and curved upwards dorsally. Pronotum long, smooth and polished, with distance from tegula to head greater than approx. [0.7] 0.6–0.7 times distance from tegula to hind margin of propodeum, and in anterior part with opening pocket-like structure not reduced longitudinally; mesoscutum smooth and polished; scutellum, in profile, convex; mesopleuron smooth and polished, with anterodorsal and posterodorsal parts bearing sparse, fine setiferous punctures; metapleuron smooth and polished, rather uniformly covered with sparse, fine setiferous punctures; propodeum smooth, polished, with sparse, fine setiferous punctures and with lateral longitudinal carina present only posteriorly. Fore wing approx. [13.0] 9.0–13.0 mm; cu-a interstitial to the base of

Figures 76–90. Tarsal claws of *Hymenoepimecis* spp. (females), lateral view **76** *H. andina* sp. nov. (holotype) **77** *H. bicolor* **78** *H. castilloi* sp. nov. (holotype) **79** *H. dolichocarinata* sp. nov. (holotype) **80** *H. duckensis* **81** *H. ecuatoriana* sp. nov. (holotype) **82** *H. kleini* **83** *H. longilobus* sp. nov. (holotype) **84** *H. manauara* **85** *H. neotropica* **86** *H. pucallpina* sp. nov. (holotype) **87** *H. rafaelmartinezi* sp. nov. (holotype) **88** *H. ribeiroi* **89** *H. tedfordi* **90** *H. uberensis*.

Rs&M; 2rs-m [0.55] 0.5–0.6 times as long as abscissa of M between 2rs-m and 2m-cu; hind wing with abscissa of Cu1 meeting cu-a equidistant between M and 1A. Hind leg with tibia + tarsus [0.6] times the fore wing length; tarsal claw with longitudinally elongated lobe, with apex of claw overtaking the lobe. Metasoma slender; tergite I [1.6] times as long as posteriorly width, centrally quite strongly convex with lateral carinae present only at extreme anterior end flanking the anterior concavity; sternite I with a low, rounded swelling posteriorly; tergite II approx. [1.2] 1.2–1.4 times as long as posteriorly width; tergites III and IV approx. [1.1] 1.1–1.3 times as long as posteriorly width; ovipositor approx. [1.6] 1.5–1.6 times as long as hind tibia.

Colour. Head black; clypeus black with apex yellowish; mouthparts yellowish, with apex mandible black; antenna brownish. Mesosoma orange. Fore and mid leg orange, the hind entirely blackish brown except base of coxa orange. Fore wing hyaline yellowish, with apex blackish and with a blackish preapical band; pterostigma with basal half black and apical half yellow; hind wing with slightly blackish band in median part. Metasoma orange, with posterior margin black in tergite V and tergites VI+ black; ovipositor and sheath brownish.

Male. (Fig. 102). Similar to female in structure and colouration, but with hind coxa orange body with 10.5–12.0 mm; face 1.0 times as broad as high; posterior ocelli separated from eyes by 0.8–1.0 times its own maximum diameter. Fore wing 8.0–10.0 mm; 2rs-m 0.3–0.5 times as long as abscissa of M between 2rs-m and 2m-cu. Tarsal claw simple. Metasoma slender; tergite I 1.6–1.7 times as long as posteriorly width; tergite II 1.2–1.5 times as long as posteriorly width; tergites III and IV 1.0–1.3 times as long as posteriorly width.

Variation. The Peruvian specimens have anterior margin of pronotum blackish. Some specimens have tergite V entirely black or black with anterior margin orange; hind coxa orange with basal part blackish.

Distribution. Ecuador**, French Guiana* and Peru* (Fig. 110).

Biological notes. Host unknown.

Etymology. The specific name refers the longitudinally elongated lobe in tarsal claw of the females.
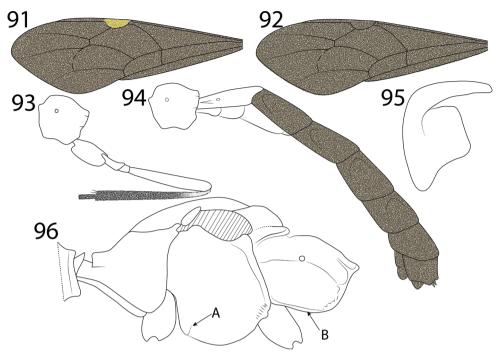
Type material. *Holotype* ♀. French Guiana, M. de Kaw, Patawa, ix.2003, (J. Cerda leg.), ZMUT. *Paratypes*: French Guiana: idem holotype, but vii.2003, 1♀, ZMUT; idem, but xi.2001, 1♂ and 1♀, ZMUT; idem, but xii.2001, 1♀, ZMUT; idem, but ii.2003 (O. Morvan leg.), 1♂, ZMUT. Ecuador: Dept. Orellana, Onkonegare, 00°39'25,7"S, 76°27'10,8"W, a.s.l.: 216 m., 23.vi.1996, Fogging, Lot #1616 (T.L. Erwin leg.), 1♂, ZMUT. Peru: Dept. of Loreto, Iquitos area, Allpahuayo, 22.ii–7.iii.2000, white sand, Malaise trap (Sääksjärvi et al. leg.), APHI, E1/2, 1♀, ZMUT; idem, but 14.ix–4.x.2000, clay, APHI, H1/13, 1♀, ZMUT; idem, but G1(15), 8.xi.2000, 1♀, ZMUT.

Comments. *Hymenoepimecis longilobus* sp. nov. closely resembles *H. neotropica* (Brues & Richardson, 1913), *Hymenoepimecis ecuatoriana* sp. nov. and *H. duckensis* Pádua & Onody, 2015 mainly by having the fore wing yellowish hyaline with two blackish bands and metasoma orange with last tergites black. It differs from all of these species by having tarsal claw with a longitudinally elongated lobe (tarsal claw with a preapical tooth in *H. neotropica* and a more or less square lobe in *H. ecuatoriana* sp. nov. and *H. duckensis*).

Hymenoepimecis manauara Pádua & Oliveira, 2015
Figures 9, 24, 39, 54, 69, 84, 103

Hymenoepimecis manauara Pádua & Oliveira, 2015: 185.

Figures 91–96. *Hymenoepimecis* spp. **91, 92** fore wing, showing colour pattern. (**91**) *H. veranii* (**92**) *H. argyraphaga* **93** *H. robertsae*, propodeum and hind leg, showing colour pattern, lateral view **94** *H. heteropus*, propodeum and metasoma, showing colour pattern, lateral view **95** *H. amazonensis* (female), tarsal claw, lateral view **96** *H. argyraphaga*, mesosoma, lateral view: Arrow "A" shows epicnemial carina and arrow "B" shows submetapleural carina.

Diagnosis. See Pádua et al. (2015).

Distribution. Brazil, French Guiana*, Ecuador** and Peru* (Fig. 111).

Biological notes. Parasitoid of *Leucauge henryi* Mello-Leitão, 1940 (Araneae: Tetragnathidae) (Pádua et al. 2016).

Material examined. French Guiana, M. de Kaw, Patawa, xi.2002 (PM) (J. Cerda leg.), 1♀, ZMUT; idem, but iii.2003, Malaise trap, 1♀, ZMUT; idem, but i.2002, 1♀, ZMUT; idem, but x.2001, 1♀, ZMUT; idem, but xi.2001, 2♀♀, ZMUT; idem, but iii.2002, 2♀♀ [one without head], ZMUT; idem, but ix.2003, 2♀♀, ZMUT; idem, but pk 35, x.2002, 1♀, ZMUT; idem, but ii.2003 (O. Morvan leg.), 1♀, ZMUT; Kourou, piste Soumourou, 2–19.iv.2002 (D. Faure leg.), 1♀, ZMUT; idem, but 12.v–10.vi.2002, 1♀, ZMUT; Montagne des Chevaux, 4.ix.2011 (SLAM leg.), 1♂ and 1♀, ZMUT. Ecuador: Napo province, Yasuni National Park, 00°38'S, 76°36'W, PUCE, Malaise trap, 20.xi.1998, Malaise trap (T. Pape & B. Viklund leg), NHRS, 4♀♀, ZMUT; Dept. Orellana, Tiputini, 00°37'55"S, 76°08'39"W, a.s.l.: 220–250 m., 9.ii.1999, Fogging, Lot #2001 (T.L. Erwin et al. leg.), 1♂, ZMUT; idem, but Yasuni, 00°37'55"S, 76°08'39"W, 5.vii.1998, Lot #1896, 1♂, ZMUT; idem, but 21.x.1998, Lot #1987, 1♂, ZMUT; idem, but Onkonegare, 00°39'25,7"S, 76°27'10,8"W, a.s.l.:

216 m., 6.x.1995, 1♀, ZMUT; idem, but 4.ii.1996, Lot #1416, 1♀, ZMUT; idem, but 9.ii.1995, Lot #984, 1♀, ZMUT; idem, but 30.ix.1996, Lot #1678, 1♀, ZMUT; idem, but 6.vii.1995, Lot #1130, 1♂, ZMUT; idem, but 8.x.1995, Lot #1263, 1♀, ZMUT. Peru: Dept. Madre de Dios, Los Amigos, 380304.85E/8611305.81, a.s.l.: 290 m., 26.vi–3.vii.2008 (I. Gómez leg.), 1♀, ZMUT; idem, but 7–14.viii.2008, 1♀, ZMUT; idem, but 14–21.viii.2008, 2♀♀, ZMUT; idem, but Tambopata, Explorer's inn, 12°50'30"S, 69°17'31"W, 161 m., 15.vi.2009, Colecta manual (M. Alvarado leg.), 1♀, ZMUT; Cusco, La Convención, Echarate, CC Timpia, 12°06'47,04"S, 72°49'34,56"W, 519 m., Bosque húmedo de montana, 29.i.2010, Light (C. Espinoza & E. Rázuri leg.), 1♀, ZMUT; idem, but Reserva Comunal Amarakaeri, 12°55'S, 70°51'W, 333–884 m., 17.ix–14.xi.2010, Malaise trap (M. Vilchez & C. Castillo leg.), 1♀, ZMUT; Loreto, Qda. Pucacuro, 18M 0501611E/9726184N, Bosque de terraza media, 173 m., 24.x.2008, Malaise trap. (M. Vilchez leg.), 1♀, ZMUT; idem, but Pucallpa, 2011 (I. Gómez leg.), 1♀, ZMUT; idem, but Iquitos area, Allpahuayo, 30°58'00"S, 73°25'16"W, 24–30.x.2011 (Gómez & Sääksjärvi leg.), 1♀, ZMUT; idem, but 17–23.x.2011, 1♀, ZMUT; idem, but 26.ix–2.x.2011, 1♀, ZMUT; idem, but 4–10.vii.2011, 1♀, ZMUT; idem, but 14–20.xi.2011, 1♀, ZMUT; idem, but iv.2011, 1♀, ZMUT; idem, but 31.x–6.xi.2011, 1♀, ZMUT; idem, but 28.xi–4.xii.2011, 1♀, ZMUT; idem, but 25–31.vii.2011, 2♀♀, ZMUT; idem, but 22–28.viii.2011, 2♀♀, ZMUT; idem, but 7–13.xi.2011, 2♀♀, ZMUT; idem, but white sand, 24.iii–16.iv.2000 (Sääksjärvi et al. leg.), APHI, E2/4, 1♀, ZMUT; idem, but 1.xii–15.xii.2000, E1(17), 1♀, ZMUT; idem, but J1, 1.xii.2000, 1♀, ZMUT.

Hymenoepimecis neotropica (Brues & Richardson, 1913)
Figures 10, 25, 40, 55, 70, 85

Epimecis neotropica Brues & Richardson, 1913: 495.
Hymenoepimecis neotropica (Brues & Richardson): Viereck, 1912: 149
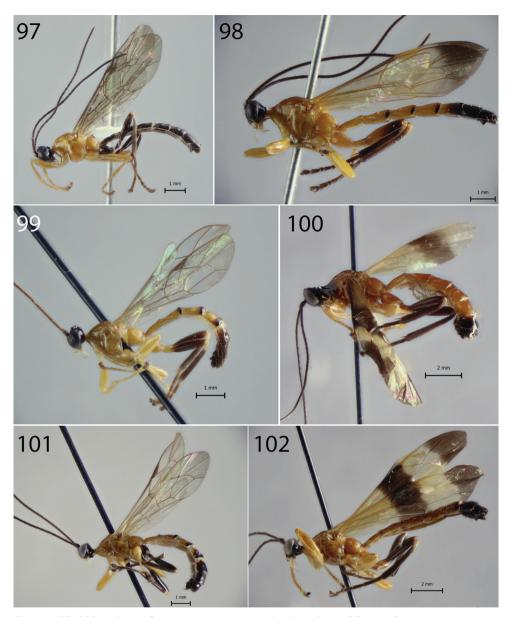
Diagnosis. See Pádua et al. (2015).
    Male. Unknown.
    Distribution. Brazil, Guiana, Ecuador** and Peru* (Fig. 112).
    Biological notes. Parasitoid of *Araneus omnicolor* (Keyserling, 1893) (Araneae: Araneidae) (Sobczak et al. 2012).
    Material examined. Ecuador, Dept. Orellana, Tiputini, 00°37'55"S, 76°08'39"W, a.s.l.: 220–250 m., 29.vi.1998, Fogging, Lot #1801 (T.L. Erwin et al. leg.), 1♀, ZMUT. Peru: Loreto, Maynas, Bosque ribereño, 18M 533166E/9583208N, 129 m., 23.vii.2008, Manual (C. Castillo leg.), 1♀, ZMUT; idem, but 18M 596425E/9520800N, 102 m., Pantano arbóreo, 8.vii.2008, 1♀, ZMUT; idem, but Pantano herbáceo, 18M 598912E/9522935N, 117 m., 12.vii.2008, Manual, 1♀, ZMUT; idem, but Alto Nanay, Qda. Lobilios, 119 m., Bosque de arena blanca, 18M 0565793E/9610621N, 20.xii.2008, Colecta manual, 1♀, ZMUT; idem,

Figures 97–102. Habitus of *Hymenoepimecis* spp. (males), lateral view **97** *H. andina* sp. nov. (paratype) **98** *H. bicolor* **99** *H. dolichocarinata* sp. nov. (paratype) **100** *H. duckensis* **101** *H. kleini* **102** *H. longilobus* sp. nov. (paratype).

but 10.xii.2008, Bosque de arena blanca, 1♀, ZMUT; idem, but Albarenga north, 195 m., Colinas fuertmnt. Disect. [sic], 18M 9646100N, 0530961E, 20.xi.2008, 1♀, ZMUT; idem, but 130 m., 18M 0532028E/9647431N, Bosque de Terraza media, 11.xi.2008, 1♀, ZMUT; idem, but Iquitos area, Allpahuayo, 22.v–11.vi.2000,

Malaise trap, white sand (I.E. Sääksjärvi et al. leg.), APHI, E3/7, 1♀, ZMUT; idem, but 16.vii–02.viii.2000, clay, APHI, J1/10, 1♀, ZMUT; idem, but 04–17.x.2000, APHI, H1/14, 1♀, ZMUT; idem, but 30°58'00"S, 73°25'16"W, 12–18.ix.2011 (Gómez & Sääksjärvi leg.), 1♀, ZMUT; idem, but Pucallpa, 7.vi.1963 (J.M. Schunke leg.), 1♀, ZMUT; idem, but Rio Nanay, ca. Diamante azul, Colinas fuertmnt disect [sic], 131 m., 18M 638497E/9570148N, 10.xi.2008, Manual (L. Huerto leg.), 1♀, ZMUT idem, but Dept. of Loreto, Iquitos area, Allpahuayo, Malaise trap, (I.E. Sääksjärvi et al. leg.), 11–16.viii.2000, 1♀, ZMUT; idem, but J1, 20.i.2001, 1♀, ZMUT; idem, but F1(3), 8.iii.2000, 1♀, ZMUT; idem, but I1 (11), 18.vii.2000, 1♀, ZMUT; Madre de Dios, Tambopata, NNRR, Explorer's inn, 12°50'S, 69°17'W, 189 msnm, 15–18.v.2008 (L. Figueroa & M. Alvarado leg.), 1♀, ZMUT; idem, but 18–19.xii.2008, Malaise trap (M. Alvarado & L. Sulca leg.), 1♀, ZMUT.

Hymenoepimecis pucallpina Pádua & Sääksjärvi, sp. nov.

http://zoobank.org/67D0DB27-DACB-42CB-8634-F4BD43FDB95A
Figures 11, 26, 41, 56, 71, 86

Diagnosis. This species can be distinguished from all other *Hymenoepimecis* by the combination of the following characters: 1) fore wing black, with a yellowish band between junction of vein R1 up to pterostigma until half vein M; 2) metasoma entirely black; 3) hind leg black; 4) occipital carina projected and curved upwards dorsally.

Description. Female. Body approx. [16.0] mm; face [1.0] times as broad as high, smooth, slightly convex with few spaced bristles; head in dorsal view, with gena slightly narrowed behind eyes; posterior ocelli separated from eyes by approx. [1.2] times its own maximum diameter; occipital carina projected and curved upwards dorsally. Pronotum long, smooth and polished, with distance from tegula to head greater than [0.6] times distance from tegula to hind margin of propodeum, and in anterior part with opening pocket-like structure not reduced longitudinally; mesoscutum smooth and polished; scutellum, in profile, convex; mesopleuron smooth and polished, with anterodorsal and posterodorsal parts bearing sparse, fine setiferous punctures; metapleuron smooth and polished, with a few sparse, fine setiferous punctures; propodeum smooth, polished, with sparse, fine setiferous punctures and with lateral longitudinal carina present only posteriorly. Fore wing approx. [13.0] mm; cu-a interstitial to the base of Rs&M; 2rs-m approx. [0.75] times as long as abscissa of M between 2rs-m and 2m-cu; hind wing with abscissa of Cu1 meet cu-a equidistant between 1A and M. Hind leg with tibia + tarsus [0.6] times the fore wing length; tarsal claw with more or less square basal lobe with apex of claw overtaking the lobe. Metasoma slender; tergite I [1.6] times as long as posteriorly width, centrally quite strongly convex with lateral carinae present only at extreme anterior end flanking the anterior concavity; sternite I with a low, rounded swelling posteriorly; tergite II approx. [1.3] times as long as posteriorly width; tergites III–IV approx. [1.2] times as long as posteriorly width; ovipositor [1.6] times as long as hind tibia.

Figures 103–106. Habitus of *Hymenoepimecis* spp. (males), lateral view **103** *H. manauara* **104** *H. rafaelmartinezi* sp. nov. (paratype) **105** *H. ribeiroi* **106** *H. uberensis*.

Colour. Head black with apical margin of clypeus and mouthparts (except apex mandible black) yellowish; antenna blackish. Mesosoma entirely orange. Fore and mid leg orange, the hind leg black. Fore wing black, with basal region yellowish and with a yellowish band between junction of vein R1 up to pterostigma until half vein M; pterostigma black, except apical margin yellowish; hind wing black with basal region and apex yellowish. Metasoma entirely black; ovipositor brownish with apex reddish brown, sheath blackish.

Male. Unknown.

Distribution. Peru (Fig. 109).

Biological notes. Host unknown.

Etymology. The specific name refers to the name given to people born in the city of Pucallpa, Peru.

Type material. *Holotype* ♀. Peru, Dept. Loreto, Pucallpa, 15.iv.1950 (J.M. Schunke leg.), B.M. 1950-559 [sic], NHM. *Paratypes*: Dept. Huánuco, Tingo Maria, Cueva de Las Pavas, 23–27.vii.1982 (C. Porter & T. O'neill leg.), 6♀♀, FSCA; idem, but 12–15.vii.1974 (C. Porter & L. Stange leg.), 2♀♀, FSCA; idem, but 20–27.i.1968 (A. Garcia & C. Porter leg.), 1♀, FSCA.
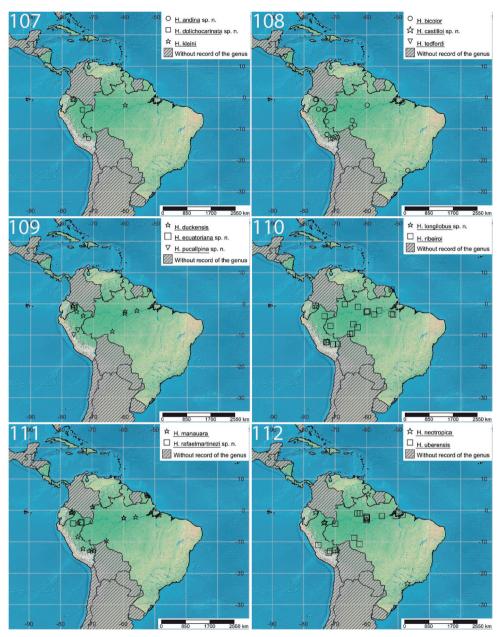
Comments. *Hymenoepimecis pucallpina* sp. nov. closely resembles *H. uberensis* Pádua & Onody, 2015 and *H. ribeiroi* Pádua & Oliveira, 2015 mainly by having fore wing black with a yellowish band between junctions of vein R1 up to pterostigma until half vein M. It differs from both of these species by having the metasoma entirely black and occipital carina projected, and curved upwards dorsally (occipital carina not curved upwards and with a concavity in the apex dorsally in *H. uberensis*, occipital carina with dorsal margin reduced, in profile view in *H. ribeiroi* and metasoma orange, with tergites VI+ black in both species).

Hymenoepimecis rafaelmartinezi Pádua & Sääksjärvi, sp. nov.
http://zoobank.org/59F648CD-2ED2-4E2E-9A0E-B7B609995608
Figures 12, 27, 42, 57, 72, 87, 104

Diagnosis. This species can be distinguished from all other *Hymenoepimecis* by the combination of the following characters: 1) fore wing hyaline yellowish, with two blackish bands; 2) face sculptured below the insertion of antennae, with a longitudinal carina in the middle part; 3) occipital carina projected, not curved upwards, with a concavity in the apex dorsally; 4) pronotum with the pocket-like structure reduced longitudinally; 5) sternite I with a ventral spine-like projection posteriorly; 6) metasoma orange, with tergites VI+ black; 7) hind leg orange, with femur, tibia and tarsus back; 8) female with tarsal claw with basal lobe more or less square and apex of claw overtaking the lobe; 9) female with ovipositor 1.0–1.2 times as long as hind tibia.

Description. Female. Body approx. [10.0] 9.0–10.0 mm; face [0.9] 0.8–1.1 times as broad as high, sculptured below the insertion of antennas, with longitudinal carina in the middle part and with few bristles spaced on the lower face; head in dorsal view with gena strongly narrowed behind eyes; posterior ocelli separated from eyes by [1.0] 0.8–1.0 times its own maximum diameter; occipital carina not curved upwards, with a concavity in the apex dorsally. Pronotum long, smooth and polished, with distance from tegula to head greater than [0.5] 0.5–0.6 times distance from tegula to hind margin of propodeum, and in anterior part with opening pocket-like structure reduced longitudinally; mesoscutum smooth and polished; scutellum, in profile, convex; mesopleuron smooth and polished, with anterodorsal and posterodorsal parts bearing sparse, fine setiferous punctures; metapleuron smooth and polished, rather uniformly covered with sparse, fine setiferous punctures; propodeum smooth, polished, with sparse, fine setiferous punctures and with lateral longitudinal carina present only posteriorly. Fore wing approx. [7.0] 7.0–8.0 mm; cu-a interstitial to the base of Rs&M; 2rs-m [0.3] 0.3–0.5 times as long as abscissa of M between 2rs-m and 2m-cu; abscissa of Cu1 meeting 1m-cu equidistant between Cu1a and Cu1b; hind wing with abscissa of Cu1 meeting cu-a closer to 1A that M. Hind leg with tibia + tarsus [0.55] 0.5–0.6 times the fore wing length; tarsal claw with basal lobe slightly more or less square, with apex of claw overtaking the lobe. Metasoma slender; tergite I approx. [1.2] 1.2–1.4 times as long as posteriorly width, centrally quite strongly convex with lateral carinae present only at extreme anterior end flanking the anterior concavity; sternite I with

Figures 107–112. Geographic distribution of the *Hymenoepimecis* species in this study.

a ventral projection, spine-like, posteriorly; tergite II [1.1] 1.0–1.1 times as long as posteriorly width; tergites III–IV [1.0] 1.0–1.05 times as long as posteriorly width; ovipositor [1.15] 1.0–1.2 times as long as hind tibia.

Colour. Head black; clypeus with apical margin yellowish, labrum and mouthparts yellowish, except apex mandible black; antenna brown. Mesosoma orange. Fore and mid leg orange, the hind leg orange, with femur, tibia and tarsus black. Fore wing

hyaline yellowish, fore wing hyaline yellowish, with apex blackish and with a blackish preapical band; pterostigma blackish brown; hind wing blackish with base and apex slightly yellowish. Metasoma orange, with tergite V with posterior margin black and tergites VI+ black; ovipositor brownish and sheath blackish brown.

Male. (Fig. 104). Similar to female in structure and colouration, but with body with 7.0–8.5 mm; face 0.9–1.0 times as broad as high; posterior ocelli separated from eyes by 0.8–0.9 times its own maximum diameter. Fore wing 6.0–7.0 mm; cu-a more or less interstitial to the base Rs&M; 2rs-m 0.3–0.4 times as long as abscissa of M between 2rs-m and 2m-cu. Tarsal claw tarsal claw simple. Metasoma slender; tergite I 1.3–1.6 times as long as posteriorly width; tergite II 1.0–1.1 times as long as posteriorly width; tergites III–IV 0.95–1.1 times as long as posteriorly width.

Distribution. Peru (Fig. 111).

Biological notes. Host unknown.

Etymology. The specific name refers to a young boy called Rafael Martinez, a friend of Yves Braet. Yves Braet has sent us many Darwin wasp samples from French Guiana, and Rafael has helped Yves in science.

Type material. *Holotype* ♀. Peru, Loreto, Maynas, Qda. Aguablanca, 151 m., Terrazas medias, 18M 0521603E/9676612N, 24.i.2009, Malaise trap (F. Meza leg.), ZMUT. *Paratypes*: idem holotype, but 18M 534463E/9584008N, Bosque rebereño, 115 m., 23.vii. 2008, Manual (C. Castillo leg.), 1♂ and 1♀, ZMUT; idem, but Rio Itaya, Colinas fuertmnt. disect., 18M 0635650E/9528654N, 127 m., 11.ii.2009, Malaise trap (W. Paredes leg.), 1♂, ZMUT; idem, but Rio Copalyacu, 03°42'59"S, 75°26'00"W, 165 m., 8.xii.2009, Malaise trap (L. Sulca leg.), 1♂, ZMUT; idem, but Rio Urituyacu, ca. Ayahuasca, 04°09'46"S, 76°00'49"W, 146 m., 19.xi.2009, Manual, 1♀, ZMUT; idem, but Mrg. Izq. Rio Nanay, Colinas fuertmnt. disect., 18M 0574494E/9614852N, 163 m., 23.i.2009, Flight-intercept trap (W. Paredes leg.), 1♀, ZMUT; idem, but Iquitos area, Allpahuayo, 2–18.viii.2000, clay, Malaise trap (Sääksjärvi et al. leg.), APHI, H1/11, 1♂, ZMUT; idem, but 19.ix–4.x.2000, APHI, J2/13, 1♂, ZMUT; idem, but 20.ii–8.iii.2000, APHI, H2/2, 1♂, ZMUT; 17.x–8.xi.2000, APHI, H2/15, 1♂, ZMUT; idem, but APHI, H1/15, 2♂♂, ZMUT; idem, but 3–22.v.2000, APHI, H1/6, 1♂, ZMUT; idem, but 18.viii–14.ix.2000, APHI, G2/12, 1♂, ZMUT; idem, but APHI, H2/12, 2♂♂ and 1♀, ZMUT; idem, but 8.iii–24.iii.2000, APHI, H1/3, 1♂, ZMUT; idem, but 22.v–11.vi.2000, APHI, H1/7, 1♂, ZMUT; idem, but 17.iv–3.v.2000, APHI, H1/5, 2♂♂, ZMUT; idem, but 2–24.iii.2000, APHI, G1/3, 1♂, ZMUT; idem, but 30°57'84"S, 73°25'39"W, 5–11.xii.2011 (Gómez & Sääksjärvi et al. leg.), 1♂, ZMUT; idem, but 7–13.xi.2011, 1♂, ZMUT; Dept. of Loreto, Iquitos area, Allpahuayo, Malaise trap, (I.E. Sääksjärvi et al. leg.), H1, 23.i.2001, 1♂, ZMUT; idem, but H2(12), 14.ix.2000, 1♂, ZMUT; idem, but I1(16), 15.xii.2000, 1♂, ZMUT; idem, but G1(15), 8.xi.2000, 1♂, ZMUT; idem, but H1, 1.xii.2000, 76, 1♂, ZMUT; idem, but H1, 23.i.2001, 1♂, ZMUT; idem, but G2(7), 11.vii.2000, 97, 1♂, ZMUT; idem, but I1, 1.xii.2000, 42, 1♀, ZMUT; idem, but J1, 1.xii.2000, 16, 1♀, ZMUT.

Comments. *Hymenoepimecis rafaelmartinezi* sp. nov. closely resembles *H. uberensis* Pádua & Onody, 2015, mainly by having wings bicoloured, face sculptured below the insertion of antennas, with longitudinal carina in the middle part and with a few

bristles spaced on the lower face, and by sternite I with a ventral spine-like projection posteriorly. It differs from *H. uberensis* mainly by having the fore wing hyaline yellowish with two black bands and hind leg orange, with femur, tibia and tarsus black (fore wing blackish, with yellowish hyaline band between junction of vein R1 up to pterostigma until half vein M and hind leg entirely black in *H. uberensis*).

Hymenoepimecis ribeiroi Pádua & Sobczak, 2015
Figures 13, 28, 43, 58, 73, 88, 105

Hymenoepimecis ribeiroi Pádua & Sobczak, 2015: 188.

Diagnosis. See Pádua et al. (2015).

Distribution. Brazil, French Guiana* and Peru* (Fig. 110).

Biological notes. Host unknown.

Material examined. French Guiana, M. de Kaw, Patawa (PM), ii.2003 (O. Morvan leg.), 1♀, ZMUT; Saül, 13.xii.2011, Malaise trap (without collector), 1♀ and 1♂, ZMUT. Ecuador: Dept. Orellana, Onkonegare, 00°39'25,7"S, 76°27'10,8"W, a.s.l.: 216.3 m., 9.ii.1995, Fogging, Lot #985 (T.L. Erwin et al. leg.), 1♂, ZMUT. Peru, Dept. of Loreto, Iquitos area, Allpahuayo, 17.xi–3.xii.1998, varillal, Malaise trap (I.E. Sääksjärvi, R. Jussila et al. leg.), APHI D2/7, 2♂♂, ZMUT; idem, but 17.xii–20.i.1998, APHI D1/9, 1♂, ZMUT; idem, but APHI C2/9, 1♂ and 1♀, ZMUT; idem, but 18.ix–4.x.1998, clay, APHI C2/3, 1♂, ZMUT; idem, but 4–20.x.1998, APHI C2/4, 2♂♂, ZMUT; idem, but 7–17.x.2000 (Sääksjärvi et al. leg.), APHI, H1/14, 1♂, ZMUT; idem, but 11–29.vi.2000, 1♂, ZMUT; idem, but 17.iv–3.v.2000, APHI, H1/5, 2♂♂, ZMUT; idem, but 16.vii–2.viii.2000, APHI H1/10, 2♂♂, ZMUT; idem, but APHI, H2/10, 1♀, ZMUT; idem, but APHI, I1/10, 1♂, ZMUT; idem, but APHI, G1/10, 1♂, ZMUT; idem, but 18.viii–14.ix.2000, APHI, H2/12, 2♂♂ [one without head], ZMUT; idem but APHI, I1/12, 1♂, ZMUT; idem, but APHI, E3/12, 1♀, ZMUT; idem, but APHI, J2/12, 1♀, ZMUT; idem, but 20.ii–2.iii.2000, white sand, APHI, G1/2, 1♂, ZMUT; idem but 14.ix–4.x.2000, 1♂, ZMUT; idem, but 19.ix–4.x.2000, APHI, I1/13, 2♂♂, ZMUT; idem, but 15.x–8.xi.2000, APHI, I1/15, 2♂♂, ZMUT; idem, but 4–15.x.2000, APHI I1/14, 2♂♂, ZMUT; idem, but 17.x–8.i.2000, APHI, G2/15, 1♂, ZMUT; idem, but 30°57'84"S, 73°25'39"W, 5–11.xii.2011 (Gómez & Sääksjärvi leg.), 1♂, ZMUT; idem, but 14–20.xi.2011, 1♂, ZMUT; idem, but Mishana, clayish soil, 16.x–1.xi.1998 (I.E. Sääksjärvi, R. Jussila et al. leg.), APHI, A1/5, 1♂, ZMUT; idem, but 1–16.xii.1998, clay, APHI, A1/8, 1♂, ZMUT; idem, but Maynas, Bosque de Terraza media, 18M 500248E/9624121N, 143 m., 2.viii.2008, Malaise trap (C. Castillo leg.), 1♂, ZMUT; idem but Alto Nanay, Albarenga north, 128 m., 18M 0533061E/9645180N, Terrazas bajas inund., 24.xi.2008, Flight intercept trap (C. Castillo leg.), 1♂ [without metasoma], ZMUT; idem, but 157 m., 0532439E/9646162N, Colinas bajas fuertmnt. dissect., 17.xi.2008, Colecta manual, 1♂, ZMUT; idem, but 130 m., 0532028E/9647431N, Bosque de terraza media, 29.xi.2008, Malaise trap, 2♂, ZMUT; idem, but 0532028E/9647431N, 28.xi.2008,

Colecta manual, 1♀, ZMUT; idem, but Qda. Lobillos, 119 m., 0565793E/9610621N, Colinas fuertmnt. dissect., 19.xii.2008, 1♀, ZMUT; Dpto. Madre de Dios, Los Amigos, 382633,452E/8610288,894N, a.s.l.: 241.7 m., 17–24.vii.2008, Malaise trap (I. Gómez leg.), 1♀, ZMUT; idem, but Explorer's Inn Amazon logde, 161 m., 12°50'30"S, 69°17'31"W, 13.ix.2009, Malaise trap (L. Sulca leg.), 1♂, ZMUT; Cusco, La Convención, 12°19'21,26"S, 73°02'44,08"W, 792 m., Bosque premontano, 26.iv.2007, Malaise trap (W. Paredes leg.), 2♂♂, ZMUT; idem, but Echarate, CC Kitaparay, 12°12'51,79"S, 72°50'04,31"W, 608 m., 8–11.xi.2009 (C. Espinoza & E. Razuri leg.), 1♂, ZMUT; idem, but Reserva Comunal Amarakaeri, 12°55'S, 70°51'W, 333–884 m., 17.ix–14.xi.2010, Malaise trap (M. Vilchez & C. Castillo leg.), 2♂♂, ZMUT; Dept. of Loreto, Iquitos area, Allpahuayo, Malaise trap, (I.E. Sääksjärvi et al. leg.), H1(16), 21.xii.2000, 1♂, ZMUT; idem, but I1, 1.xii.2000, 1♂, ZMUT; idem, but I1(16), 15.xii.2000, 1♂, ZMUT; idem, but H1(16), 21.xii.2000, 1♂, ZMUT; idem, but I1, 1.xii.2000, 1♂, ZMUT; idem, but I1, 1.xii.2000, 1♂, ZMUT; idem, but I1, 20.i.2001, 1♂, ZMUT; idem, but H1(4), iv.2000, 1♂, ZMUT; idem, but I1(16), 15.xii.2000, 1♂, ZMUT.

Hymenoepimecis tedfordi **Gauld, 1991**
Figures 14, 29, 44, 59, 74, 89

Hymenoepimecis tedfordi Gauld, 1991: 340.

Diagnosis. This species can be distinguished from all other *Hymenoepimecis* by the combination of the following characters: 1) fore wing hyaline; 2) mesosoma orange with propleuron, pronotum, metapleuron ventrally, and propodeum black (metapleuron entirely orange in Nicaraguan specimens); 3) epicnemial carina present ventrally, sometimes visible laterally; 4) metasoma entirely blackish; 5) female with ovipositor 1.0–1.1 times as long as hind tibia.

   Distribution. Costa Rica and Nicaragua* (Fig. 108).

   Biological notes. Parasitoid of *Leucauge mariana* (Keyserling, 1881) (Araneae: Tetragnathidae) (Gauld, 1991; Eberhard, 2013).

   Material examined. Nicaragua, Jinotega, RN Cerro Kilambé, 1310 ± 10 m., 13.56541/-85.69785, Pasture/cloud, forest edge, 22–26.v.2011, Malaise trap (without collector), LLAMA#Ma-D-05-1-01 [sic], 1♀, ZMUT.

Hymenoepimecis uberensis **Pádua & Onody, 2015**
Figures 15, 30, 45, 60, 75, 90, 106

Hymenoepimecis uberensis Pádua & Onody, 2015: 190.

Diagnosis. See Pádua et al. (2015).

   Distribution. Brazil and Peru* (Fig. 112).

Biological notes. Host unknown.

Material examined. Peru, La Merced, Fundo Genova, 21.vi.2008, Malaise trap (without collector), AECID: A/013484/07, 1♀, ZMUT; idem, but 7.vi.2008, 1♂, ZMUT; Cusco, ca. P.V. Tono, 12°57'48"S, 71°32'06"W, 862 m., 26.ix.2007, Malaise trap (C. Castillo leg.), 1♂, ZMUT; Dept. Madre de Dios, Los Amigos, 380955, 769E/8610042,474N, a.s.l.: 240.2 m., 26.vi–3.vii.2008, Malaise trap (I. Gómez leg.), 1♀, ZMUT; idem, but 380792,164E/8610919,14N, a.s.l.: 280.5 m., 7–14.viii.2008, 1♂, ZMUT; Marcapata [without others information], NHRS-HEVA #2908, 1♀, ZMUT.

Discussion

The present study increases the number of recognized *Hymenoepimecis* species to 27 species. In addition, is presented a large amount of faunistic records from different parts of Central and South America. It is also shown that *H. rafaelmartinezi* sp. nov. belongs to the *H. jordanensis* species group (Pádua et al. 2015) which is characterised by the following set of characters: 1) face sculptured below the insertion of antennae, with a longitudinal carina in the middle part of the face; 2) head with occipital carina projected, not curved upwards, with a dorsal concavity in the apex; 3) pronotum with the pocket-like structure reduced longitudinally; 4) sternite I with a ventral spine-like projection posteriorly. After the present study this species group is composed of five species (*H. amazonensis*, *H. jordanensis*, *H. kleini*, *H. rafaelmartinezi* sp. nov., and *H. uberensis*),

A noteworthy new character state was recorded for *Hymenoepimecis*: in *H. dolichocarinata* sp. nov., the epicnemial carina is ventrally present and extending to the level of the lower lateral corner of the pronotum. This character state is shared with most species of *Acrotaphus* (Pádua et al. 2020), and likely represents a homoplastic trait in the two genera.

Finally, the genus is reported for the first time from the Andes (Figs 107, 108). Two Peruvian species, both collected by Carol Castillo, were found from the Andean-Amazonian interface (Cusco, San Pedro, Cosñipata valley, 1302–1520 m). *Hymenoepimecis andina* sp. nov. and *H. castilloi* sp. nov. are both remarkable because they resemble *Polysphincta* Gravenhorst (and *Ticapimpla amazonica* Palacio, Broad, Sääksjärvi & Veijalainen, 2010) by the shape of the occiput. All other species of *Hymenoepimecis* have the occipital carina strongly raised and produced into a neck-like structure.

Acknowledgements

References

Brues CT, Richardson CH (1913) Descriptions of new parasitic Hymenoptera from British Guiana. Bulletin of the American Museum of Natural History 32: 485–503.

Brullé MA (1846) Tome Quatriene. Des Hymenopteres. Les Ichneumonides. Lepeletier de Saint-Fargeau A. "Histoire Naturelles des Insectes." Paris, 680 pp.

Cresson ET (1865) On the Hymenoptera of Cuba. Proceedings of the Entomological Society of Philadelphia 4: 1–200.

Eberhard WG (2013) The Polysphinctine Wasps *Acrotaphus tibialis*, *Eruga* ca. *gutfreundi*, and *Hymenoepimecis tedfordi* (Hymenoptera, Ichneumonidae, Pimplinae) Induce Their Host Spiders to Build Modified Webs. Annals of the Entomological Society of America 106(5): 652–660. https://doi.org/10.1603/AN12147

Gauld ID (1991) The Ichneumonidae of Costa Rica I. Memoirs of the American Entomological Institute 47: 1–589.

Gauld ID (2000) The re-definition of Pimplinae genus *Hymenoepimecis* (Hymenoptera: Ichneumonidae) with a description of a plesiomorphic new Costa Rica species. Journal of Hymenoptera Research 9: 213–219.

Gonzaga MO, Sobczak JF, Penteado-Dias AM, Eberhard WG (2010) Modification of *Nephila clavipes* (Araneae, Nephilidae) webs induced by the parasitoids *Hymenoepimecis bicolor* and *H. robertsae* (Hymenoptera, Ichneumonidae). Ethology Ecology & Evolution 22: 151–165. https://doi.org/10.1080/03949371003707836

Kriechbaumer J (1890) Ichneumoniden-Studien. Neue Ichneumoniden des Wiener Museums. II. Annalen des Naturhistorischen Hofmuseums Wien 5: 479–491.

Kumagai AF, Graf V (2002) Biodiversidade de Ichneumonidae (Hymenoptera) e monitoramento das espécies de Pimplinae e Poemeniinae do Capão da Imbuia, Curitiba, Párana. Revista Brasileira de Zoologia 19(2): 445–452. https://doi.org/10.1590/S0101-81752002000200010

Loffredo APS, Penteado-Dias AM (2009) New species of *Hymenoepimecis* Viereck (Hymenoptera, Ichneumonidae, Pimplinae) from Brazilian Atlantic forest. Revista Brazileira de Entomologia 53: 11–14. https://doi.org/10.1590/S0085-56262009000100004

Pádua DG, Sääksjärvi IE, Monteiro RF, Oliveira ML (2020) Review of the New World genus *Acrotaphus* Townes, 1960 (Hymenoptera: Ichneumonidae: Pimplinae), with descriptions of fifteen new species. Zootaxa 4719: 1–062. https://doi.org/10.11646/zootaxa.4719.1.1

Pádua DG, Oliveira ML, Onody HC, Sobczak JF, Sääksjärvi IE, Gómez IC (2015) The Brazilian Amazonian species of *Hymenoepimecis* Viereck, 1912 (Hymenoptera: Ichneumonidae: Pimplinae). Zootaxa 4058(2): 175–194. hhttps://doi.org/10.11646/zootaxa.4058.2.2

Pádua DG, Salvatierra L, Sobczak JF, Oliveira ML (2016) Parasitism of *Hymenoepimecis manauara* Pádua & Oliveira (Hymenoptera: Ichneumonidae: Pimplinae) on *Leucauge*

henryi Mello-Leitão (Araneae: Tetragnathidae) in Brazilian Amazonian. Biodiversity Data Journal 4: e11219. https://doi.org/10.3897/BDJ.4.e11219

Sobczak JF, Loffredo APS, Penteado-Dias AM, Gonzaga MO (2009) Two new species of *Hymenoepimecis* (Hymenoptera: Ichneumonidae: Pimplinae) with note on their spider hosts and behavior manipulation. Journal of Natural History 43(43): 2691–2699. https://doi.org/10.1080/00222930903244010

Sobczak JF, Loffredo APS, Camargo LF, Penteado-Dias AM (2012) *Hymenoepimecis neotropica* (Brues & Richardson) (Hymenoptera, Ichneumonidae, Pimplinae) parasitoid de *Araneus omnicolor* (Keyserling) (Araneae, Araneidae): first host record and new occurrence to Brazil. Revista Brasileira de Entomologia 56(3): 390–392. https://doi.org/10.1590/S0085-56262012005000055

Townes H, Townes M (1966) A catalogue and reclassification of neotropic Ichneumonidae. Memories of the American Entomological Institute 8: 1–367. https://doi.org/10.1080/00222930903244010

Wahl DB, Gauld ID (1998) The cladistics and higher classification of the Pimpliformes (Hymenoptera: Ichneumonidae). Systematic Entomology 23: 265–298. https://doi.org/10.1046/j.1365-3113.1998.00057.x

Yu DS, van Achterberg C, Horstmann K (2012) World Ichneumonoidea 2011: Taxonomy, Biology, Morphology and Distribution. Taxapad 2012, Vancouver. htpp://www.taxapad.com/ [accessed 20 May 2018]

RESEARCH ARTICLE

A new genus of Languriinae from Mexico (Coleoptera, Erotylidae), with comments on the potential mimic phenomenon of some languriines

Zheng-Zhong Huang[1], Xing-Ke Yang[1], Si-Qin Ge[1]

I *Insititue of Zoology, Chinese Academy of Sciences, 1 Beichen West Road, Chaoyang District, Beijing, 100101, China*

Corresponding author: Si-Qin Ge (gesq@ioz.ac.cn)

Citation: Huang Z-Z, Yang X-K, Ge S-Q (2020) A new genus of Languriinae from Mexico (Coleoptera, Erotylidae), with comments on the potential mimic phenomenon of some languriines. ZooKeys 935: 93–101. https://doi.org/10.3897/zookeys.935.49957

Abstract

A new genus of Languriinae, *Tomolanguria* Huang, **gen. nov.** is erected for a single species, *Languria aculeata* Gorham, 1887 from Mexico. It is similar to the Neotropical genus *Languria* Latreille, 1802. The differential diagnosis of this new genus is based on the structural features of the elytral apices and slight impressions present on each elytron. *Languria aculeata* is designated as the type species of the new genus. This species is redescribed and illustrated (all the three specimens examined are shown in the dorsal, ventral, and lateral views). Finally, a mimic relationship between this new genus and genus *Paederus* Fabricius, 1775 (Staphylinidae) is discussed.

Keywords

Cucujoidea, Neotropical Region, new combination, *Tomolanguria*

Introduction

Languria aculeata was first described by Gorham (1887), based on three specimens in the Sallé collection. Martins and Perreira (1965) accomplished a revision of the Neotropical Languriinae, but they did not examine the specimens of *L. aculeata* and just cited Gorham's original description in their work. In 2017, we had a chance to examine specimens of Languriinae, including the syntypes of *L. aculeata*, in the Natu-

ral History Museum, London. The elytral structure of *L. aculeata* clearly separates this species from all known Neotropical genera of Languriinae. Hence, we propose a new genus and a new combination for its type species.

Materials and methods

The type series of *Tomolanguria* gen. nov., *Anadastus ornatus* Arrow, 1925, *A. pulchellus* Arrow, 1925, *A. jucundus* (Gorham, 1903), *Clerolanguria tricolor* (Fabricius, 1787), and *Stenolanguria tricolor* Fowler, 1885 are deposited in the Natural History Museum, London, United Kingdom (**BMNH**). The holotypes of *Paederolanguria holdhausi* Mader, 1939 and *P. klapperichi* Mader, 1955 are deposited in the Naturhistorisches Museum, Basel, Switzerland (**NHMB**). The holotype of *Paederolanguria alternata* (Zia, 1959) and non-type specimen of *P. holdhausi* are deposited in the Institute of Zoology of the Chinese Academy of Sciences, Beijing, China (**IZCAS**). The holotype of *Stenolanguria robusta* Villiers, 1958 is deposited in the Muséum national d'Histoire naturelle, Paris, France (**MNHN)**. Label data are given with separate lines on labels indicated by / and separate labels by //. Other comments and remarks are in square brackets [].

All photographs were taken with a Canon 5D Mark III digital camera equipped with a Canon MP-E 65 mm lens. The images were stacked with Helicon Focus 6.7.1 and modified in Adobe Photoshop CS6 to correct for contrast, brightness, and imperfections.

Body length was measured from the apices of mandibles to the apices of elytra.

Taxonomy

Family Erotylidae Latreille, 1802
Subfamily Languriinae Hope, 1840
Tribe Languriini Hope, 1840

Genus *Tomolanguria* Huang, gen. nov.
http://zoobank.org/9EBD53DE-64BC-4284-8E6E-81BDB8098B34

Type species. *Languria aculeata* Gorham, 1887.
Diagnosis. The new genus is a member of tribe Languriini, based on the presence of a frontoclypeal suture; the antennal club composed of more than three antennomeres and relatively oval in cross-section. The only species of *Tomolanguria* can be separated from other languriine genera by the following combination of characters: body length 8.5–9.5 mm, body slender without unified metallic luster, at least prothorax without any metallic luster; antennal club not very dilated; eyes moderate in size and with fine facets; mandibles similar to each other; pronotum finely punctured, without basal foveae; lateral sides of pronotum rounded and prothorax more or less subcylindric, not flattened; elytral epipleura distinct, each elytron with transverse and

very weak depressions, apices of elytra being produced and strongly tapering, rounded and with several small denticles.

Comparision. The elytral structure, which often shows the differences among genera of Languriinae, is a relatively reliable morphological character. *Tomolanguria* is closely related to genus *Languria* Latreille, 1802, sharing with the latter a similar external appearance. From *Languria*, it can be distinguished by having the antennal club not very dilated; lateral sides of pronotum rounded and prothorax more or less subcylindric; each elytron with transverse and weak depressions, and apices of elytra being more or less produced and strongly tapering, and also with several small denticles. However, the elytral apex of *Languria* is simply rounded and somewhat tapering, and neither produced nor with denticles. *Tomolanguria* also resembles the Neotropical genera *Acropteroxys* Gorham, 1887 and *Langurites* Motschulsky, 1860. *Tomolanguria* differs from *Acropteroxys* in having the pronotum finely punctured, with lateral side rounded, and apices of the elytra produced and bearing small denticles. *Tomolanguria* differs from *Langurites* in having the lateral side of pronotum rounded and the apices of the elytra with neither a sharp sutural angle nor an outer angle.

On the other hand, a similar structure of the elytra is demonstrated in the Oriental genus *Paederolanguria* Mader, 1939 and African genus *Stenolanguria* Fowler, 1885 (Fig. 3G, H). The new genus can be easily separated from the former by the following characters: 1) elytral epiplerura broader and more distinct; 2) apex of prosternal process bent sharply downward (Fig. 2G, H); 3) mesoventrite without punctation and nearly smooth (Fig. 2B, C); 4) apex of elytra produced and with several small denticles (Fig. 2I, J); 5) abdomen without postmetacoxal lines. (Fig. 2D, E). *Tomolanguria* can be easily separated from *Stenolanguria* in having the head with fine punctures and the apex of elytra rounded; in *Stenolanguria*, the sutural angle is not produced and the outer angle of the elytra is produced and sharp, without denticles.

Etymology. The name is derived from the Greek word Τομός (Latin transliteration as *tomós*, meaning "sharp", referring to the apex of the elytra) and the generic name *Languria* (as in *Paederolanguria*, *Megalanguria*, *Caenolanguria*, etc.). Gender feminine.

Distribution. Mexico, San Andrés Tuxtla.

Included taxa. Only one species.

Tomolanguria aculeata **(Gorham, 1887), comb. nov.**
Figure 1A–L

Languria aculeata: Gorham 1887: 11, tab. I, fig 17; Fowler 1908: 29; Schenkling 1928: 16; Blackwelder 1945: 426; Martins and Perreira 1965: 154.

Type locality. Mexico, San Andrés Tuxtla.

Redescription. Body length 8.5–9.5 mm. Body narrow and elongate, moderately convex. Integument finely and sparsely punctured. Head pitch black. Antenna brown except for last five antennomeres yellowish. Prothorax orange. Basal third of elytra coppery green or metallic blue, remainder deep brown or black, without metallic luster.
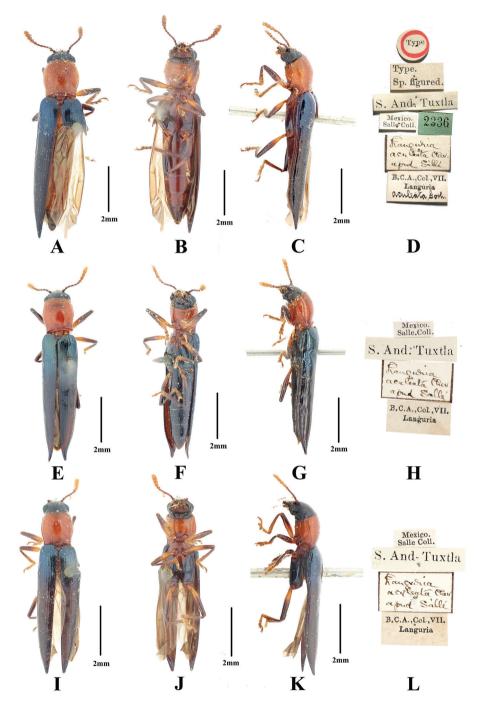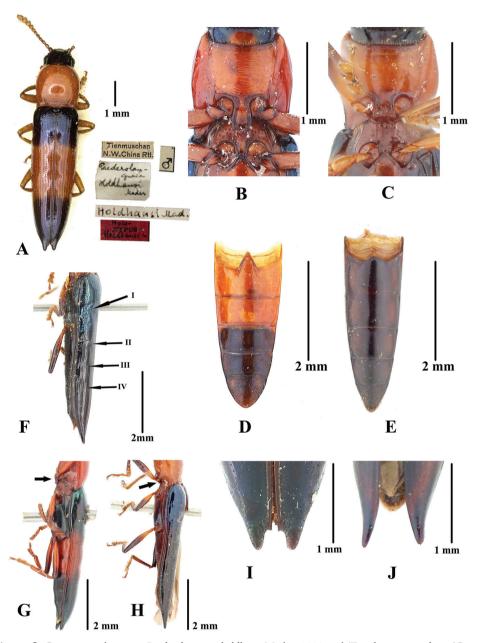
Figure 1. *Tomolanguria aculeata* (Gorham, 1887), comb. nov. **A–D** lectotype of *T. aculeata*: **A** dorsal habitus **B** ventral habitus **C** lateral view **D** labels **E–H** paralectotype of *T. aculeata*: **E** dorsal habitus **F** ventral habitus **G** lateral view **H** labels **I–L** second paralectotype of *T. aculeata*: **I** dorsal habitus **J** ventral habitus **K** lateral view **L** labels. Scale bars: 2mm.

Figure 2. Comparison between *Paederolanguria holdhausi* Mader, 1939 and *Tomolanguria aculeata* (Gorham, 1887), comb. nov. **A** Holotype of *Paederolanguria holdhausi* Mader, 1939 **B** *P. holdhausi*, prosternum and mesoventrite with punctures, non-type **C** *T. aculeata*, prosternum and mesoventrite without punctures, paralectotype **D** *P. holdhausi*, abdomen, non-type **E** *T. aculeata* comb. nov., abdomen, paralectotype **F** lateral view of *T. aculeata*, black arrows show the depressions on the elytron, paralectotype **G** later view of body of *P. holdhausi*, black arrow shows the prosternal process nearly straight, non-type **H** same of *T. aculeata*, black arrow shows the prosternal process downwards, paralectotype **I** *P. holdhausi*, apex of the elytra, non-type **J** *T. aculeata* comb. nov., apex of elytra, paralectotype. Scale bars: 1 mm (**A–C, I, J**); 2 mm (**D–H**).
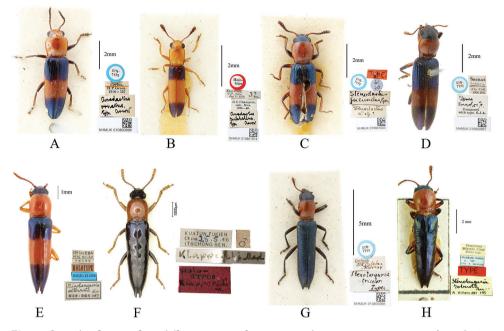
Figure 3. Body of species from different genera of Languriinae that may imitate genus *Paederus*. **A** *Anadastus ornatus* Arrow, 1925, syntype **B** *A. pulchellus* Arrow,1925, holotype **C** *A. jucundus* (Gorham, 1903), syntype, synonym of *A. bifasciatus* (Motschulsky, 1860) **D** *Clerolanguria tricolor* (Fabricius, 1787), syntype **E** *Paederolanguria alternata* (Zia, 1959), holotype **F** *P. klapperichi* Mader, 1955, holotype **G** *Stenolanguria tricolor* Fowler, 1885, syntype **H** *S. robusta* Villiers, 1958, holotype. Scale bar: 2 mm (**A–D, H**); 1 mm (**E, F**); 5 mm (**G**).

Antenna with 11 antennomeres and club composed of five fringed antennomeres. Antennomere III almost as long as antennomere IV, antennomere V subequal to antennomere VI, both of them shorter than each of antennomeres III or IV, antennomere VII subtriangular but slightly dilated, antennomeres VIII–XI dilated, apex of antennomere XI rounded. Head with fine punctation, nearly smooth. Clypeus broader than long. Eyes large, finely faceted. Mandibles robust and with outer side nearly straight.

Pronotum slightly convex, distinctly longer than broad, with sides rounded, constricted at the base. Pronotum finely punctured, without basal foveae. Anterior angle rounded, posterior angle acute but not produced. Lateral and basal margins beaded. Prohypomera smooth, without punctation or folds. Prosternal process long, with apex strongly bent downwards. Procoxal cavities open. Mesoventrite without punctation, nearly smooth (Fig. 2C).

Scutellar shield short and cordiform, apex not acute. Elytra regularly striate-punctate, vanishing before apex. Elytral epipleura distinct, narrow. Elytra at humeri slightly broader than base of pronotum. Sides of elytra parallel, narrowed posteriorly. Each elytron with four shallow transverse depressions (Fig. 2F). Elytral apex distinctly pro-

duced and acute, laterally curved, with four or five coarse denticles (Fig. 2J). Abdomen finely punctured, postmetacoxal lines absent (Fig. 2E).

Material examined. *Lectotype* (BMNH), female, here designated, labeled: "Type" [circular label with red margin]// "Type. /Sp. figured." // "S. And. Tuxtla" // "Mexico./ Salle Coll."// "2336" [green label]// "*Languria/ aculeata* Chev./ apud Sallé" [handwriting]// "B. C. A., Col., VII./ *Languria/ aculeata*, Gorh."(Fig. 1D). *Paralectotypes* (BMNH), two females, with the same labels (Fig. 1H, L).
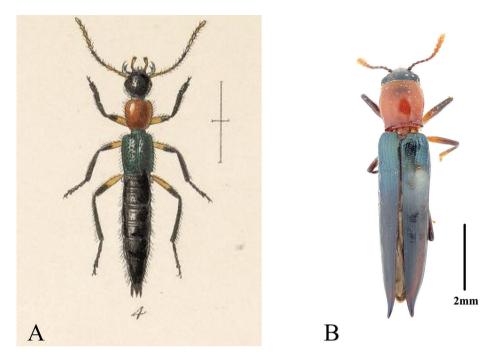
Distribution. Mexico, San Andrés Tuxtla.

Discussion

The potential mimicry between Languriinae and Staphylinidae has been recorded (Mader 1939; Reid and Noerdjito 1994). When Mader (1939) erected the genus *Paederolanguria*, which was named after the genus *Paederus* Fabricius, 1775, he designated *P. holdhausi* (Fig. 2A) as the type species and mentioned that it displayed a color pattern similar to that in species of *Paederus*. (Staphylinidae). Reid and Noerdjito (1994) also reported a similarity between an undetermined species of Languriinae and *Paederus* from Java. The specimens examined in this study and an additional search of the Internet shows that such a mimic phenomenon is not rare in Languriinae and that it demonstrates two different forms. Some languriines show only the characteristic color pattern of *Paederus*, with red and alternative blue or dark stripes, including several species from the genus *Anadastus* Gorham, 1887 (Fig. 3A–C): *Clerolanguria tricolor* (Fabricius, 1787) (Fig. 3D), and *Languria trifasciata* Say, 1823. Some others not only have the similar color pattern but also somewhat modified structure, such as their bodies are more slender, with antennae not very dilated, pronotum rounded, elytra with weak transverse depressions, and elytral apex more or less produced or acute, which can be observed in species from the genera *Paederolanguria*, (Fig. 3E, F), *Stenolanguria* (Fig. 3G, H), and *Tomolanguria* (Fig. 1A, E, I).

After discussion with Dr José Luis Navarrete-Heredia, a specialist of Staphylinidae, we suggest that *Paederus signaticornis* Sharp, 1886 should be a suitable model for *Tomolanguria aculeata* (Fig. 4A, B). Both *P. signaticornis* and *T. aculeata* share the same distribution in Mexico, and the elytral color pattern of *T. aculeata* matches with that of *P. signaticornis*. For example, the basal third of the elytra of *T. aculeata* with a green metallic luster mimics the elytral color of *P. signaticornis*, the remaining part of the nearly black elytra mimics the color of the staphylinid abdomen. Besides, the color pattern and depressions on the elytra probably mimic the segmentation of the abdomen, and the produced apex of elytra may mimic tergite IX of *P. signaticornis*.

The genus *Paederus* is famous for their toxic, paederus dermatitis (Frank and Kanamitsu 1987). Kellner and Dettner (1996) suggested that the toxin is the basis for prey rejection. Their classic color pattern may be an example of aposematism, a warning signal to potential predators. Languriines may imitate the warning signals, even the appearances of *Paederus*, as an anti-predator strategy. In summary, we suppose that there may be a potential mimic relationship between this new genus *Tomolanguria* and genus *Paederus*.

Figure 4. Comparison between *Paederus signaticornis* Sharp, 1886 and *Tomolanguria aculeata* (Gorham, 1887), com. nov. **A** habitus of *P. signaticornis* (from Sharp 1886: pl. XVI, fig. 4) **B** habitus of *T. aculeata* comb. nov. Scale bars: 2 mm.

Acknowledgements

References

Blackwelder RE (1945) Checklist of the coleopterous insects of Mexico, Central America, the West Indies, and South America. Part 3. Bulletin of the United States National Museum 185: i–iv, 343–550. https://doi.org/10.5479/si.03629236.185.3

Frank JH, Kanamitsu K (1987) *Paederus*, *Sensu Lato* (Coleoptera: Staphylinidae): natural history and medical importance. Journal of Medical Entomology 24(2): 155–191. https://doi.org/10.1093/jmedent/24.2.155

Fowler WW (1908) Coleoptera fam. Erotylidae subfam. Languriinae. In: Wytsman P (Ed.) Genera Insectorum. Vol. 78. P. Wytsman, Bruxelles, 1–45.

Gorham HS (1887) Erotylidae, Endomychidae and Coccinellidae. In: Porter RH (Ed.) Biologia Centrali-Americana. Insecta. Coleoptera, Vol. III. Taylor & Francis, London, 276 pp.

Kellner RLL, Dettner K (1996) Differential efficacy of toxic pederin in deterring potential arthropod predators of *Paederus* (Coleoptera: Staphylinidae) offspring. Oecologia 107(3): 293–300. https://doi.org/10.1007/BF00328445

Mader L (1939) Neue Coleopteren aus China. Entomologisches Nachrichtenblatt 13: 41–51.

Martins UR, Perreira FS (1965) Revisão dos Languriinae neotropicais (Coleoptera, Languriidae). Archivos de Zoologia do Estado de São Paulo 13: 139–300.

Navarrete-Heredia JL, Newton AF, Thayer MK, Ashe JS, Chandler DS (2002) Guía Ilustrada para los Géneros de Staphylinidae (Coleóptera) de México. Illustrated Guide to the Genera of Staphylinidae (Coleóptera) of Mexico. Universidad de Guadalajara and CONABIO, Mexico, 401 pp.

Reid CAM, Noerdjito WA (1994) Mimicry of a *Paederus* species (Col., Staphylinidae) by a species of Languriinae (Col., Languriidae) in Java. Entomologist's Monthly Magazine 130: 63–65.

Schenkling S (1928) Languriidae. In: Junk W, Schenkling S (Eds) Coleopterorum Catalogus, Pars 100, W. Junk, Berlin, 40 pp.

Sharp D (1886) Fam. Staphylinidae. Biologia Centrali-Americana. Insecta, Coleoptera. Vol. 1. Part 2. Taylor & Francis, London, 537–672. [pls 14–17] https://biodiversitylibrary.org/page/577032

RESEARCH ARTICLE

A peer-reviewed open-access journal
ZooKeys
Launched to accelerate biodiversity research

Even hotter hotspot: description of seven new species of many-plumed moths (Lepidoptera, Alucitidae) from Mount Cameroon

Peter Ustjuzhanin[1,2], Vasily Kovtunovich[3], Vincent Maicher[4,5,6], Szabolcs Sáfián[5,7], Sylvain Delabye[4,5], Alexander Streltzov[8], Robert Tropek[4,6]

1 *Altai State University, Lenina 61, Barnaul, RU-656049, Russia* **2** *Biological Institute, Tomsk State University, Lenina Prospekt 36, Tomsk 634050, Russia* **3** *Moscow Society of Nature Explorers, Bolshaya Nikitskaya 2, Moscow, RU-125009, Russia* **4** *Institute of Entomology, Biology Centre of the Czech Academy of Sciences, Branišovská 31, CZ-37005 České Budějovice, Czech Republic* **5** *Faculty of Science, University of South Bohemia, Branišovská 1760, CZ-37005 České Budějovice, Czech Republic* **6** *Department of Ecology, Faculty of Science, Charles University, Viničná 7, CZ-12844 Prague, Czech Republic* **7** *Institute of Silviculture and Forest Protection, University of Sopron, Bajcsy-Zsilinszky u. 4. H-9945 Sopron, Hungary* **8** *Herzen State Pedagogical University of Russia, 48, Moika Emb., Saint-Petersburg, 191186, Russia*

Corresponding author: Robert Tropek (robert.tropek@gmail.com)

Citation: Ustjuzhanin P, Kovtunovich V, Maicher V, Sáfián S, Delabye S, Streltzov A, Tropek R (2020) Even hotter hotspot: description of seven new species of many-plumed moths (Lepidoptera, Alucitidae) from Mount Cameroon. ZooKeys 935: 103–119. https://doi.org/10.3897/zookeys.935.49843

Abstract

Mount Cameroon, SW Cameroon, has already been described as a unique hotspot of the many-plumed moth (Lepidoptera, Alucitidae), with their local diversity unrivalled in the entire Afrotropics. We confirm its importance with description of seven new species: *Alucita bakweri* Ustjuzhanin & Kovtunovich, **sp. nov.**, *Alucita jana* Ustjuzhanin & Kovtunovich, **sp. nov.**, *Alucita bakingili* Ustjuzhanin & Kovtunovich, **sp. nov.**, *Alucita tatjana* Ustjuzhanin & Kovtunovich, **sp. nov.**, *Alucita zuza* Ustjuzhanin & Kovtunovich, **sp. nov.**, *Alucita deja* Ustjuzhanin & Kovtunovich, **sp. nov.**, and *Alucita bokwango* Ustjuzhanin & Kovtunovich, **sp. nov.** These descriptions have raised the known local diversity of many-plumed moth species on Mount Cameroon to 22, i.e., over a quarter of the known Afrotropical biodiversity of this group. This study also emphasises the great conservation importance of the area.

Introduction

Mount Cameroon has recently been recognised as a unique biodiversity hotspot for many-plumed moths (Lepidoptera, Alucitidae) (Ustjuzhanin et al. 2018), an easily recognisable family of Lepidoptera because of their characteristic six-lobed wings. As reviewed in Ustjuzhanin et al. (2018), Alucitidae are strongly understudied in the Afrotropics. While several recent faunistic (Maicher et al. 2016; Przybyłowicz et al. 2019; Delabye et al. 2020) and taxonomic (Przybyłowicz 2013; Sáfián and Tropek 2016; Yakovlev and Sáfián 2016; Sáfián et al. 2019) discoveries have shown the Mount Cameroon region as an important but largely understudied locality for lepidopteran biodiversity, its importance for Alucitidae biodiversity in particular remains unrivalled. Of 70 Afrotropical species of many-plumed moths, 32 are known from the Guineo-Congolian forest zone (De Prins and De Prins 2019); 15 of these have been already described or reported from Mount Cameroon (Ustjuzhanin et al. 2018).

In this study, we report on a second part of the material sampled during our long-term study of lepidopteran diversity in rainforests of Mount Cameroon (e.g., Maicher et al. 2018, 2019). Seven species of *Alucita* are described as new for science.

Materials and methods

Abbreviations

CUK   personal collections of P. Ustjuzhanin and V. Kovtunovich, Novosibirsk and Moscow, Russia.
NECJU   Nature Education Centre, Jagiellonian University, Kraków, Poland.

Material sampling and processing

All specimens were collected in eight rainforest localities on the south-western and southern slopes of Mount Cameroon at elevations ranging from 350 to 2200 m a.s.l. between November 2014 and October 2017 (Fig. 1). All specimens were attracted to light. The detailed sampling protocol was described in Ustjuzhanin et al. (2018). Holotypes will be stored in NECJU, paratypes will be split between NECJU and CUK.

Genitalia of most specimens were dissected and examined. For their dissection and preparation of permanent slides, we followed a protocol described in Ustjuzhanin et al.
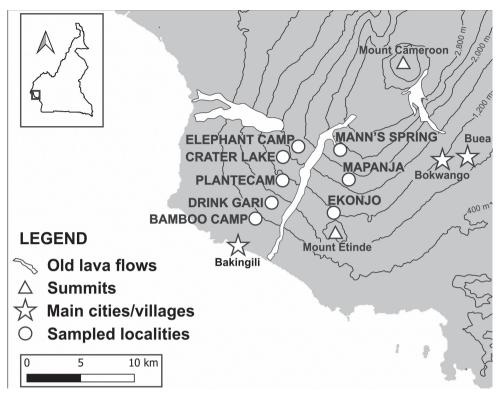
Figure 1. Map of the Mount Cameroon region with the sampling localities.

(2018). Each permanent preparation received a unique code under which it is searchable in the collections where they are stored; the relevant numbers are listed in captions of the genitalia figures.

Sampling localities

All sampling localities (Fig. 1) are listed below; the localities not included in Ustjuzhanin et al. (2018) are marked with *:

Bamboo Camp. Bamboo Camp (350 m a.s.l.), Mount Cameroon (SW slope), 4.0879°N, 9.0505°E; a lowland rainforest with historical disturbances from selective logging.

*__Crater Lake.__ Crater Lake camp (1450 m a.s.l.), Mount Cameroon (SW slope), 4.1443°N, 9.0717°E; a submontane rainforest locally disturbed by forest elephants.

Drink Gari. Drink Gari camp (650 m a.s.l.; also known as "Drinking Gari"), Mount Cameroon (SW slope), 4.1014°N, 9.0610°E; a lowland rainforest with canopy layer presumed to be closed.

*__Ekonjo.__ Ekonjo camp (1150 m a.s.l.), Mount Cameroon (S slope), 4.0881°N, 9.1168°E; an upland closed-canopy rainforest.

Elephant Camp. Elephant Camp (1850 m a.s.l.), Mount Cameroon (SW slope), 4.1170°N, 9.0729°E; a montane forest with a sparse canopy layer as a consequence of natural disturbances by forest elephants.

*Mann's Spring.** Mann's Spring camp (2200 m a.s.l.), Mount Cameroon (SW slope), 4.1428°N, 9.1225°E; a montane forest at the natural timberline.

*Mapanja.** Mapanja camp (1850 m a.s.l.), Mount Cameroon (S slope), 4.1157°N, 9.1315°E; a montane forest with canopy layer presumed to be closed.

PlanteCam. PlanteCam camp (1100 m a.s.l.; also misspelled as "Planticamp"), Mount Cameroon (SW slope), 4.1175°N, E9.0709°E; an upland rainforest in the transition between the lowland and montane zones, with a sparse canopy layer as a consequence of natural disturbances by forest elephants.
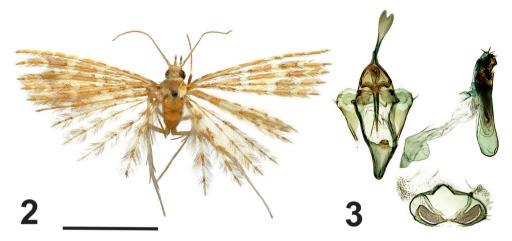
Species descriptions

Alucita bakweri Ustjuzhanin & Kovtunovich, sp. nov.
http://zoobank.org/4CCBE08C-2366-40FF-B52F-D7B3D60DF816
Figs 2, 3

Type material. *Holotype* • 1 male, (NECJU 201901) Cameroon, PlanteCam, 1100 m a.s.l., Mount Cameroon (SW slope), 4.1175°N, 9.0709°E, 11–18.XII.2014, lgt. V. Maicher, Sz. Sáfián, Š. Janeček, R. Tropek.

Diagnosis. In the yellowish colour of its wings, this species resembles *Alucita ferruginea* Walsingham, 1881, *Alucita balioxantha* (Meyrick, 1921), and *Alucita compsoxantha* (Meyrick, 1924), from which it differs in the structure of male genitalia. Genitalia of the new species differ from *A. balioxantha* by a thin sharp gnathos, prolonged saccus, and short, wide and wing-like valvae (Fig. 19). *Alucita balioxantha* gnathos is wider, with a blunt and round top, the saccus is archlike and not prolonged, and valvae are thin and lancet-like. In the shape of the uncus and gnathos of the male genitalia, *A. bakweri* is similar to *A. ferruginea*, from which it differs in having an elongated, narrowing saccus without the distinct notch on its outer edge. Additionally, unlike *A. ferruginea*, *A. bakweri* has clusters of small acicular cornuti apically on the aedaeagus. Moreover, its valvae are short, wide and wing-like, with a bundle of thin needle-like cornuti in its apical part. Whilst male genitalia of the new species have a forked uncus and comparatively short aedeagus, *A. compsoxantha* has a simple short uncus and a very long aedeagus.

External characters. Wingspan 18 mm. Head with white scales, thorax and tegulae yellowish-brown. Labial palpus yellow, thin, straight, twice as long as longitudinal eye diameter. Third segment discrete, directed forward, median part framed by brown lines, apically pale and sharp. Antenna white, basally thickened. Wings yellowish-brown, with four white transverse lines. Wings basally darkened with brown scales. Abdomen yellowish-brown. Hind leg pale yellow.

Male genitalia. Uncus long, distally widened, apically with triangle notch. Gnathos narrow, apically tapered, in length equal to uncus. Gnathos arms short, thick,

Figures 2, 3. *Alucita bakweri* Ustjuzhanin & Kovtunovich, sp. nov. **2** adult male, Holotype, NEJCU **3** male genitalia, Holotype, preparation slide no. 201901. Scale bar: 5 mm.

smoothly bent inwards. Valves short, wide, wing-shaped, apically with bundle of fine acicular setae. Anellus arms wide, short. Saccus elongated, narrow triangular. Aedeagus almost straight, with an elongated uncinate cornutus in middle, groups of fine acicular cornuti distally, and narrow sharp cornuti sticking out apically.

Distribution. Cameroon.

Flight period. December.

Etymology. We name the species after the Bakweri people, the main ethnic group of the Mount Cameroon region. Without the priceless assistance of numerous local people our project would not be possible. We hope such dedication will encourage protection of the species' habitats.

Alucita jana Ustjuzhanin & Kovtunovich, sp. nov.
http://zoobank.org/2EE6AAB9-8CCB-4123-B957-786B6776CB92
Figs 4, 5

Type material. *Holotype* • male, (NECJU 201902) Cameroon, PlanteCam, 1100 m a.s.l., Mount Cameroon (SW slope), 4.1175°N, 9.0709°E, 09–14.IV.2015, lgt. V. Maicher, Sz. Sáfián, S. Janeček, R. Tropek. *Paratypes* • 1 male, (CUK), Ekonjo, 1150 m a.s.l., Mount Cameroon (SW slope), 4.0881°N, 9.1168°E, 24.X.2017, lgt.V. Maicher, P. Potocký, S. Delabye • 1 male, (CUK), Mapanja camp, 1850 m a.s.l., Mount Cameroon (SW slope), 4.1157°N, 9.1315°E, 25.X.2017, V. Maicher, P. Potocký, S. Delabye.

Diagnosis. The new species is similar in the shape of the uncus and valves of the male genitalia to *Alucita tesserata* (Meyrick, 1918) (Fig. 20), but it differs in the apically narrow gnathos and the presence of a group of fine acicular cornuti in the aedeagus. *Alucita jana* also differs from *A. tesserata* in the wing colouration.

Figures 4, 5. *Alucita jana* Ustjuzhanin & Kovtunovich, sp. nov. **4** adult male, Holotype, NEJCU **5** male genitalia, Holotype, preparation slide no. 201902. Scale bar: 5 mm.

External characters. Wingspan 15 mm. Head, thorax and tegulae with brown appressed scales. Labial palpus wide, short, 1.5 longer than longitudinal eye diameter, slightly bent upwards, brown scaled inside and outside. Third segment discrete, apically sharp. Antenna yellowish-brown. Wings yellowish-brown, distinctive pale brown band medially. Forewings show a dark brown postmedial band. Forewing basally with dark brown scales, hindwing basally light. Distally, alternating portions of brown and yellowish scales. Fringe of wings yellow, with alternating portions of brown hairs. Hind leg pale yellow.

Male genitalia. Uncus long, apically slightly widened. Gnathos long, distally widened, apically slightly tapered, equal to uncus in length. Valve short, finger-like, membranous. Anellus arms narrow, long, apically slightly widened. Saccus with oval outer edge. Aedeagus straight, basally widened, apically with a group of fine acicular cornuti.

Distribution. Cameroon.

Flight period. April, October.

Etymology. The species name is a noun in apposition in honour to Robert Tropek's mother, Jana Tropková.

Alucita bakingili Ustjuzhanin & Kovtunovich, sp. nov.

http://zoobank.org/C1503460-2901-4437-BFA7-49D660E2462F

Figs 6–8

Type material. *Holotype* • male (NECJU 201903) Cameroon, Bamboo Camp, 350 m a.s.l., Mount Cameroon (SW slope), 4.0879°N, 9.0505°E, 12–20.XII.2014, lgt. V. Maicher, Sz. Sáfián, S. Janeček, R. Tropek. *Paratypes* • 1 male (CUK), same data as the holotype • 1 female (NECJU 201908), same data as the holotype • 1 male, (CUK), PlanteCam, 1100 m a.s.l., Mount Cameroon (SW slope), 4.1175°N, 9.0709°E, 29.I.-07.II.2016, lgt. V. Maicher, Sz. Sáfián, R. Tropek.

Figures 6–8. *Alucita bakingili* Ustjuzhanin & Kovtunovich, sp. nov. **6** adult male, Holotype, NEJCU **7** male genitalia, Holotype, preparation slide no. 201903 **8** female genitalia, Paratype, preparation slide no. 201908. Scale bar: 5 mm.

Diagnosis. The new species resembles *Alucita fokami* Ustjuzhanin & Kovtunovich, 2018 in external appearance but it substantially differs in both male and female genitalia (for genitalia of *A. fokami*, see Ustjuzhanin et al. 2018). *Alucita bakingili* is similar to *Alucita seychellensis* (T.B. Fletcher, 1910) in male genitalia (illustrated in Ustjuzhanin and Kovtunovich 2016), specifically in the sclerotized process on the sacculus. *Alucita bakingili* also differs from *A. seychellensis* in its wide gnathos, the narrow triangular valves and the short narrow uncus. In the female genitalia, the new species is similar to *Alucita rhaptica* (Meyrick, 1920) (Fig. 21), from which it differs in its rectangular lamina postvaginalis and in the longer and narrower ductus.

External characters. Wingspan 12–15 mm, holotype 12 mm. Head, thorax and tegulae with dark grey scales and an admixture of white scales. Labial palpus grey outside, white inside, 1.5 times longer than longitudinal eye diameter, directed forward. Third segment short, apically slightly sharpened. Antenna pale grey, distinct dark elongated spot basally just beyond scape. Wings mottled, yellowish-grey, medially with a poorly expressed yellowish-brown band. Alternating portions of grey and white scales shaped as elongated strokes, spots and points on lobe of all wings. Fringe with alternating portions of grey and white hairs. Hind leg pale yellow.

Male genitalia. Uncus short, straight, slightly widened apically. Gnathos wide, sharply narrowing apically, a little longer than uncus. Valve short, narrow triangular, membranous. Sacculus with membranous process containing a large sclerotized uncinate process in lower part. Anellus arms very long, basally wide, medially narrowing, apically widened and slightly bent. Saccus with oval outer edge. Aedeagus long, straight, with two robust cornute in this medial part.

Female genitalia. Papilla analis narrow, elongated. Posterior apophyses thin, straight. Anterior apophyses also thin, straight, equal in length to posterior apophyses. Lamina postvaginalis sclerotized, wide, rectangular, with blunt angular lateral projections. Antrum corrugated, wide, short. Ductus wide, medially swollen. Ductus seminalis short,

well expressed. Bursa copulatrix small, oval, with robust elongated comb-shaped signum located basally and reaching base of ductus seminalis.

Distribution. Cameroon.

Flight period. December to February.

Etymology. The species is named after Bakingili, a village at the southern foothills of Mount Cameroon, in which area it was collected. Numerous people from the village helped our project as field assistants and by many other ways, and therefore the community was crucial for its success. The Bakingili people are also necessary for protection of the species' natural area.

Alucita tatjana Ustjuzhanin & Kovtunovich, sp. nov.
http://zoobank.org/2CCDE55D-7D9C-413C-A5B0-42833DE8F770
Figs 9, 10

Type material. *Holotype* • female, (NECJU 201904) Cameroon, PlanteCam, 1100 m a.s.l., Mount Cameroon (SW slope), 4.1175°N, 9.0709°E, 09–14.IV.2015, V. Maicher, Sz. Sáfián, S. Janeček, R. Tropek; *Paratype* • 1 female, (CUK), Ekonjo, 1150 m a.s.l., Mount Cameroon (S slope), 4.0881°N, 9.1168°E, 24.X.2017, lgt. V. Maicher, P. Potocký, S. Delabye.

Diagnosis. The new species resembles *Alucita mischenini* Ustjuzhanin & Kovtunovich, 2018 in the light colour of its wings and the wide medial band, but it differs in its larger size (21 mm vs. 12–15 mm wingspan). Additionally, the position and shape of dark markings in the basal and distal portions of the wings differentiates *A. tatjana* from *A. mischenini* whose forewings bear extensive brown areas in in the basal portions and almost continuous dark brown marks covering the distal halves of the first two forewing lobes (Ustjuzhanin et al. 2018). Additionally, forewings of the new species differ from *A. mischenini* by the continuation of the brown medial band through most of the length of the second forewing lobe. In female genitalia, *A. tatjana* is similar to *A. compsoxantha* Meyrick, 1924 (Fig. 22), especially in the shape of the antrum and the absence of any signa in the bursa copulatrix. However, *A. tatjana* differs in its shorter and wider ductus and substantially shorter anterior and posterior apophyses. These species also differ in the colouration of their wings.

External characters. Wingspan 21 mm. Head, thorax and tegulae with appressed white scales. Labial palpus twice as long as longitudinal eye diameter, white, with a brown band of the third segment, thin, apically tapered, sharp. Antenna white. Scape extended and flattened. Wings white with well-expressed wide median band, brown on forewing and almost black on hindwing. Subterminal band narrower, consisting of brown spots of scales, intermittently traced throughout all lobes. First forewing lobe apically brown. Second forewing lobe with brown colouration continuous between median band and subterminal band. Forewing basally white with well-expressed dark brown fringes near the base of the cleft between the second and third lobes. Hindwing basally white with scattered dark brown scales and a prominent dark brown marking across base of second to sixth lobes. Hind leg pale yellow (although not so apparent in Fig. 9).

Figures 9, 10. *Alucita tatjana* Ustjuzhanin & Kovtunovich, sp. nov. **9** adult female, Holotype, NEJCU **10** female genitalia, Holotype, preparation slide no. 201904. Scale bar: 5 mm.

Female genitalia. Papilla analis narrow, elongated. Posterior and anterior apophyses thick, straight. Anterior apophyses equal in length to posterior apophyses. Antrum wide, goblet-like. Ductus short, expanded in median part around junction with ductus seminalis, and corrugated at junction with bursa copulatrix. Bursa copulatrix small, oval, without signa.

Distribution. Cameroon.

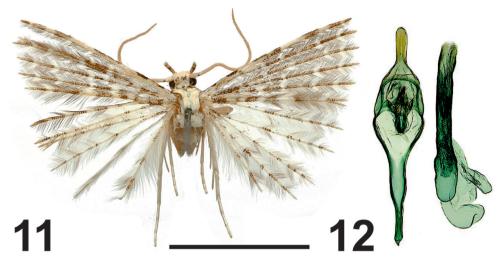**Flight period.** April, October.

Etymology. The species is a noun in apposition in honour to Petr Ustjuzhanin's sister, Tatjana Ustjuzhanina.

Alucita zuza Ustjuzhanin & Kovtunovich, sp. nov.

http://zoobank.org/3EFBC3D5-E44D-4F58-A1D4-3E5D049D58E3
Figs 11, 12

Type material. *Holotype* • 1 male, (NECJU 201905) Cameroon, Drink Gari, 650 m a.s.l., Mount Cameroon (SW slope), 4.1014°N, 9.0610°E, 11–23.IV.2015, lgt. V. Maicher, Sz. Sáfián, Š. Janeček, R. Tropek; *Paratypes* • 1 male, (CUK), same data as the holotype • 1 male (CUK), PlanteCam, 1100 m a.s.l., Mount Cameroon (SW slope), 4.1175°N, 9.0709°E, 29.I–07.II.2016, lgt. V. Maicher, Sz. Sáfián, R. Tropek • 1 male (CUK), Drink Gari, 650 m a.s.l., Mount Cameroon (SW slope), 4.1014°N, 9.061°E, 20.XI–10.XII.2014, lgt. V. Maicher, Sz. Sáfián, R. Tropek.

Diagnosis. In its male genitalia, the new species shares the elongated saccus and absence of valves with *A. fokami* (illustrated in Ustjuzhanin et al. 2018), but it differs in the narrow uncus which is not expanded apically, and in the absence of a long needle-like cornutus in the aedeagus.

Figures 11, 12. *Alucita zuza* Ustjuzhanin & Kovtunovich, sp. nov. **11** adult male, Holotype, NEJCU **12** male genitalia, Holotype, preparation slide no. 201905. Scale bar: 5 mm.

External characters. Wingspan 12 mm. Head white, with two brown spots between antennae. Thorax and tegulae white. Labial palpus straight, 1.5 times as long as longitudinal eye diameter, with alternating white and dark bands on each segment. Third segment short, not tapered apically. Antenna yellow, with small dark brown spots basally, just above scape. Wings mottled in their dark parts. Forewing darker than hindwing, with predominance of dark brown spots and strokes, while these spots and strokes are less expressed on the hindwing, with predominance of pale-yellow portions. Wings basally white, although locally darkened with dark brown scales. Fringe with alternating portions of light and brown hairs. Hind leg pale yellow.

Male genitalia. Uncus straight, finger-like, of even width. Gnathos and its arms wide, short. Valves absent. Anellus arms short, narrow, arched, apically sharp. Saccus very long, narrow, elongated, slightly expanded medially. Aedeagus straight, medially with two small, spinous cornuti (not apparent on Fig. 12).

Distribution. Cameroon.

Flight period. November till February, April.

Etymology. The species name is a noun in apposition. It was named in honour of the ichthyologist Zuzana Musilová, Robert Tropek's wife.

Alucita deja **Ustjuzhanin & Kovtunovich, sp. nov.**
http://zoobank.org/9C094272-0A16-4CEA-AB05-CD4E3C04D27B
Figs 13–15

Type material. *Holotype* • male (NECJU 201906), Cameroon, Bamboo Camp, 350 m a.s.l., Mount Cameroon (SW slope), 4.0879°N, 9.0505°E, 20.XII.2014, lgt. V. Maicher, Sz. Sáfián, Š. Janeček, R. Tropek. *Paratypes* • 1 female (CUK), PlanteCam,

Figures 13–15. *Alucita deja* Ustjuzhanin & Kovtunovich, sp. nov. **13** adult female, Paratype, NEJCU **14** male genitalia, Holotype, preparation slide no. 201906 **15** female genitalia, Paratype, preparation slide no. 201909. Scale bar: 5 mm.

1100 m a.s.l., Mount Cameroon (SW slope), 4.1175°N, 9.0709°E, 11–18.XII.2014, lgt. V. Maicher, Sz. Sáfián, Š. Janeček, R. Tropek • 1 female (NECJU 201909), PlanteCam, 1100 m a.s.l., Mount Cameroon (SW slope), 4.1175°N, 9.0709°E, 11–23. IV.2015, lgt. V. Maicher, Sz. Sáfián, Š. Janeček, R. Tropek.

Diagnosis. *Alucita deja* differs from other *Alucita* species by the distinctive white mirrors on its abdomen. The new species' male genitalia are similar to *A. janeceki* Ustjuzhanin & Kovtunovich, 2018 in the absence of valves and the shape of the saccus (illustrated in Ustjuzhanin et al. 2018), but *A. deja* differs in the smoothly rounded apex of its uncus, the apically sharp anellus arms, jagged acicular cornuti in the aedeagus, and the wing colouration.

External characters. Female wingspan 15 mm, male wingspan 13 mm. Head with pure-white appressed scales. Thorax and tegulae also pure white anteriorly, sharply contrasting with dark brown posterior portions. Labial palpus short, 1.5 times as long as longitudinal eye diameter. Third segment short, not tapered apically. Antenna brown. Scape pure white. Wings and fringes dark brown. First lobe of forewing with white band around 1/3, narrow white band around 3/5 and yellowish-brown band edged with white around 4/5. Several irregular fine white cross-lines across all other lobes and fringes of both wings. Hind leg yellowish-brown. Fourth, sixth and last tergites of abdomen with mirrors of pure-white scales. Abdomen completely pure-white ventrally.

Male genitalia. Uncus straight, long, of even width. Gnathos short, wide, apically expanded. Valves not developed. Anellus arms straight, apically sharp. Saccus shaped as elongated oval, with small notch at apex. Aedeagus robust, slightly shorter than entire genital structure, with jagged acicular cornuti from its medial part to apex.

Female genitalia. Papilla analis narrow, elongated. Posterior apophyses thin, straight, shorter than anterior apophyses. Antrum wide, sclerotized, shaped as truncated tube with extended ostium. Outer edge of ostium jagged. Ductus wide and corrugated at its confluence to antrum and bursa copulatrix. Ductus seminalis short, bag-like, membranous, departing from confluence of ductus to antrum. Bursa copulatrix of irregular oval shape with elongated protrusion at apex.

Distribution. Cameroon.

Figures 16–18. *Alucita bokwango* Ustjuzhanin & Kovtunovich, sp. nov. **16** adult male, Paratype, NE-JCU **17** male genitalia, Holotype, preparation slide no. 201907 **18** female genitalia, Paratype, preparation slide no. 201910. Scale bar: 5 mm.
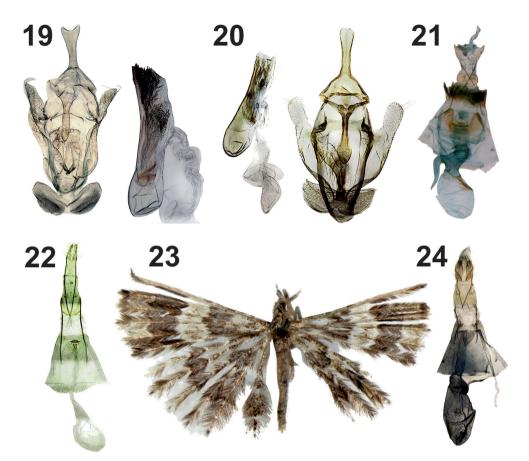
Flight period. April, December.

Etymology. The species name is a noun in apposition in honour of the limnologist and cyanobacteria specialist, Andreja Kust, a dear soulmate of Vincent Maicher.

Alucita bokwango Ustjuzhanin & Kovtunovich, sp. nov.
http://zoobank.org/C84BA8AD-3588-494F-86C8-55DEA44AC841
Figs 16–18

Type material. *Holotype* • male (NECJU 201907), Cameroon, Elephant Camp, 1850 m a.s.l., Mount Cameroon (SW slope), 4.1170°N, 9.0729°E, 19–24.XI.2014, lgt. V. Maicher, Sz. Sáfián, Š. Janeček, R. Tropek. *Paratypes* • 1 female, (NECJU 201910), + 16 ex., (NECJU, CUK), same data as holotype • 1 male, (CUK), PlanteCam, 1100 m a.s.l., Mount Cameroon (SW slope), 4.1175°N, 9.0709°E, 06–15.II.2016, lgt. V. Maicher, Sz. Sáfián, R. Tropek • 2 ex., (CUK, NECJU), PlanteCam, 1100 m a.s.l., 4.1175°N, 9.0709°E, 11–18.XII.2014, lgt. V. Maicher, Sz. Sáfián, Š. Janeček, R. Tropek • 1 male (CUK), Crater Lake, 1500 m a.s.l., Mount Cameroon (SW slope), 4.1443°N, 9.0717°E, 11–21.II.2016, lgt. P. Potocký, Sz. Sáfián, J. Mertens, Š. Janeček, R. Tropek • 1 male (CUK), Elephant Camp, 1850 m a.s.l., Mount Cameroon (SW slope), 4.1170°N, 9.0729°E, 17–22.II.2017, lgt. P. Potocký, Sz. Sáfián, J. Mertens, Š. Janeček, R. Tropek • 1 male (NECJU), Mann's Spring, 2200 m a.s.l., Mount Cameroon (SW slope), 4.1428°N, 9.1225°E, 16–21.IV.2017, lgt. V. Maicher, P. Potocký, S. Delabye • 1 male (CUK), Crater Lake, 1500 m a.s.l., Mount Cameroon (SW slope), 4.1443°N, 9.0717°E, 23–29. IV.2017, lgt. V. Maicher, P. Potocký, S. Delabye • 8 ex., (NECJU, CUK), Elephant Camp, 1850 m a.s.l., Mount Cameroon (SW slope), 4.1170°N, E9.0729°E, 18–26.IV.2017, lgt. V. Maicher, P. Potocký, S. Delabye • 5 ex. (CUK, NECJU), Mapanja, 1850 m a.s.l., Mount Cameroon (S slope), 4.1157°N, 9.1315°E, 05–14.V.2017, lgt. V. Maicher, P. Potocký, S. Delabye • 6 ex. (CUK, NECJU), Mapanja, 1850 m a.s.l., Mount Cameroon (SW slope), 4.1157°N, 9.1315°E, 23–28.X.2017, lgt. V. Maicher, P. Potocký, S. Delabye.

Figures 19–24. Comparative illustrations of other *Alucita* species mentioned in the new species' diagnoses **19** *A. balioxantha* (Meyrick, 1921), type, male genitalia **20** *A. tesserata* (Meyrick, 1918), type, male genitalia **21** *A. rhaptica* (Meyrick, 1920), female genitalia **22** *A. compsoxantha* (Meyrick, 1924), type, female genitalia **23** *A. chloracta* (Meyrick, 1908), type, adult female **24** *A. chloracta*, type, female genitalia.

Diagnosis. The new species resembles *Alucita chloracta* (Meyrick, 1908) in its external characters and the structure of the male genitalia. Genitalia of *A. bokwango* differs from *A. chloracta* in the needle-like apex of the uncus and the oval apical expansions of the valvae, whilst the uncus of *A. chloracta* is noticeably widened apically with a notch and valvae have a rounded apex. In its female genitalia, *A. bokwango* differs from *A. chloracta* (Fig. 24) in the short narrow ductus, wide funnel-shaped antrum and absence of a plaque-like signum in the bursa copulatrix. The wing colouration of *A. bokwango* is more contrasted than in *A. chloracta* (Fig. 23), and the new species is also substantially larger (23–25 mm vs. 15–16 mm wingspan).

External characters. Wingspan 23–25 mm. Head, thorax, tegulae and abdomen all dark brown. Labial palpus yellowish-brown, three times as long as longitudinal eye diameter, directed forward. Third segment thin, apically tapered. Antenna pale brown, with small dark brown spots basally, just above scape. Wings brown, outer edge slightly

lighter. Medial band on all wings whitish, almost transparent, interspersed with brown portions of hairs on lobes fringe. Hind leg yellow.

Male genitalia. Uncus thin, long, needle-shaped. Gnathos equal to uncus in length, apically sharp. Valves long, membranous, smoothly forming an oval apically. Anellus arms straight, narrow, equal to gnathos in their length. Saccus oval. Aedeagus robust, thick, almost equal in length to genital structure without uncus, two spinous cornuti distally.

Female genitalia. Papilla analis oval, wide throughout length. Posterior apophyses slightly shorter than anterior, thick and slightly undulated. Antrum wide, funnel-like. Ductus short, thin, membranous. Bursa copulatrix large, oval, with two large, lanceolate signa (although not clearly apparent in Fig. 18).

Distribution. Cameroon.

Flight period. October-May

Etymology. The species is named after Bokwango, a village on the eastern slope of Mount Cameroon where our project established its main base and where we made a lot of good friends. Many of the species records were also made in forests belonging to the village. Last but not least, most of our field assistants and other helpers came from Bokwango and we are thankful to all of them for the success of the project. We strongly believe this dedication will also help protect the unique biodiversity of the region.

Note. 18 specimens from Elephant Camp, 19–24.XI.2014, and two specimens from PlanteCam, 11–18.XII.2014, (all lgt. V. Maicher, Sz. Sáfián, Š. Janeček, R. Tropek), were erroneously indicated as *A. chloracta* by Ustjuzhanin et al. (2018). The other *A. chloracta* specimens referred by Ustjuzhanin et al. (2018) from Bamboo Camp, Drink Gari and PlanteCam were identified correctly.

Discussion

With the seven newly described *Alucita* species, the known diversity of many-plumed moths on Mount Cameroon has been increased to 22 species (Table 1). Altogether, 19 of these species were collected in the single locality, PlanteCam (Table 1), but the general diversity patterns will be analysed only once the complete *Alucita* material from our collections is processed. This comprises more than a quarter of the known Afrotropical diversity of many-plumed moths. At most, only a few species of the group are known from other localities in the region (Ustjuzhanin et al. 2018; De Prins and De Prins 2019). Although microlepidopteran diversity in the Guineo-Congolian forest zone remains largely unknown, discoveries of multiple undescribed species of many-plumed moths from a single locality is unexpected (Ustjuzhanin et al. 2018).

Mount Cameroon is known to harbour high diversity in many groups, including Lepidoptera (e.g., Ballesteros-Mejia et al. 2013; Maicher et al. 2016; Przybyłowicz et al. 2019; Delabye et al. 2020). This is usually explained as a result of the combination of its position at the border between the Guinean and Congolian biogeographic regions, its diversity of habitats along the elevational and precipitation gradients,

Table 1. Summary of all specimens of *Alucita* moths sampled on Mount Cameroon in this study and by Ustjuzhanin et al. (2018).

Sampling locality	Altitude	A. acalyptra	A. bakingili	A. bakweri	A. besongi	A. bokwango	A. chloracta	A. coffeina	A. deja	A. escobari	A. fokami	A. jana	A. janeceki	A. lidiya	A. longipenis	A. ludmila	A. megaphimus	A. mischenini	A. olga	A. spicifera	A. tatjana	A. zinovievi	A. zuza
Bimbia-Bonadikombo	30 m																	1					
Bamboo Camp	350 m	1	3		3		7		1	2	2		2	1		2	6		4				
Drink Gari	650 m						1				1		1	1	1	3							3
PlanteCam	1100 m		1	1		3	3	1	2	2	1	1		2	1	1	5	2	1	1	1	1	1
Ekonjo	1150 m											1								1			
Crater Lake	1450 m					2																	
Elephant Camp	1850 m					27							7							7			
Mapanja	1850 m					11						1											
Mann's Spring	2200 m					1																	

and its isolated "sky island" character (Ustjuzhanin et al. 2018). Nevertheless, even such unique combination of conditions can hardly explain why Mount Cameroon so strongly outnumbers all other Afrotropical localities in the species richness of its many-plumed moths. Of the known 22 *Alucita* species, 16 have been described from the site and have not yet been found anywhere else. Although it is highly expected that some of these will be distributed more widely, several of the newly described species are distinctive and unmistakable in their appearance. These are unlikely to have been overlooked in collections. Therefore, we expect that most of this many-plumed moth diversity is endemic to the study area. Several other potentially endemic species of moths (e.g., Yakovlev and Sáfián 2016; De Prins and De Prins 2019; Przybyłowicz et al. 2019;) and butterflies (e.g., Larsen 2005; Sáfián and Tropek, 2016; Sáfián et al. 2019) are already known from Mount Cameroon. Nevertheless, the real character of the endemism within Alucitidae on Mount Cameroon, as well as the mechanisms underlying the group's speciation (or even local radiation), will need more detailed research.

Acknowledgements

References

Ballesteros-Mejia L, Kitching IJ, Jetz W, Nagel P, Beck J (2013) Mapping the biodiversity of tropical insects: species richness and inventory completeness of African sphingid moths. Global Ecology and Biogeography 22: 586–595. https://doi.org/10.1111/geb.12039

De Prins J, De Prins W (2019) AfroMoths. Online database of Afrotropical moth species (Lepidoptera). Available from: http://www.afromoths.net [Accessed 20 November 2019]

Delabye S, Maicher V, Sáfián Sz, Potocký P, Mertens JEJ, Przybyłowicz Ł, Murkwe M, Kobe IN, Fokam EB, Janeček Š, Tropek R (2020) First records of 31 species of butterflies and moths (Lepidoptera) in Cameroon, with remarks on their elevational ranges. Biodiversity Data Journal 8: e50543. https://doi.org/10.3897/BDJ.8.e50543

Larsen TB (2005) Butterflies of West Africa. Apollo Books, Stenstrup, 865 pp.

Maicher V, Sáfián Sz, Ishmeal KN, Murkwe M, Kimbeng TJ, Janeček Š, Tropek R (2016) Two Genera and Nineteen Species of Fruit-Feeding Erebid Moths (Lepidoptera: Erebidae) Recorded in Cameroon for the First Time. Entomological News 126: 64–70. https://doi.org/10.3157/021.126.0108

Maicher V, Sáfián Sz, Murkwe M, Przybyłowicz Ł, Janeček Š, Fokam EB, Pyrcz T, Tropek R (2018) Flying between raindrops: Strong seasonal turnover of several Lepidoptera groups in lowland rainforests of Mount Cameroon. Ecology and Evolution 8: 1–12. https://doi.org/10.1002/ece3.4704

Maicher V, Sáfián Sz, Murkwe M, Delabye S, Przybyłowicz Ł, Potocký P, Kobe IN, Janeček Š, Mertens JEJ, Fokam EB, Pyrcz T, Doležal J, Altman J, Hořák D, Fiedler K., Tropek R (2019) Seasonal shifts of biodiversity patterns and species' elevation ranges of butterflies and moths along a complete rain forest elevational gradient on Mount Cameroon. Journal of Biogeography. https://doi.org/10.1111/jbi.13740

Przybyłowicz Ł (2013) Review of subgenus *Compsochromia* Kiriakoff 1953 (Lepidoptera: Erebidae: Arctiinae, genus *Balacra*) with identification keys and description of a new species from Cameroon. Annales de la Société entomologique de France 49: 53–60. https://doi.org/10.1080/00379271.2013.763459

Przybyłowicz Ł, Maicher V, László GM, Sáfián Sz, Tropek R (2019) *Amerila* (Lepidoptera: Erebidae: Arctiinae) of Cameroon with morphological remarks on male and female genitalia. Zootaxa 4674: 283–295. https://doi.org/10.11646/zootaxa.4674.2.8

Sáfián Sz, Tropek R (2016) Two new butterfly species (Lepidoptera: Rhopalocera) from Mount Cameroon, Gulf of Guinea Highlands, Cameroon. Zootaxa 4150: 123–132. https://doi.org/10.11646/zootaxa.4150.2.2

Sáfián Sz, Belcastro C, Tropek R (2019) Two new species in the genus *Andronymus* Holland, 1896 (Lepidoptera, Hesperiidae). Zootaxa 4624: 108–120. https://doi.org/10.11646/zootaxa.4624.1.7

Ustjuzhanin P, Kovtunovich V (2016) The Alucitidae (Lepidoptera) of Malawi with descriptions of five new species. Zootaxa 4126: 533–547. http://dx.doi.org/10.11646/zootaxa.4126.4.5

Ustjuzhanin P, Kovtunovich V, Sáfián Sz, Maicher V, Tropek R (2018) A newly discovered biodiversity hotspot of many-plumed moths in the Mount Cameroon area: first report on species diversity, with description of nine new species (Lepidoptera, Alucitidae). ZooKeys 777: 119–139. https://doi.org/10.3897/zookeys.777.24729

Yakovlev RV, Sáfián Sz (2016) *Geraldocossus* gen. nov. (Lepidoptera, Cossidae) from Mount Cameroon (West Africa). Zootaxa 4114: 595–599. http://doi.org/10.11646/zootaxa.4114.5.8

RESEARCH ARTICLE

ZooKeys
A peer-reviewed open-access journal
Launched to accelerate biodiversity research

Integrative taxonomy reveals three new taxa within the *Tylototriton asperrimus* complex (Caudata, Salamandridae) from Vietnam

Marta Bernardes[1,2], Minh Duc Le[3,4,5], Truong Quang Nguyen[6,7], Cuong The Pham[6,7], Anh Van Pham[8], Tao Thien Nguyen[7,9], Dennis Rödder[10], Michael Bonkowski[2], Thomas Ziegler[1,2]

1 *Cologne Zoo, Riehler Str. 173, 50735 Cologne, Germany* **2** *Terrestrial Ecology, Institute of Zoology, University of Cologne, Zülpicher Str. 47b, 50674 Cologne, Germany* **3** *Faculty of Environmental Sciences, University of Science, Vietnam National University, Hanoi, 334 Nguyen Trai Road, Hanoi, Vietnam* **4** *Central Institute for Natural Resources and Environmental Studies, Vietnam National University, Hanoi, 19 Le Thanh Tong, Hanoi, Vietnam* **5** *Department of Herpetology, American Museum of Natural History, Central Park West at 79th Street, New York, New York 10024, USA* **6** *Institute of Ecology and Biological Resources, Vietnam Academy of Science and Technology, 18 Hoang Quoc Viet, Hanoi, Vietnam* **7** *Graduate University of Science and Technology, Vietnam Academy of Science and Technology, 18 Hoang Quoc Viet, Cau Giay, Hanoi, Vietnam* **8** *Faculty of Natural Science and Technology, Tay Bac University, Quyet Tam Ward, Son La City, Son La Province, Vietnam* **9** *Vietnam National Museum of Nature, 18 Hoang Quoc Viet St., Hanoi, Vietnam* **10** *Zoologisches Forschungsmuseum Alexander Koenig, Adenauerallee 160, 53113 Bonn, Germany*

Corresponding author: Marta Bernardes (mrtbernardes@gmail.com)

Abstract

The *Tylototriton asperrimus* complex from northern Vietnam is reviewed based on morphological comparisons and analysis of the mitochondrial marker NADH dehydrogenase subunit 2 (ND2). Based on molecular divergences, which were revealed to be higher than in other congeners, in concert with morphological differences, two new species and one subspecies are described herein: *Tylototriton pasmansi* **sp. nov.** differs from *T. asperrimus sensu stricto* by 3.2 to 3.6 % genetic divergence and a combination of distinct morphological characters, such as head slightly longer than wide, distinct mid-dorsal ridge, relatively wide distance between the eyes, tips of fingers reaching the eye when foreleg is laid forward, labial and

gular folds present, central belly skin with tubercles shaped like transverse wrinkles and distinct, pointy to round rib nodules. The population of *T. pasmansi* **sp. nov.** consists of two subclades, the nominotypic one occurring on the eastern side of the Da River (or Black River, including Hoa Binh and Phu Tho provinces), and another occurring on the western side (including Son La and Thanh Hoa provinces). These two subclades differ by 2.5 to 3.1 % genetic divergence and distinct morphological characters. The western subclade is herein described as *Tylototriton pasmansi obsti* **ssp. nov.**, which differs from the nominotypic form by a wider head, longer and narrower snout, shorter femur length, and an overall less granulose skin, without an increased concentration of warts on the body sides.

A second new species, *Tylototriton sparreboomi* **sp. nov.** is described from Lai Chau Province. It differs from *T. asperrimus sensu stricto* by 4.1 to 4.2 % and from *Tylototriton pasmansi* **sp. nov.** by 3.6 to 4.5 % genetic divergences as well as by a combination of distinct morphological characters, such as head longer than wide, tips of fingers reaching nostril when foreleg adpressed along head, rib nodules distinct, round and relatively enlarged, and wide distance between the eyes.

Introduction

Tylototriton asperrimus Unterstein, 1930 was the second salamander species within the genus described after *T. verrucosus*. It was considered a common species due to its relatively wide distribution from central and southern China to northern Vietnam (Bain and Nguyen 2004; Weisrock et al. 2006; van Dijk et al. 2008; Nguyen et al. 2009; Sun et al. 2011; Qin et al. 2012). The increasing amount of field work conducted in these regions, combined with the incorporation of new technologies in taxonomic analyses (e.g., molecular studies, X-ray scans), has since resulted in a vast increase of knowledge on the taxonomy of this genus, turning it into the most speciose genus within the Salamandridae (Fig. 1).

The widely distributed taxon has been revealed to consist of several different species with smaller ranges, and accordingly with a more critical conservation status. For example *T. vietnamensis*, recorded from Bac Giang, Quang Ninh, and Lang Son provinces, Vietnam (Bernardes et al. 2017), currently listed as Endangered (IUCN SSC ASG 2016), *T. ziegleri* from Ha Giang and Cao Bang provinces, Vietnam (Nishikawa et al. 2013b) and Yunnan Province, China (Jiang et al. 2017), listed as Vulnerable (IUCN SSC ASG 2017), *T. broadoridgus*, known from Hunan, China (Shen et al. 2012) and *T. anhuiensis*, known from Anhui, China (Qian et al. 2017), both not yet assessed were some of the species recently described within the *T. asperrimus* species complex.

However, the taxonomic assignments of some populations of *T. asperrimus* have not been completely resolved. The population from Thuong Tien District, Hoa Binh Province, Vietnam, was identified as *T. asperrimus* due to low genetic differences in partial mitochondrial (Yuan et al. 2011; Nishikawa et al. 2013b) and partial nuclear genes (Wang et al. 2018) compared with the Chinese population. Nonetheless, other authors regarded this population as an undescribed species, *T.* cf. *asperrimus*, based

on genetic differentiation, including complete mitochondrial sequence data (Phimmachak et al. 2015a; Hernandez 2016). Taxonomic decisions, however, should at best not be based on genetic variation alone, but also be accompanied by other evidence, such as morphological and/or ecological differences. Given the high degree of morphological conservatism within the genus *Tylototriton*, identifying phenotypic divergence can be especially challenging (Stuart et al. 2010; Nishikawa et al. 2013b), but nonetheless crucial due to its repercussions on species delimitations.

In order to further understand the taxonomy of species within the *T. asperrimus* complex in Vietnam, we examined specimens of the population from Hoa Binh Province and other newly collected specimens from the region, and compared them with the holotype of *T. asperrimus* from Guangxi, China. We combined molecular and detailed morphological analyses to infer the taxonomic status and phylogenetic relationships among these populations. As a consequence, we herein describe three new taxa of the *T. asperrimus* complex from northern Vietnam.
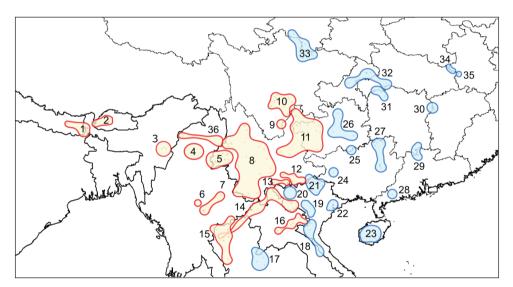

Figure 1. Current distribution map of the genus *Tylototriton*, from South and Central China, to northern Vietnam, Laos, Thailand, Myanmar, India, Bhutan and Nepal (Hernandez 2016; Qian et al. 2017; Grismer et al. 2018; Wang et al. 2018; Grismer et al. 2019; Hernandez et al. 2019; Zaw et al. 2019). In red the distribution areas belonging to the subgenus *Tylototriton*, and in blue the distribution areas belonging to the sub–genus *Yaotriton* (Dubois and Raffaëlli 2009). The numerical identification corresponds to the different species and undescribed taxa as follow: **1** *T. himalayanus* **2** *T.* cf. *himalayanus* (Bhutan) **3** *T.* cf. *verrucosus* (Manipur) **4** *T. kachinorum* **5** *T. verrucosus* **6** *T. ngarsuensis* **7** *T. shanorum* **8** *T. shanjing* **9** *T. pseudoverrucosus* **10** *T. taliangensis* **11** *T. kweichowensis* **12** *T. yangi* **13** *T. pulcherrimus* **14** *T. anguliceps* **15** *T. uyenoi* **16** *T. podichthys* **17** *T. panhai* **18** *T. notialis* **19** *Tylototriton* taxon 2, this study **20** *Tylototriton* taxon 3, this study **21** *T. ziegleri* **22** *T. vietnamensis* **23** *T. hainanensis* **24** *T.* cf. *hainanensis* (Baise) **25** *T.* cf. *wenxianensis* (Libo) **26** *T.* cf. *wenxianensis* (Guizhou) **27** *T. asperrimus* **28** *T.* cf. *asperrimus* (Guangdong) **29** *T. lizhengchangi* **30** *T. liuyangensis* **31** *T. broadoridgus* **32** *T.* cf. *wenxianensis* (Chongqing and Hubei) **33** *T. wenxianensis* **34** *T. dabienicus* **35** *T. anhuiensis* and **36** *T. panwaensis*.
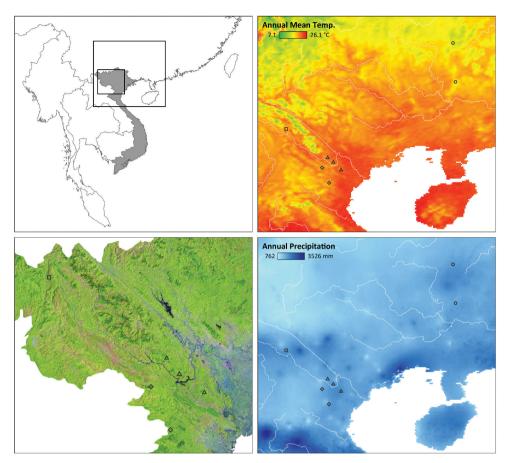
Materials and methods

Sampling

Field surveys were conducted in northern Vietnam by: 1) A. V. Pham and M. A. Vang in Sa De Phin Commune, Sin Ho District, Lai Chau Province in May 2015, and in Xuan Nha Nature Reserve, Van Ho District, Son La Province on 15 June 2016; 2) H. N. Ngo et al. in Phu Canh Nature Reserve, Da Bac District, Hoa Binh Province on 11 June 2016; 3) T. D. Le et al. in Xuan Son National Park, Du Village, Xuan Son Commune, Tan Son District, Phu Tho Province on 7 July 2016; and 4) T. S. Nguyen in Xuan Lien Nature Reserve, Bat Mot Commune, Thuong Xuan District, Thanh Hoa Province in July 2015 (Fig. 2).

Specimens were anaesthetized and euthanized in a closed vessel with a piece of cotton wool containing ethyl acetate (Simmons 2002), fixed in 80% ethanol for five hours, and subsequently transferred to 70% ethanol for permanent storage. Tissue samples were preserved separately in 70% ethanol prior to fixation. Specimens were subsequently deposited in the collections of the Institute of Ecology and Biological Research (**IEBR**), Hanoi, the Tay Bac University (**TBU**), Son La Province, Vietnam, and the Zoologisches Forschungsmuseum Alexander Koenig (**ZFMK**), Bonn Germany.

Molecular analyses

Tissue samples from muscle of preserved specimens were extracted using the DNeasy blood and tissue kit, Qiagen (California, USA). A fragment of a mitochondrial gene, the NADH dehydrogenase subunit 2 (ND2), was amplified by PCR mastermix (Fermentas, Burlington, ON, Canada) using the primer pair, Sal_Nd2_F1 (5'- AA-GCTTTTGGGCCCATACC-3') (Nishikawa et al. 2013b) and a newly design primer TyloR1 (5'- GGTCTTTGGTCTYATTATCCTAA -3'). The PCR volume consisted of 21 µl (10 µl of mastermix, 5 µl of water, 2 µl of each primer at 10 pmol/µl and 2 µl of DNA or higher depending on the quantity of DNA in the final extraction solution). The following temperature profile for PCR was used: 95 °C for 5 minutes to activate the taq; with 40 cycles at 95 °C for 30 s, 58 °C for 45 s, 72 °C for 60 s; and the final extension at 72 °C for 6 minutes. PCR products were subjected to electrophoresis through a 1 % agarose gel (UltraPure™, Invitrogen, La Jolla, CA). Gels were stained for 10 min in 1 X TBE buffer with 2 pg/ml ethidium-bromide and visualized under UV light. Successful amplifications were purified to eliminate PCR components using a GeneJET™ PCR Purification kit (Fermentas). Purified PCR products were sent to FirstBase Malaysia for sequencing. We included 12 new samples from five populations distributed in north and north central Vietnam to another 21 known species' samples of *Tylototriton* (Table 1). Additionally, five species were selected as outgroups: *Echinotriton andersoni*, *E. chinhaiensis*, *Lyciasalamandra atifi*, *Notophthalmus viridescens*, and *Pleurodeles waltl*, to root the tree (Qian et al. 2017; Wang et al. 2018).

Figure 2. Distribution map of the new populations of *Tylototriton* from North Vietnam, based on the following symbols: **square** (taxon 3, this study) the population from Sin Ho District, Lai Chau Province; **diamond** (taxon 1, this study) the upper one identifies the population from Van Ho District, Son La Province, and the lower one identifies the population from Thuong Xuan District, Thanh Hoa Province; **triangle** (taxon 2, this study) the upper one identifies the population from Tan Son District, Phu Tho Province, the middle one identifies the population from Da Bac District, Hoa Binh Province, and the lower one identifies the population from Lac Son District, Hoa Binh Province. The two populations identified by the **circles** represent *T. asperrimus* sensu stricto from China. High resolution remote sensing land cover information was extracted from "GLAD-UMD and SERVIR-Mekong, Natural annual tree canopy structure and surface water dynamics products, 2017" (lower left panel). Bioclimatic variables (right side) were extracted from remote sensing data provided by Deblauwe et al. (2016).

The sequences were aligned in Clustal X v2 (Thompson et al. 1997) with default settings. Data were analyzed using maximum parsimony (MP) and maximum likelihood (ML) as implemented in PAUP 4.0b10 (Swofford 2001), and Bayesian analysis in MrBayes 3.2 (Ronquist et al. 2012). For MP analysis, heuristic analysis was conducted with 100 random taxon addition replicates using tree-bisection and reconnection (TBR) branch swapping algorithm, with no upper limit set for the maximum number

Table 1. Samples of *Tylototriton* species used in the molecular analyses of this study. Country label key: CH = China; L = Laos; VN = Vietnam.

ID	Species	Voucher	Locality	Genbank no.	Source
1	*T. anhuiensis*	AHU-16-EE-001	Yuexi, Anhui, CH	KY321388	Qian et al. 2017
2	*T. asperrimus* lineage 1	CIB 70063	Longsheng, Guangxi, CH	KC147816	Shen et al. 2012
3	*T. asperrimus* lineage 1	CIB 200807055	Jinxiu, Guangxi, CH	KC147815	Shen et al. 2012
4	*T. asperrimus* lineage 2	CIB XZ20091201	Xinyi, Guangdong, CH	KY800876	Wang et al. 2018
5	*T. broadoridgus*	CIB 200085	Sangzhi, Hunan, CH	KC147814	Shen et al. 2012
6	taxon 1	IEBR 4471	Van Ho, Son La, VN	MT210168	This study
7	taxon 1	IEBR 4473	Van Ho, Son La, VN	MT210169	This study
8	taxon 1	IEBR 4474	Van Ho, Son La, VN	MT210170	This study
9	taxon 1	IEBR 4318	Thuong Xuan, Thanh Hoa, VN	MT210171	This study
10	taxon 1	IEBR 4319	Thuong Xuan, Thanh Hoa, VN	MT210172	This study
11	taxon 2	IEBR 4320	Tan Son, Phu Tho, VN	MT210164	This study
12	taxon 2	IEBR 4321	Tan Son, Phu Tho, VN	MT210165	This study
13	taxon 2	IEBR 4466	Da Bac, Hoa Binh VN	MT201166	This study
14	taxon 2	IEBR 4467	Da Bac, Hoa Binh VN	MT210167	This study
15	taxon 2	VNMN TAO1214 / VFUA.2009.8	Xuan Lien, Lac Son, Hoa Binh, VN	AB769531	Nishikawa et al. 2013b
16	*T. dabienicus* lineage 1	HNNU10042015	Shangcheng, Anhui, CH	KC147811	Nishikawa et al. 2013b
17	*T. dabienicus* lineage 2	CIB 08042905-2	Yuexi, Anhui, CH	KY800853	Wang et al. 2018
18	*T. hainanensis*	CIB 20081048	Diaoluoshan, Hainan, CH	KC147817	Nishikawa et al. 2013b
19	*T. liuyangensis*	CSUFT20100108	Liuyang, Hunan, CH	KJ205598	Yang et al. 2014
20	*T. lizhengchangi*	KUHE 42317	Yizhang, Hunan, CH	AB769533	Nishikawa et al. 2013b
21	*T. notialis*	VNMN TAO1235	Pu Hoat, Nghe An, VN	AB769536	Nishikawa et al. 2013b
22	*T. panhai*	NUOL 00437	Botene, Xaignabouli, L	KT304306	Phimmachak et al. 2015a
23	taxon 3	IEBR 4477	Sin Ho, Lai Chau, VN	MT210167	This study
24	taxon 3	IEBR 4476	Sin Ho, Lai Chau, VN	MT210162	This study
25	*T. taliangensis*	KUHE 43361	Pet Trade	AB769543	Nishikawa et al. 2013b
26	*T. verrucosus*	KIZ 201306058	Husa, Yunnan, CH	AB922820	Nishikawa et al. 2014
27	*T. vietnamensis*	KUHE 55172	Yen Tu, Bac Giang, VN	AB769538	Nishikawa et al. 2013b
28	*T. vietnamensis*	IEBR A.2014.43	Hoanh Bo, Quang Ninh, VN	KX609961	Bernardes et al. 2017
29	*T. vietnamensis*	IEBR A.2014.45	Loc Binh, Lang Son, VN	KX609963	Bernardes et al. 2017
30	*T. wenxianensis* lineage 1	CIB 20090527	Wenxian, Gansu, CH	KC147813	Nishikawa et al. 2013b
31	*T. wenxianensis* lineage 2	CIB Wg20090730001	Libo, Guizhou, CH	KY800842	Wang et al. 2018
32	*T. wenxianensis* lineage 3	CIB WH10003	Wufeng, Hubei, CH	KY800865	Wang et al. 2018
33	*T. ziegleri*	VNMN 3390	Quan Ba, Ha Giang, VN	AB769539	Nishikawa et al. 2013b

of trees saved. Bootstrap support (BP) (Felsenstein 1985) was calculated using 1,000 pseudo-replicates and 100 random taxon addition replicates. All characters were equally weighted and unordered. For ML analysis, we used the optimal evolution model as selected by ModelTest v3.7 (Posada and Crandall 1998). To estimate BP in the ML analysis, a simple taxon addition option and 100 pseudo-replicates were employed. We considered BP values of ≥ 70 % to represent strong support (Hillis and Bull 1993).

For Bayesian analyses, we used the optimal model, GTR+I+G as selected by Modeltest v3.7, for ML and combined Bayesian analyses. Two simultaneous analyses with four Markov chains (one cold and three heated) were run for 10 million generations with a random starting tree and sampled every 1,000 generations. Log-likelihood scores of sample points were plotted against generation time to determine stationarity of Markov chains. The cutoff point for the burn-in function was set to 21, equivalent to 21,000 generations, in the Bayesian analysis, as -lnL scores reached stationarity after 21,000 generations in both runs. Nodal support was evaluated using Bootstrap in PAUP and posterior probability in MrBayes v3.2. Uncorrected pairwise divergences were calculated in PAUP*4.0b10.

We selected the relaxed-clock method (Drummond et al. 2006) to estimate divergence times. The obtained dataset was used as input for the computer program BEAST v1.8.0 (Drummond and Rambaut 2007). *A priori* criteria for the analysis were set in the program BEAUti v1.8.0. One calibration point, the split between the clade containing *Tylototriton vietnamensis* + *T. panhai* and the clade consisting of *T. asperrimus* and other related species, estimated for 12.4 ± 2.3 million years ago (MYA) (Wang et al. 2018), was used to calibrate the phylogeny. A general time-reversible (GTR) model using gamma + invariant sites with four gamma categories was employed along with the assumption of a relaxed molecular clock. As for the priors, we used all default settings, except for the Tree Prior category that was set to Yule Process, as recommended for species-level analyses. The codon-partitioned dataset was used for a single run. In addition, a random tree was employed as a starting tree. The length chain was set to 10^7, and the Markov chain was sampled every 1,000 generations. After the dataset with the above settings was analyzed in BEAST, the resulting likelihood profile was then examined by the program Tracer v1.6 to determine the burn-in cutoff point. The final tree with calibration estimates was computed using the program TreeAnnotator v1.8.0 as recommended in the BEAST program manual.

Morphological examination

All specimens were sexed by evaluating the size of the opening of the cloacal fissure: females show a puncture-like opening and males a wider slit-like opening. The holotype of *T. asperrimus* (ZMB 34089), collected from Guangxi Province, China, was loaned from the Zoologisches Museum Berlin (Museum für Naturkunde Berlin) and evaluated as a female (Fig. 3). In addition we investigated two other Vietnamese female specimens, one from IEBR: JJLR01195 from Pu Hoat Nature Reserve, Nghe An Prov-

Figure 3. Holotype of *Tylototriton asperrimus* (ZMB 34089). In sequence: dorsal view; ventral view; lateral view with detail of ovaries; and detail of dorsal view of the head. Photographs T. Ziegler.

ince (*T. notialis*) and another from the Vietnam Forestry University (VFU) in Hanoi: VFUA.2009.8 (also known as voucher Tao1214 in Nishikawa et al. [2013b]) from Thuong Tien Nature Reserve, Hoa Binh Province (*T.* cf. *asperrimus*). Morphological comparisons were only performed among animals of the same sex, and only males had a sufficiently large number of specimens (*N*) to perform statistical analysis.

A total of 23 morphological characters were measured following Bernardes et al. (2017) to the nearest 0.01 mm with a digital caliper as follows: snout-vent length (**SVL**); head length (**HL**); head width (**HW**) measured behind the eyes and before the beginning of the parotoids; maximum head width (**MHW**); parotoid width (**PW**); maximum parotoid height (**PH**); eye length (**EL**); inter-eye distance (**IE**); inter-narial distance (**IN**); eye-narial distance (**EN**); lower jaw length (**LJL**) from tip of lower jaw to jaw angle; maximum upper eyelid length (**UEL**); humerus length (**HUM**); radius length (**RAD**); femur length (**FEM**); tibia length (**TIB**); axilla to groin (**AG**); trunk length (**TkL**) from wrinkle of throat to anterior tip of vent; length of the 5th anterior dorsal nodule (**L5N**); width of vertebral cord (**WVr**) measured at the height of the 5th nodule; cloaca length (**ClL**) length of cloaca muscle; tail length (**TL**); tail height (**TH**). The following ratios were calculated based on the measures above: total forelimb length (**FORE**); total hindlimb length (**HIND**); hind-limb to forelimb lengths (**HIND/FORE**); the relative length of radius to humerus (**RAD/HUM**); tibia to femur (**TIB/FEM**); and tail length to tail height (**TL/TH**).

The morphological comparison between the new taxa and their congeners were based on the specimen examination and the following literature: Fei et al. (1984), Böhme et al. (2005), Stuart et al. (2010), Shen et al. (2012), Nishikawa et al. (2013a), Nishikawa et al. (2013b), and Yang et al. (2014). When measurements were involved, only the ones taken in similar ways were found suitable for comparison and used as reference.

Statistical analysis

We first compared the morphological characters of males between the two clades originating on both sides of the Da River: the western clade from Son La and Thanh Hoa provinces (referred to as taxon 1) and the eastern clade from Hoa Binh and Phu Tho provinces (referred to as taxon 2; for reference see Fig. 2). Subsequently we compared the above-mentioned males (jointly referred to as *T.* cf. *asperrimus*) and the males originating from Lai Chau Province (referred to as taxon 3).

The statistical analyses had to be conducted on different subsets of morphological characters according to data availability. Morphological characters that could not be obtained for all the species had to be excluded from the overall analysis. These included: PW, PH, EL, IE, UEL, AG, and ClL. Whether the measured morphological characters showed a linear increase with body size was analyzed through correlation analyses (see Suppl. material 1). Accordingly, measurements of morphological characters and character ratios were standardized by SVL (R[character]: % SVL) to exclude the effect of body size, and log-transformed. A Principal Component Analysis (PCA)

was tested by a one-way Analysis of Variance (ANOVA) between populations. Because morphological traits within individuals are not independent of each other, comparisons between different morphological traits of species were based on Multivariate Analysis of Variance (MANOVA) and proceeding to ANOVA and Tukey HSD test only if the MANOVA yielded a significant result (i.e., 'protected ANOVA' (van Ende 2001). Roy's Greatest Root was chosen as test of significant differences among groups in the MANOVA procedure.

Significance levels were set to 95 %. All statistical analyses were performed in R v 3.1.2, the vegan package was used to calculate PCA (Oksanen et al. 2015).
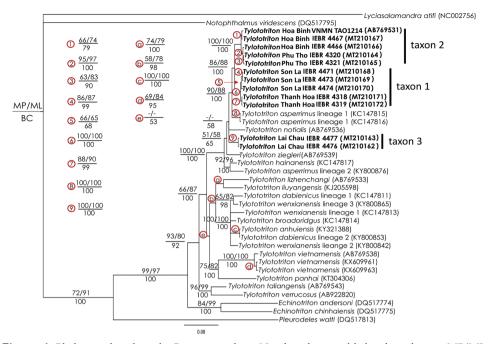
Macroclimatic information

Climatic information at the sample sites were extracted from remote sensing data (Deblauwe et al. 2016). Representing averages across last decades with a spatial resolution of 0.1°, the following bioclimatic variables were available: Annual Mean Temperature BIO1, Mean Diurnal Range BIO2, Isothermality BIO3, Temperature Seasonality BIO4, Max Temperature of Warmest Month BIO5, Min Temperature of Coldest Month BIO6, Temperature Annual Range BIO7, Mean Temperature of Wettest Quarter BIO8, Mean Temperature of Driest Quarter BIO9, Mean Temperature of Warmest Quarter BIO10, Mean Temperature of Coldest Quarter BIO11, Annual Precipitation BIO12, Precipitation of Wettest Month BIO13, Precipitation of Driest Month BIO14, Precipitation Seasonality BIO15, Precipitation of Wettest Quarter BIO16, Precipitation of Driest Quarter BIO17, Precipitation of Warmest Quarter BIO18, and Precipitation of Coldest Quarter BIO19.

Results

Molecular analyses

The combined matrix contained 1036 aligned characters. Of those, 370 were parsimony informative. MP analysis of the dataset recovered 2 most parsimonious trees with 1400 steps (CI = 0.54; RI = 0.65). Our phylogenetic analyses recovered the Vietnamese *T.* cf. *asperrimus* as a sister taxon to *T. asperrimus* from China with strong support values from all analyses (MP_{BP} = 90, ML_{BP} = 88, PP = 100) (Fig. 4). The genetic differences between Vietnamese populations and the Chinese lineage were 3.3 to 3.6 % for the population from Son La Province; 3.2 to 3.4 % for the population from Thanh Hoa Province; 3.3 to 3.6 % for the population from Phu Tho Province; 3.2 to 3.6 % for the population from Da Bac District, Hoa Binh Province; and 3.4 to 3.5 % for the population from Lac Son District, Hoa Binh Province, respectively (Table 2).

Furthermore, our genetic analyses identified different lineages within the Vietnamese clade of *T.* cf. *asperrimus*. The genetic variation between taxon 1 and taxon 2 varied between 2.5 % (between Thanh Hoa and Hoa Binh populations) and 3.1 % (between

Figure 4. Phylogram based on the Bayesian analysis. Number above and below branches are MP/ML bootstrap values and Bayesian posterior probabilities (> 50 %), respectively. Dashes represent values < 50 %. Sample AB769531 is from Nishikawa et al. 2013b.

Son La and Phu Tho populations). In contrast, within-population differences were only 0.0 to 0.6 % in taxon 1 and 0.1 to 0.9 % in taxon 2.

The population from Lai Chau Province turned out to be a distinct and basal lineage within a weakly supported clade, including *T. notialis*, *T. asperrimus* from China, and taxon 1 and taxon 2 from Vietnam (Fig. 4). In this case the genetic differences of taxon 3 to the topotypical population of *T. asperrimus* ranged between 4.1 to 4.2 % to taxon 1 between 3.6 to 4.0 %, and to taxon 2 between 4.1 to 4.5 % (see Table 2 for genetic distances). Our time estimates are very similar to those generated by Wang et al. (2018), and the results show that *T. asperrimus* from China split from taxon 1 about 2.5 MYA (95% highest posterior densities – 95% HPD = 1.4–3.7), while taxon 3 diverged from the two taxa approximately 3.4 MYA (95% HPD = 2.3–4.8) (see Suppl. material 2).

Morphological examination

Vietnamese species compared to the Chinese holotype

This comparison was only based on three female specimens: the holotype of *T. asperrimus*, one from Hoa Binh Province (taxon 2), and one from Nghe An Province (*T. notialis*) (Table 3). Due to the lack of replicates it was not possible to perform statistical analyses between the Chinese and the Vietnamese clades. After correcting the absolute measures to

Table 2. Uncorrected p-distances of the mitochondrial DNA sequences used in this study for members of the *Tylototriton asperrimus* species complex.

ID	Taxon–Locality	1	2	3	4	5	6	7	8	9	10	11	12	13	14
1	*T. asperrimus*–China	–													
2	*T. asperrimus*–China	0.001	–												
3	taxon 1–Son La	0.034	0.034	–											
4	taxon 1–Son La	0.036	0.035	0.001	–										
5	taxon 1–Thanh Hoa	0.034	0.033	0.005	0.006	–									
6	taxon 1–Son La	0.034	0.033	0.004	0.005	0.005	–								
7	taxon 1–Thanh Hoa	0.033	0.032	0.005	0.006	0.000	0.005	–							
8	taxon 2–Phu Tho	0.034	0.033	0.029	0.030	0.028	0.029	0.028	–						
9	taxon 2–Phu Tho	0.036	0.035	0.030	0.031	0.029	0.030	0.029	0.001	–					
10	taxon 2–Hoa Binh	0.036	0.034	0.030	0.030	0.028	0.029	0.028	0.002	0.003	–				
11	taxon 2–Hoa Binh	0.033	0.032	0.026	0.027	0.025	0.026	0.025	0.005	0.006	0.005	–			
12	taxon 2–Hoa Binh	0.035	0.034	0.029	0.031	0.029	0.029	0.028	0.007	0.008	0.007	0.002	–		
13	taxon 3–Lai Chau	0.042	0.041	0.039	0.040	0.038	0.039	0.038	0.044	0.045	0.044	0.041	0.044	–	
14	taxon 3–Lai Chau	0.041	0.041	0.039	0.040	0.036	0.039	0.036	0.044	0.045	0.044	0.041	0.044	0.002	–

ratios of snout-vent length, the most prominent differences between the female of taxon 2 and the female holotype of *T. asperrimus* from China were: a wider and longer head (MHW = 28.99, HL = 29.15 in taxon 2 vs. MHW = 25.35, HL = 26.60 in *T. asperrimus*), a longer lower jaw (LJL = 17.40 in taxon 2 vs. 14.85 in *T. asperrimus*), and higher values for most of the measured head features (including the distance between the eyes) for taxon 2. The exceptions were found in the distance between eye and nostril (EN = 6.37 in *T. asperrimus* vs. 4.86 in taxon 2) and head width (HW = 18.54 in *T. asperrimus* vs. 13.67 in taxon 2) which in these cases the values were higher in *T. asperrimus*. The female from taxon 2 also had higher values for tail length (TL = 85.62 in taxon 2 vs. 77.28 in *T. asperrimus*), cloacal muscles (ClL = 11.39, ClW = 7.63 in taxon 2 vs. ClL = 7.01, ClW = 3.65 in *T. asperrimus*), and vertebra width (WVr = 4.46 in taxon 2 vs. 2.80 in *T. asperrimus*).

Table 3. Morphological comparisons between the available females. Measures as absolute values (in mm) and ratios of characters to snout vent length (% SVL) between *Tylototriton asperrimus* holotype from China (ZMB 34089), *T.* cf. *asperrimus* from Thuong Tien Nature Reserve, Hoa Binh Province, Vietnam (taxon 2) (VFUA.2009.8), and *T. notialis* (JJLR01195) from Pu Hoat Nature Reserve, Nghe An Province, Vietnam. For abbreviations see Materials and methods.
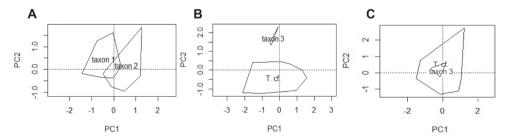
Character	Absolute measures			Ratios to SVL		
	T. asperrimus	taxon 2	*T. notialis*	*T. asperrimus*	taxon 2	*T. notialis*
SVL	73.45	76.82	76.16	–	–	–
MHW	18.62	22.27	19.64	25.35	28.99	25.79
HW	13.62	10.50	–	18.54	13.67	–
HL	19.54	22.39	20.86	26.60	29.15	27.39
PL	10.74	13.03	12.78	14.62	16.96	16.78
PH	5.78	7.45	7.54	7.87	9.70	9.90
EL	3.17	3.86	2.94	4.32	5.02	3.86
EN	4.68	3.73	3.79	6.37	4.86	4.98
IN	5.78	7.37	6.46	7.87	9.59	8.48
IE	9.40	10.13	9.11	12.80	13.19	11.96
LJL	10.91	13.37	–	14.85	17.40	–
UEL	4.27	5.06	–	5.81	6.59	–
HUM	8.98	7.91	8.63	12.23	10.30	11.33
RAD	16.04	16.88	18.11	21.84	21.97	23.78
FEM	7.17	7.69	9.89	9.76	10.01	12.99
TIB	17.07	18.29	18.37	23.24	23.81	24.12
FORE	25.02	24.79	26.74	34.06	32.27	35.11
HIND	24.24	25.98	28.26	33.00	33.82	37.11
HIND.FORE	0.97	1.05	1.06	1.32	1.36	1.39
RAD.HUM	1.79	2.13	2.10	2.43	2.78	2.76
TIB.FEM	2.38	2.38	1.86	3.24	3.10	2.44
TL	56.76	65.77	65.14	77.28	85.62	85.53
TH	7.87	9.44	9.39	10.71	12.29	12.33
TL.TH	7.21	6.97	6.94	9.82	9.07	9.11
ClL	5.15	8.75	5.87	7.01	11.39	7.71
ClW	2.68	5.86	5.25	3.65	7.63	6.89
WVr	2.06	3.43	2.49	2.80	4.46	3.27
L5W	2.39	2.66	2.29	3.25	3.46	3.01
AG	37.12	37.56	–	50.54	48.89	–
TkL	54.78	53.52	–	74.58	69.67	–

The female from China had a longer trunk length (TkL = 74.58 in *T. asperrimus* vs. 69.67 in taxon 2). The female from Nghe An Province differed by having the smallest eye length, the shortest distance between both eyes, the smallest glandular warts and by having the longest limbs, while other measurements did not separate it from other lineages.
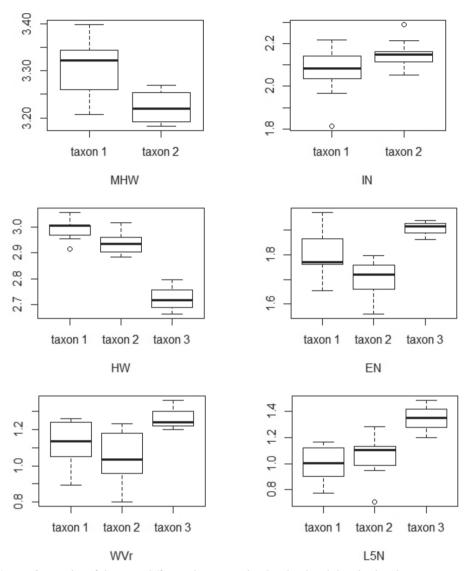
Comparisons within *T.* cf. *asperrimus* from Vietnam

The comparison between taxon 1 and taxon 2 included only males. Absolute measures and ratios of species' morphological traits corrected by snout vent length are shown in Table 4. Taxon 1 and taxon 2 did not differ in their respective SVL (*t*-test = -1.55, DF = 18, *p* = 0.14). Taxon 1 presented wider head than taxon 2 (MHW = 27.37 ± 1.67, HW = 19.86 ± 0.95 for taxon 1 vs. MHW = 25.11 ± 0.81, HW = 18.75 ± 0.99 taxon 2). The ratios of EN and IN also differed between lineages, with taxon 1 having a relatively longer snout (EN = 6.16 ± 0.68) than taxon 2 (5.50 ± 0.37) and taxon 2 having a wider snout (IN = 8.58 ± 0.57) than taxon 1 (7.94 ± 0.85). Taxon 2 showed the highest variation range in limb data. The ratio of FEM was longer in taxon 2 (12.59 ± 0.78) than in taxon 1 (10.99 ± 0.67), as well as the ratio of TIB (23.69 ± 2.35 in taxon 2 vs. 22.41 ± 0.61 in taxon 1), which together also resulted in longer hind limbs (HIND = 36.28 ± 2.89 in taxon 2 vs. 33.40 ± 0.99 in taxon 1). The ratio of the fore-limbs on the other hand was alike between lineages. Although taxon 2 presented lower minimum values for both RAD (18.80) and HUM (9.30) than in taxon 1 (RAD = 20.08 and HUM = 11.04). The tail in taxon 1 was longer (87.06 ± 5.25) and less high (11.79 ± 1.14) than in taxon 2 (TL = 84.61 ± 5.20, TH = 12.43 ± 2.46). Taxon 1 showed longer trunk (70.28 ± 3.41) than taxon 2 (68.78 ± 1.24).

The statistical analysis was based on nine males of taxon 1 and ten males of taxon 2. A PCA analysis resulted in six principal components (PC) explaining 87 % of the total variation. The first two PCs accounted for 52 % of the variation. The scatterplot between PC1 and PC2 showed a clear separation of the two clades, with only a small overlap area (Fig. 5A).

Figure 5. Scatterplot between PC1 and PC2 of the morphological characters corrected to SVL and log–transformed, for **A** taxon 1 and taxon 2 of the Vietnamese *Tylototriton* cf. *asperrimus* **B** the head- and dorso- related data of taxon 3 from Lai Chau Province and *T.* cf. *asperrimus* from Vietnam *sensu lato*; and **C** the limb related data of taxon 3 from Lai Chau Province and *T.* cf. *asperrimus* from Vietnam *sensu lato*. In the graphics *T.* cf. refers to *T.* cf. *asperrimus*.

Figure 6. Boxplot of the most differing characters related to head and dorsal values between taxon 1, taxon 2, and taxon 3. Characters were corrected to SVL and log–transformed. For abbreviations see Materials and methods.

The head related data (MANOVA: $F_{1, 17}$ = 11.75, DF = 6, $p < 0.001$), and the limb related data (MANOVA: $F_{1, 17}$ = 5.10, DF = 9, p = 0.01) were significantly different between the two lineages. Tail and dorsal morphological traits were not significantly different (MANOVA: $F_{1, 17}$ = 1.42, DF = 6, p = 0.3). Our results identified MHW, HW, EN, IN, RAD/HUM, FEM, TIB/FEM, HIND, and HIND/FORE as important traits separating both lineages (Table 5). Taxon 1 has a wider head (both as MHW +8.3 %; and as HW +5.6 %) and a longer snout (EN +10.7 %). Taxon 2 has a wider snout (IN +7.5 %) (Fig. 6).

Table 4. Morphological measurements between the *Tylototriton* males from Son La and Thanh Hoa provinces (taxon 1), from Phu Tho and Hoa Binh provinces (taxon 2), and from Lai Chau Province (taxon 3). Measures as absolute values (in mm) and ratios of characters to snout vent length (% SVL). Values are presented as mean ± standard deviation above minimum and maximum ranges, and for abbreviations see Materials and methods.

Character	N			Absolute measures			Ratios to SVL		
				taxon 1	taxon 2	taxon 3	taxon 1	taxon 2	taxon 3
SVL	10	11	5	64.98 ± 1.87, 62.00–67.95	66.59 ± 2.81, 61.57–70.69	65.14 ± 2.12, 63.20–68.71			
MHW	10	11	5	17.78 ± 1.11, 16.00–19.63	16.71 ± 0.64, 15.66–17.90	17.12 ± 0.43, 16.68–17.60	27.37 ± 1.67, 24.71–29.91	25.11 ± 0.81, 24.11–26.31	26.30 ± 0.86, 25.61–27.75
HW	10	11	3	12.89 ± 0.48, 12.10–13.70	12.47 ± 0.63, 10.98–13.13	10.00 ± 0.53, 9.56–10.59	19.86 ± 0.95, 18.44–21.29	18.75 ± 0.99, 16.98–20.45	15.29 ± 1.04, 14.34–16.40
HL	10	11	5	18.67 ± 0.71, 17.24–19.54	18.79 ± 0.89, 17.64–20.39	18.71 ± 0.93, 17.42–19.95	28.75 ± 1.16, 26.63–30.32	28.23 ± 1.23, 25.41–29.80	28.72 ± 0.75, 27.56–29.62
PL	10	11	5	9.74 ± 0.80, 8.52–10.92	9.64 ± 0.58, 8.79–10.27	10.34 ± 0.43, 9.92–11.02	14.99 ± 1.31, 13.02–16.64	14.80 ± 0.46, 14.28–15.48	15.88 ± 0.79, 14.82–16.92
PH	10	5	5	5.70 ± 0.68, 4.77–6.98	5.28 ± 0.73, 4.50–6.11	5.77 ± 0.21, 5.58–6.12	8.78 ± 1.10, 7.13–10.81	8.10 ± 0.97, 7.01–9.52	8.87 ± 0.18, 8.64–9.15
EL	10	5	5	3.14 ± 0.24, 2.60–3.40	3.24 ± 0.12, 3.06–3.40	3.26 ± 0.23, 3.02–3.49	4.84 ± 0.41, 3.89–5.24	4.99 ± 0.32, 4.54–5.31	5.01 ± 0.31, 4.68–5.45
EN	10	11	5	4.00 ± 0.41, 3.43–4.75	3.66 ± 0.25, 3.24–4.11	4.40 ± 0.46, 3.74–5.05	6.16 ± 0.68, 5.23–7.19	5.50 ± 0.37, 4.75–6.03	6.77 ± 0.78, 5.74–7.88
IN	10	11	5	5.16 ± 0.60, 4.03–5.97	5.71 ± 0.40, 5.17–6.43	5.67 ± 0.54, 5.01–6.26	7.94 ± 0.85, 6.13–9.18	8.58 ± 0.57, 7.79–9.88	8.70 ± 0.63, 7.93–9.35
IE	10	5	5	8.56 ± 0.17, 8.24–8.82	8.61 ± 0.48, 8.11–9.17	8.78 ± 0.56, 8.00–9.50	13.18 ± 0.37, 12.53–13.67	13.22 ± 0.45, 12.64–13.85	13.48 ± 0.73, 12.66–14.58
LJL	10	11	3	11.20 ± 0.61, 10.20–12.11	12.59 ± 1.76, 10.05–14.73	10.66 ± 0.62, 10.00–11.24	17.25 ± 1.05, 15.54–18.88	18.88 ± 2.30, 14.22–21.33	16.29 ± 0.98, 15.63–17.41
UEL	10	5	3	4.59 ± 0.36, 4.00–5.07	4.42 ± 0.33, 3.92–4.83	4.80 ± 0.15, 4.70–4.97	7.07 ± 0.65, 5.98–7.95	6.79 ± 0.64, 6.11–7.42	7.35 ± 0.49, 6.90–7.86
HUM	10	11	5	7.86 ± 0.40, 7.15–8.61	7.98 ± 0.99, 5.97–9.22	9.03 ± 0.98, 7.81–10.47	12.11 ± 0.74, 11.04–13.89	11.96 ± 1.15, 9.30–13.54	13.89 ± 1.69, 11.99–16.57
RAD	10	11	5	14.01 ± 0.61, 13.21–14.96	14.46 ± 1.13, 12.50–15.96	14.20 ± 1.12, 12.71–15.86	21.56 ± 0.72, 20.08–22.42	21.72 ± 1.52, 18.80–23.60	21.78 ± 1.21, 19.84–23.08

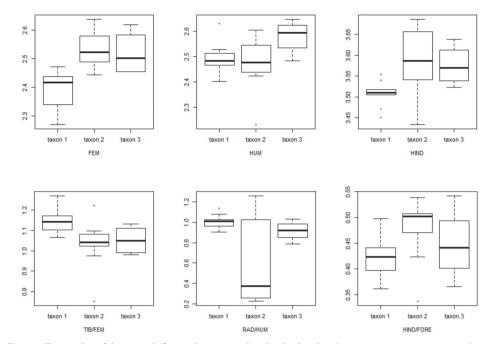| Character	N			Absolute measures			Ratios to SVL		
				taxon 1	taxon 2	taxon 3	taxon 1	taxon 2	taxon 3
FEM	10	11	4	7.14 ± 0.39 6.31 –7.54	8.40 ± 0.81 7.08 –9.59	8.17 ± 0.79 7.46 –8.93	10.99 ± 0.67 9.67 –11.83	12.59 ± 0.78 11.50 –13.97	12.44 ± 0.99 11.65–13.71
TIB	10	11	4	14.57 ± 0.60 13.73 –15.75	15.78 ± 1.77 13.14 –17.91	15.29 ± 0.82 14.25 –16.03	22.41 ± 0.61 21.27 –23.19	23.69 ± 2.35 18.59 –26.67	23.30 ± 0.86 22.24–24.34
FORE	10	11	5	21.87 ± 0.62 21.11 –23.08	22.44 ± 1.86 19.48 –25.18	23.23 ± 1.54 21.75 –25.13	33.67 ± 0.89 32.43 –35.35	33.68 ± 2.11 30.36 –36.97	35.67 ± 2.13 33.88–38.94
HIND	10	11	4	21.70 ± 0.78 20.34 –22.80	24.18 ± 2.41 21.14 –27.06	23.46 ± 1.58 21.71 –24.80	33.40 ± 0.99 31.51 –34.96	36.28 ± 2.89 30.98 –39.90	35.74 ± 1.78 33.89–38.05
HIND/FORE	10	11	4	0.99 ± 0.03 0.95 –1.03	1.08 ± 0.05 0.99 –1.15	1.03 ± 0.06 0.99 –1.12	1.53 ± 0.06 1.44 –1.65	1.62 ± 0.09 1.40 –1.71	1.57 ± 0.12 1.44–1.72
RAD/HUM	10	11	5	1.79 ± 0.13 1.55 –2.02	1.34 ± 0.54 0.86 –2.26	1.59 ± 0.20 1.35 –1.83	2.75 ± 0.20 2.47 –3.12	2.03 ± 0.89 1.26 –3.53	2.43 ± 0.27 2.14–2.80
TIB/FEM	10	11	4	2.05 ± 0.13 1.91 –2.32	1.88 ± 0.15 1.50 –2.09	1.88 ± 0.10 1.78 –2.00	3.15 ± 0.18 2.90 –3.56	2.83 ± 0.30 2.12 –3.40	2.87 ± 0.21 2.66–3.10
TL	10	11	4	54.94 ± 3.02 50.47 –60.71	57.96 ± 4.12 53.64 –64.13	55.97 ± 2.81 53.16 –59.70	84.61 ± 5.20 77.37 –93.13	87.06 ± 5.25 76.88 –94.16	85.92 ± 2.47 82.34–88.00
TH	10	10	5	8.06 ± 1.67 6.13 –11.34	7.87 ± 0.71 6.69 –8.83	8.00 ± 0.64 7.03 –8.57	12.43 ± 2.46 9.47 –17.28	11.79 ± 1.14 9.82 –13.76	12.28 ± 0.90 10.97–13.10
TL/TH	9	10	4	7.06 ± 1.35 4.80 –8.82	7.49 ± 1.04 6.21 –9.59	6.97 ± 0.75 6.31 –8.02	10.93 ± 2.22 7.31 –13.62	11.22 ± 1.51 8.79 –14.07	10.72 ± 1.23 9.78–12.52
CIL	10	5	4	8.98 ± 0.96 8.02 –10.96	9.41 ± 1.70 8.13 –12.12	8.34 ± 0.93 7.54 –9.66	13.82 ± 1.43 12.39 –16.98	14.39 ± 1.91 12.67 –17.15	12.78 ± 0.98 11.68–14.06
CIW	10	5	0	5.06 ± 0.67 4.16 –5.91	4.63 ± 0.66 4.09 –5.77		7.79 ± 1.03 6.38 –9.06	7.08 ± 0.61 6.64 –8.16	
WVr	10	10	5	1.99 ± 0.23 1.58 –2.30	1.93 ± 0.27 1.43 –2.37	2.30 ± 0.17 2.10 –2.52	3.06 ± 0.37 2.44 –3.53	2.90 ± 0.37 2.23 –3.43	3.53 ± 0.25 3.32–3.90
L5N	10	11	5	1.73 ± 0.26 1.41 –2.12	1.93 ± 0.24 1.39 –2.31	2.17 ± 0.63 1.44 –3.04	2.67 ± 0.39 2.12 –3.21	2.91 ± 0.41 2.02 –3.60	3.31 ± 0.87 2.25–4.42
AG	10	5	5	30.28 ± 2.41 26.26 –35.45	30.26 ± 4.05 27.36 –37.20	30.56 ± 1.80 27.97 –32.66	46.59 ± 3.42 40.68 –54.01	46.31 ± 3.91 42.64 –52.62	46.92 ± 2.47 44.26–50.13
TkL	10	10	3	45.66 ± 2.43 41.48 –50.25	45.81 ± 2.16 42.19 –50.20	43.31 ± 1.58 42.10 –45.10	70.28 ± 3.41 64.26 –76.57	68.78 ± 1.24 67.35 –71.01	66.22 ± 3.86 62.17–69.86

Table 5. Results from the MANOVA of the log–transformed ratio of characters to SVL of males. The variation was analyzed between the populations from Son La and Thanh Hoa provinces (taxon 1; $N = 9$) and the populations from Phu Tho and Hoa Binh provinces (taxon 2; $N = 10$), and between these (jointly referred to as *Tylototriton* cf. *asperrimus*) and the population from Lai Chau Province (taxon 3; in the comparison based on head and dorsum related data: $N_{T. cf. asperrimus} = 19$ and $N_{taxon3} = 3$; and in the comparison of limb related data, $N_{T. cf. asperrimus} = 21$ and $N_{taxon3} = 4$). F: F–test; DF: degrees of freedom; P: p–value. For abbreviations of characters see Materials and methods. In **Bold** significant results.

	taxon 1 × taxon 2			*T.* cf. *asperrimus* × taxon 3		
	F	**DF**	**P**	**F**	**DF**	**P**
MHW	17.62	17	**< 0.001**	0.08	20	0.79
HW	7.48	17	**0.01**	52.48	20	**< 0.001**
EN	4.85	17	**0.04**	7.52	20	**0.01**
HL	0.76	17	0.4	0.09	20	0.77
IN	4.56	17	**0.05**	0.09	20	0.77
LJL	2.51	17	0.13	2.22	20	0.15
RAD/HUM	5.92	17	**0.03**	0.34	23	0.56
FEM	21.13	17	**< 0.001**	1.10	23	0.30
TIB/FEM	7.07	17	**0.02**	0.42	23	0.52
HIND	7.47	17	**0.01**	0.43	23	0.52
HIND/FORE	4.95	17	**0.04**	0.03	23	0.87
HUM	0.14	17	0.72	4.66	23	**0.04**
RAD	0.17	17	0.7	<0.001	23	0.98
TIB	1.99	17	0.18	0.83	23	0.78
FORE	0.01	17	0.91	1.87	23	0.19
TL	1.10	17	0.31	0.07	20	0.79
TH	0.35	17	0.56	0.71	20	0.41
TL.TH	0.25	17	0.63	0.56	20	0.46
L5N	0.84	17	0.37	12.43	20	**< 0.01**
WVr	1.61	17	0.22	5.02	20	**0.04**
TkL	0.90	17	0.36	3.74	20	0.07

Regarding the limb data, FEM was 12.7 % longer on taxon 2, as well as the overall hind-limb length (HIND +7.9 %) and the ratio of HIND to FORE (+5.6 %). On the contrary, the ratios of tibia to femur (TIB/FEM +10.2 %) and radius to humerus (RAD/HUM +26.2 %) were larger in taxon 1 (Fig. 7).

Comparison of taxon 3 from Lai Chau Province with taxon 1 and taxon 2

This analysis is only based on males. Absolute measures and ratios of species' morphological traits corrected by snout vent length are shown in Table 4. All three taxa had similar measures for SVL, TL, and TH. The narrowest head was recorded in taxon 3 (HW 15.29 ± 1.04; 19.86 ± 0.95 in taxon 1; 18.75 ± 0.99 in taxon 2) and its maximum values were still below the minima recorded for taxon 1 and taxon 2 (max HW = 16.40 in taxon 3; min HW = 18.44 in taxon 1 and = 16.98 in taxon 2). The snout length was longer in taxon 3 (EN 6.77 ± 0.78), than in taxon 1 (6.16 ± 0.68) or taxon 2 (5.50 ± 0.37). HUM was longer in taxon 3 (13.89 ± 1.69) and showed a maximum range (11.99 to 16.57) not repeated in taxon 1 (11.04 to 13.89) nor in taxon 2 (9.30 to 13.54). Consequently, the sizes of the fore-limbs were also longer in

Figure 7. Boxplot of the most differing characters related to limb values between taxon 1, taxon 2, and taxon 3. Characters were corrected to SVL and log–transformed. For abbreviations see Materials and methods.

taxon 3 (35.67 ± 2.13, range = 33.88 - 38.9) than in taxon 1 (33.67 ± 0.89, range = 32.43–35.35) and in taxon 2 (33.68 ± 2.11, range = 30.36 - 36.97). In taxon 3 the width of the vertebral cord (WVr 3.53 ± 0.25) and the length of the rib nodules (L5N 3.31 ± 0.87) were wider than in taxon 1 (3.06 ± 0.37, and 2.67 ±0.39, respectively) and taxon 2 (2.90 ± 0.37, and 2.91 ±0.41, respectively). Trunk length, on the other hand was shorter in taxon 3 (TkL 66.22 ± 3.86), than in taxon 1 (70.28 ± 3.41) or taxon 2 (68.78 ± 1.24) (Table 4).

The data set of head and dorsal morphological traits was based on 19 observations of taxon 1 and taxon 2 together and three observations of taxon 3 from Lai Chau. A PCA identified five principal components (PCs) which together explained 84 % of the morphological variation (cumulative explanation of the first 3 PCs = 66 %; of the first 4 PCAs = 75 %). The first two PCs accounted for 48 % of the variation graphically showing a clear separation of the two clades (Fig. 5B). HW, EN, WVr, and L5N were identified as the characters differentiating between the species (MANOVA: $F_{1,\,20}$ = 20.52, p < 0.001) (Table 5). Head width (HW) was 21 % smaller in taxon 3 than in taxon 1 and taxon 2 ($F_{2,\,19}$ = 36.79, p < 0.001), and the size of the rib nodules (L5N) was 15 % longer in taxon 3 than in taxon 1 and taxon 2 ($F_{2,\,19}$ = 6.59, p < 0.01). The two remaining characters were only different between taxon 3 and taxon 2. Both the snout length (EN) and the width of the vertebral cord (WVr) were longer in taxon 3 than in taxon 2, by 17 % ($F_{2,\,19}$ = 7.21, p < 0.01) and 16 % ($F_{2,\,19}$ = 3.45, p < 0.05), respectively (Fig. 6).

The limb data included 21 observations of taxon 1 and taxon 2 together and four of taxon 3 and resulted in a PCA with three PCs explaining 88 % of the variation. The

Table 6. Bioclimatic conditions at the species records. Abbreviations: Annual Mean Temperature BIO1, Mean Diurnal Range BIO2, Isothermality BIO3, Temperature Seasonality BIO4, Max Temperature of Warmest Month BIO5, Min Temperature of Coldest Month BIO6, Temperature Annual Range BIO7, Mean Temperature of Wettest Quarter BIO8, Mean Temperature of Driest Quarter BIO9, Mean Temperature of Warmest Quarter BIO10, Mean Temperature of Coldest Quarter BIO11, Annual Precipitation BIO12, Precipitation of Wettest Month BIO13, Precipitation of Driest Month BIO14, Precipitation Seasonality BIO15, Precipitation of Wettest Quarter BIO16, Precipitation of Driest Quarter BIO17, Precipitation of Warmest Quarter BIO18, and Precipitation of Coldest Quarter BIO19.

Variables	Unit	taxon 1	taxon 1	taxon 2	taxon 2	taxon 3	*T. asperrimus*	*T. asperrimus*
BIO1	°C	20.7	20.4	20.4	19.9	19.3	16.8	16.9
BIO2	°C	5.3	5.5	6.1	6.0	6.6	7.4	5.9
BIO3	°C	37.4	38.1	39.7	42.0	45.7	32.0	32.5
BIO4	°C	1.0	1.0	1.0	0.9	0.8	2.0	1.5
BIO5	°C	26.3	26.1	27.1	26.1	26.1	26.0	23.9
BIO6	°C	12.1	11.5	11.7	11.7	11.6	3.0	5.7
BIO7	°C	14.2	14.6	15.4	14.4	14.5	23.0	18.2
BIO8	°C	23.6	23.0	22.8	22.2	20.4	22.1	20.9
BIO9	°C	16.6	16.3	16.5	16.0	15.9	9.5	10.8
BIO10	°C	23.5	23.2	22.3	22.4	21.4	22.7	21.2
BIO11	°C	16.6	16.3	16.3	16.0	15.9	8.5	10.8
BIO12	mm	1884.2	1624.6	1648.3	1603.5	1843.7	1703.7	1558.2
BIO13	mm	379.8	351.2	324.4	373.0	421.6	316.5	335.5
BIO14	mm	7.3	8.2	4.3	6.8	9.6	43.5	25.5
BIO15	mm	92.2	88.6	89.0	93.9	85.8	59.2	74.1
BIO16	mm	984.9	888.1	821.4	910.9	1041.8	784.6	813.5
BIO17	mm	42.6	56.4	45.8	37.8	80.4	189.2	169.6
BIO18	mm	986.2	843.3	403.8	856.8	424.9	390.7	738.1
BIO19	mm	42.6	56.4	43.7	37.8	80.4	233.0	169.6

overall MANOVA ($F_{1, 23}$ = 1.92, p = 0.13) was not significantly different between both lineages (Fig. 5C).

Macroclimatic comparison

Our data show that *T. asperrimus* in Guangxi, China experiences the lowest temperatures during the coldest months (3–6 °C) than any of the remaining three taxa in North Vietnam (12 °C). This species also shows the highest amount of precipitation during the coldest (169–233 mm vs. 38–80 mm for the remaining three taxa) and driest (170–180 mm vs. 38–80 mm for the three remaining taxa) quarter of the year, as well as in the driest month (26–44 mm vs. 4–10 mm for the three remaining taxa) (Table 6).

Integrative taxonomy

Genetic and morphological differences found in this study support the taxonomic separation between *T.* cf. *asperrimus* from Vietnam and *T. asperrimus sensu stricto* (from China), thus confirming the distinctness of the Vietnamese clade. Furthermore, we uncovered genetic and morphological variations within the Vietnamese *T.* cf. *asperrimus*

clade. However, based on our current knowledge these should be evaluated with caution regarding taxon 1 and taxon 2. Therefore these taxa are treated herein at the subspecies level until further evidence is presented. In addition, due to distinct morphological and molecular divergence, the population from Lai Chau Province was revealed to be distinct at the species level.

Taxonomic accounts

Tylototriton pasmansi **M. Bernardes, M. D. Le, T. Q. Nguyen, C. T. Pham, A. V. Pham, T. T. Nguyen & T. Ziegler, sp. nov.**
http://zoobank.org/3B901B94-4741-40BD-BDC1-75086A06A8FA
Figures 8, 9

Tylototriton taxon 2 (this study).
T. vietnamensis (referring to the population from Phu Tho Province): Nguyen et al. 2009, page 327.
T. asperrimus (referring to the population from Hoa Binh Province): Yuan et al. 2011, page 583; Nishikawa et al. 2013b, page 39; Luu et al. 2014, page 55.
T. cf. *asperrimus* (1) (referring to the population from Hoa Binh Province): Phimmachak et al. 2015a, page 293.
T. cf. *asperrimus* "Lao Cai/Hoa Binh" (referring to the populations from Lac Son, Hoa Binh): Hernandez 2016, page 254.
T. cf. *asperrimus* "northern Vietnam" (referring to the populations from Lai Chau, Lao Cai, Hoa Binh, and Phu Tho) Hernandez 2018, page 80.

Holotype. IEBR 4466, adult male, collected in Phu Canh Nature Reserve, Da Bac District, Hoa Binh Province, on 11 June 2016 by H. N. Ngo et al.
Paratypes. Four adult males, same data as the holotype: IEBR 4467–IEBR 4470; two adult males collected from Xuan Son National Park, Tan Son District, Phu Tho Province, unknown collector: IEBR 4322 and IEBR 4323; four adult males collected from Xuan Son National Park, Tan Son District, Phu Tho Province, on 7 July 2016 by T. D. Le: IEBR 4320, IEBR 4321, IEBR 4500 and IEBR 4501. One adult female collected from Thuong Tien Nature Reserve (Cot Ca forest, Quy Hoa Commune), Lac Son District, Hoa Binh Province at 720 m elevation on 24 July 2009 by V. Q. Luu: VFU A.2009.8.
Etymology. The species is named after Prof. Dr. Frank Pasmans, Ghent University (Belgium), who has made considerable and path-breaking contributions in the field of infectious diseases driven amphibian declines.
Diagnosis. The new species is diagnosed by the following combination of characters: head slightly longer than wide; snout truncate in dorsal view and slightly angular in profile; relative wide distance between the eyes; distinct mid-dorsal ridge on head; tips of fingers reaching the eye when foreleg adpressed along head; labial and gular folds present; rib nodules distinct and varying from pointy to more rounded; glandular vertebral ridge high, slightly rough and segmented; dorsal skin more granulose

Figure 8. *Tylototriton pasmansi* sp. nov. (holotype). In sequence: dorsal view; ventral view; lateral view; and detail of dorsal view of the head. Photographs T. Ziegler.
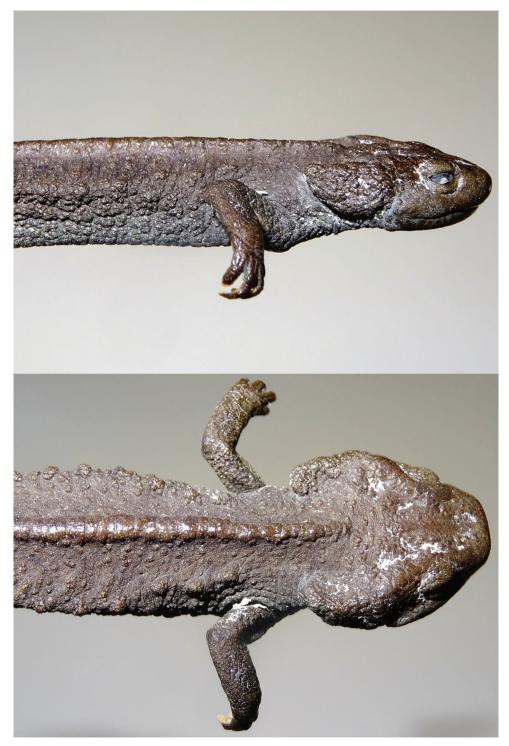
Figure 8. Continued.

than ventral skin; and skin in middle of abdomen with smooth tubercles shaped like transverse wrinkles.

Description of holotype. Habitus moderately slender; head broader than body, slightly longer than wide, depressed and slightly oblique in profile; snout wider than long (IN > EN), truncate in dorsal view, slightly angular shaped in profile and protruding beyond lower jaw; nostrils close to snout tip and slightly visible from above; labial fold slightly evident; dorsolateral bony ridges on head prominent, moderately protruding, from above eye to above anterior end of parotoid, posterior ends relatively thick and scrolled inside; mid-dorsal ridge on head distinct and thin; parotoids enlarged, projecting backwards; ventral skin with tubercles shaped like transverse wrinkles; gular fold weak; glandular vertebral ridge high, slightly rough and segmented, anteriorly thinner, extending from top of head to base of tail, separated from mid-dorsal ridge, with slight scoliosis at height of anterior limbs; number of trunk vertebras around 13; rib nodules distinct, rounded and small, with slightly bigger sizes reached at mid-trunk; tips of fore- and hind limbs touch when adpressed along body; tips of fingers reaching eye when foreleg laid forward; one toe missing on right hind-limb; and tail laterally compressed, thin and tip acuminated.

Color of holotype. In preservative, the overall dorsal coloration faded dark grayish green, the ventral coloration dark brown, with faded yellow markings on vent, ventral margin of tail, tip of fingers and toes, and part of palms. For color in life see Fig. 9.

Measurements of holotype (in mm). SVL 64.16; MHW 16.07; HW 11.87; HL 17.67; PL 9.61; PH 4.50; EL 3.06; EN 3.69; IN 5.55; IE 8.11; LJL 10.8; UEL 4.52; HUM 5.97; RAD 13.51; FEM 7.44; TIB 13.70; FORE 19.48; HIND 21.14; TL 53.91; TH 7.78; ClL 8.13; ClW 4.37; WVr 2.18; L5W 2.31; AG 27.36; and TkL 44.00.

Variation. Paratypes from Hoa Binh Province are very similar to the holotype. Paratypes from Phu Tho seem to present a stouter habitus, more distinct middorsal ridge but slightly less protruding dorsolateral ridges on head and slightly enlarged round rib nodules. The variation of the morphological characters in males is summarized in Table 4 and the additional measurements of one female can be found in Table 3.

Comparisons. *Tylototriton pasmansi* sp. nov. differs from other related species of *Tylototriton* as follows: from *T. anhuiensis* by distinctly separated rib nodules (versus continuous nodule-like warts in *T. anhuiensis*); from *T. asperrimus* by a wider (versus shorter) distance between the eyes, tips of fingers reaching eye (versus nostril) when foreleg laid forward, and head slightly longer than wide (versus wider than long in *T. asperrimus* according to Nishikawa et al. 2013b; Sparreboom 2014; Hernandez 2016), however, the female holotype shows similar head proportions–see Discussion); from *T. broadoridgus* by a head longer than wide (versus equally long and wide), wider (versus shorter) distance between eyes, presence (versus absence) of gular fold, smoother (versus extremely rough) skin on ventral side shaped like transverse wrinkles (versus rounded shaped, uniform to dorsal side), distinctly separated rib nodules (versus continuous nodule-like warts), and narrower vertebral ridge (versus broader in *T. broadoridgus*); from *T. hainanensis* by the head being slightly longer than wide (versus much wider than long), and a snout truncate in dorsal view (versus rounded in *T. hainanensis*);

Figure 9. Dorsal and ventral views of the new taxa in life. Top: *Tylototriton pasmansi* sp. nov. (holotype); Center: *Tylototriton pasmansi obsti* ssp. nov. (holotype); Bottom: *Tylototriton sparreboomi* sp. nov. Photographs: C. T. Pham (upper row) and A. V. Pham (central and lower rows).

from *T. liuyangensis* by a wider (versus shorter) distance between eyes, distinctly separated rib nodules (versus continuous nodule-like warts), and ventral side skin shaped like transverse wrinkles (versus covered by warts in *T. liuyangensis*); from *T. notialis* by a broader (versus narrower) head, a slightly angular (versus rounded) shaped snout in profile, longer (versus shorter) hind-limbs, and higher tail (versus thinner tail in *T. notialis*); from *T. panhai* by wider (versus shorter) distance between the eyes, presence (versus absence) of labial fold, distinct (versus absent) middorsal ridge on head, and dorsal color uniformly dark (versus dorsal color with characteristic colorful markings in *T. panhai*); from *T. vietnamensis* by round to pointy (versus slightly flattened) rib nodules, presence (versus absence) of gular fold, and high vertebral ridge (versus low vertebral ridge in *T. vietnamensis*); from *T. wenxianensis* by a truncate snout in dorsal view (versus round), wider (versus shorter) distance between the eyes, distinctly separated rib nodules (versus continuous nodule-like warts), presence (versus absence) of gular fold, smoother (versus extremely rough) skin on ventral side shaped like transverse wrinkles (versus rounded shaped and uniform to dorsal side), and colored marking on ventral slit (versus black colored ventral slit in *T. wenxianensis*); and from *T. ziegleri* by head slightly longer than wide (versus wider than long), smaller (versus enlarged knob-like) rib nodules, dispersed granules (versus more granulose) on dorsal skin and vertebral ridge slightly less (versus more) segmented and glandular.

The morphological comparison resulting from the measurements performed on the two females of *T. pasmansi* and *T. asperrimus sensu stricto* (Table 3) showed that the first one presents: wider (versus narrower) and longer (versus less long) head, longer (versus shorter) lower jaw length, wider (versus shorter) distance between the eyes, as well as higher values for all of the remaining head features, with the exception of snout length and head width, which were, in these cases, higher in *T. asperrimus*. *T. pasmansi* additionally presents longer and higher (versus shorter and thinner) tail, bigger (versus smaller) cloacal muscles, wider (versus narrower) vertebral ridge, slightly bigger (versus smaller) rib nodules and shorter trunk length (versus longer trunk length in *T. asperrimus*).

Distribution. Phu Canh Nature Reserve, Da Bac District and Thuong Tien Nature Reserve, Lac Son District in Hoa Binh Province, and Xuan Son National Park, Tan Son District, Phu Tho Province, Vietnam (Fig. 2).

Natural history. Based on remote sensing information the species is known from sites with an annual mean temperature of 20.4 to 20.7 °C, ranging from 11.5 to 26.3 °C during the year. Annual precipitation is about 1624 to 1884 mm ranging throughout the year from 7.3 to 379.8 mm. Further bioclimatic information is provided in Table 6.

Tylototriton pasmansi obsti **M. Bernardes, M. D. Le, T. Q. Nguyen, C.T. Pham, A. V. Pham, T. T. Nguyen & T. Ziegler, ssp. nov.**
http://zoobank.org/7A124E44-4F79-499F-AFD3-5B429D1AB4FB
Figures 9, 10

Tylototriton taxon 1 (this study).

Holotype. IEBR 4471, adult male, collected in Xuan Nha Nature Reserve, Van Ho District, Son La Province, at an elevation of 1090 m a.s.l., on 15 June 2016 by A. V. Pham and N. B. Sung.

Paratypes. Eight adult males, the same data as the holotype: IEBR 4472–4475, TBU 11–14; two adult males collected at elevation of 950 m a.s.l. in Xuan Lien Nature Reserve, Vin Village, Bat Mot Commune, Thuong Xuan District, Thanh Hoa Province, and in July 2015 by T. S. Nguyen: IEBR 4318 and IEBR 4319.

Etymology. The new subspecies is named after Prof. Fritz-Jürgen Obst, the former herpetologist and director of the Museum für Tierkunde Dresden, Germany, as well as passionate *Tylototriton* keeper, who passed away on the 10 June 2018.

Diagnosis. The new subspecies is diagnosed from the nominotypic subspecies *Tylototriton pasmansi pasmansi* by the following combination of characters: a wider head (both as head width and maximum head width), versus narrower head; a longer and narrower snout, versus shorter and wider snout; a shorter femur and associated hind-limb lengths, versus longer femur and longer hind-limbs length; less overall concentration of warts and small granules on skin, versus overall skin more granulose; and skin on lateral body with apparently same concentration of warts than dorsal side, versus higher concentration of warts on ventral side of the body than on dorsum in *T. p. pasmansi*.

Figure 10. *Tylototriton pasmansi obsti* ssp. nov. (holotype) In sequence: dorsal view; ventral view; lateral view; and detail of dorsal view of the head. Photographs T. Ziegler.
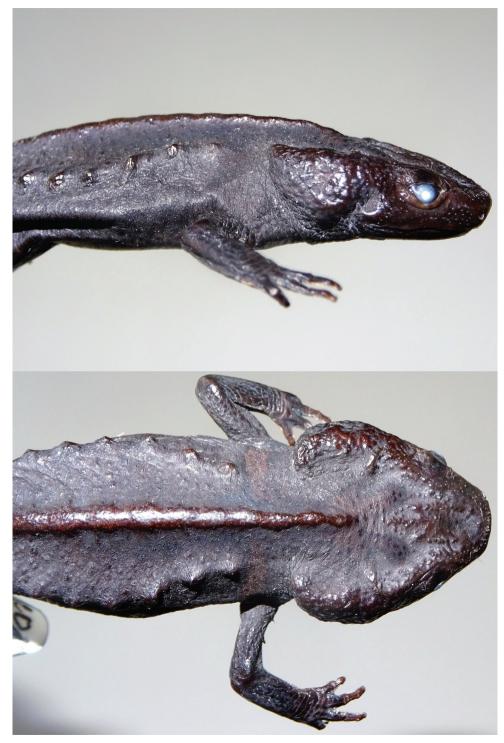
Figure 10. Continued.

Description of holotype. Habitus moderately stout; head broader than body, slightly longer than wide, depressed and slightly oblique in profile; snout wider than long (IN > EN), truncate in dorsal view, slightly angular shaped in profile and protruding beyond lower jaw; nostrils close to snout tip and not visible from above; labial fold slightly evident; dorsolateral bony ridges on head prominent, moderately protruding, from above eye to above anterior end of parotoid, posterior ends thin and scrolled inside; distinct middorsal ridge on head; parotoids enlarged, projecting backwards; dorsal skin granulose; skin on lateral body and between axilla-groin smooth, with no obvious presence of small glands; throat skin visibly more rough than in between axilla-groin region; gular fold present; glandular vertebral ridge high, slightly rough and segmented, anteriorly thinner, extending from top of head to base of tail, separated from middorsal ridge; number of trunk vertebrae 12; rib nodules distinct, rounded and pointy, with similar sizes throughout their length; fingers from fore- and hind limbs overlap when adpressed along body; tips of fingers reaching eye when adpressed along head; and tail laterally compressed, thin and tip acuminated.

Color of holotype. In preservative, with overall dark brown to blackish with faded yellow markings in vent margin, ventral tail fin, and tips of fingers and toes. For color in life see Fig. 9.

Measurements of holotype (in mm). SVL 67.95; MHW 18.1; HW 12.53; HL 19.44; PL 10.4; PH 5.5; EL 3.4; EN 3.99; IN 5.44; IE 8.64; LJL 12.11; UEL 5.07; HUM 8.12; RAD 14.43; FEM 7.05; TIB 15.75; FORE 22.55; HIND 22.80; TL 60.71; TH 8.46; ClL 8.86; ClW 5.88; WVr 2.18; L5W 2.12; AG 30.57; and TkL 46.48.

Variation (based on preserved paratypes). Some paratypes also show slightly bigger and rounded rib nodules, an overall more granulose skin, and faded yellow coloration on: anterior upper arms (like mating pads), posterior end of parotoids and first rib nodules. The remaining characters were similar to the holotype. Further measurements are summarized in Table 4.

Comparisons. In addition to the diagnostic characteristics already mentioned above, *Tylototriton pasmansi obsti* ssp. nov. differs from *T. p. pasmansi* by having a moderately stout habitus (versus moderately slender, when excluding the population from Phu Tho), nostrils usually not visible (versus usually visible) from dorsal view, usually thinner (versus usually thicker) posterior end of the dorsolateral bony ridges on head, gular fold more evident (versus weaker), rib nodules with similar sizes throughout their length (versus with slightly bigger sizes at mid-trunk), and rib nodules sometimes pointy (versus rounded in *T. p. pasmansi*).

Distribution. Xuan Nha Nature Reserve, Van Ho District, Son La Province and Xuan Lien Nature Reserve, Thuong Xuan District, Thanh Hoa Province, Vietnam (Fig. 2).

Natural history. Specimens were found between 14:00 and 16:00 h inside breeding ponds. The surrounding habitat was characterized by secondary forest of large, medium and small hardwoods mixed with shrubs and vines. Air temperature at the collection time was about 25 to 30 °C and relative humidity was about 75 to 80 %. Based on remote sensing information the species occurs at sites with an annual mean temperature of 19.9 to 20.4 °C, ranging from 11.7 to 27.1 °C during the year. Annual

precipitation is about 1603.5 to 1648.3 mm with yearly variations from 4.3 to 373.0 mm monthly. Further bioclimatic information is provided in Table 6.

Tylototriton sparreboomi M. Bernardes, M. D. Le, T. Q. Nguyen, C. T. Pham, A. V. Pham, T. T. Nguyen & T. Ziegler, sp. nov.
http://zoobank.org/4599D131-7C89-4D62-B43A-15E24C6473B9
Figures 9, 11

Tylototriton taxon 3 (this study).
T. sp.: Laking et al. 2017, page 2.
T. verrucosus: Orlov et al. 2002, page 101; van Dijk et al. 2009, page 1; Nguyen et al. 2009, page 329.
T. cf. *asperrimus* "North Vietnam": Hernandez 2018, page 80.

Holotype. IEBR 4476, adult male, collected in Sa De Phin Commune, Sin Ho District, Lai Chau Province, Vietnam, at an elevation of 1670 m a.s.l., in May 2015 by A. V. Pham and M. A. Vang.

Paratypes. Two adult males, same data as the holotype: IEBR 4477 and TBU 10; two adult males, collector unknown: IEBR 4478 and IEBR 4479.

Etymology. The specific epithet is dedicated to late Prof. Dr. Max Sparreboom, who has made great contributions to the understanding of Urodela.

Diagnosis. The new species is distinguished from other species of the genus by the following combination of characters: head longer than wide; snout truncate in dorsal view; tips of fingers reaching nostril when foreleg is laid forward; skin tubercles on ventral side shaped like transverse wrinkles; rib nodules distinct and round; vertebral ridge segmented, high and relatively wide; relatively wide distance between the eyes; and gular and labial folds present.

Description of holotype. Habitus stout; head broader than body, longer than wide, depressed and slightly oblique in profile; snout wider than long (IN > EN), truncate in dorsal view, rounded in profile and protruding beyond lower jaw; nostrils close to snout tip and not visible from above; labial fold slightly evident; dorsolateral bony ridges on head prominent, wide, moderately protruding, from above eye to above anterior end of parotoid, posterior ends slightly scrolled inside; middorsal ridge on head almost indistinct; parotoids enlarged, projecting backwards; ventral skin smoother than dorsal skin, with tubercles shaped like transverse wrinkles; gular fold weak; glandular vertebral ridge high, wide, smooth and segmented extending from top of head to base of tail, separated from middorsal ridge; number of trunk vertebrae 13; rib nodules distinct and roundish, the third anterior rib nodule on right side is located below the second nodule and the fourth nodule seems to not be associated with the fourth vertebra, nodules appear knob-like anteriorly, becoming smaller posteriorly; tips of fore- and hind limbs overlap when adpressed along body; tips of fingers reaching nostril when foreleg laid forward; and tail laterally compressed, thin and tip acuminated.

Figure 11. *Tylototriton sparreboomi* sp. nov. (holotype). In sequence: dorsal view; ventral view; lateral view; and detail of dorsal view of the head. Photographs T. Ziegler.

Figure 11. Continued.

Color of holotype. In preservative, with an overall faded dark brown coloration, with faded yellow markings on vent, ventral margin of tail, tips of fingers and toes, and part of palms. For color in life see Fig. 9.

Measurements of holotype (in mm). SVL 68.71; MHW 17.60; HW 9.85; HL 19.95; PL 10.18; PH 6.12; EL 3.43; EN 4.43; IN 6.26; IE 9.04; LJL 10.74; UEL 4.74; HUM 9.27; RAD 15.86; FEM 8.77; TIB 16.03; TL 59.70; TH 8.57; ClL 9.66; WVr 2.37; L5W 3.04; AG 30.99; and TkL 42.72.

Variation. TBU 10 (in worse preserved condition) presents rib-nodules thinner than holotype, glandular vertebral ridge more tubercular, and tail tip slightly rounded. The remaining characters were similar to the holotype in morphology. For detailed measurements see Table 4.

Comparisons. *Tylototriton sparreboomi* sp. nov. differs from other related species of *Tylototriton* as follows: from *T. anhuiensis* by distinctly separated rib nodules (versus continuous nodule-like warts in *T. anhuiensis*); from *T. asperrimus* by a head longer than wide (versus wider than long in *T. asperrimus* according to Nishikawa et al. 2013b; Sparreboom 2014; Hernandez 2016), however the female holotype shows similar head proportions–see Discussion); from *T. broadoridgus* by head slightly longer than wide (versus equally long and wide), presence of skin on ventral side shaped like transverse wrinkles (versus covered with round shaped tubercles, like the dorsal side), distinctly separated rib nodules (versus continuous nodule-like warts), and narrower vertebral ridge (versus wider vertebral ridge in *T. broadoridgus*); from *T. hainanensis* by a head longer than wide (versus much wider than long), tips of fingers reaching nostril (versus eyes) when foreleg is laid forward, and a snout truncate in dorsal view (versus rounded in *T. hainanensis*); from *T. liuyangensis* by a wider (versus shorter) distance between eyes, distinctly separated rib nodules (versus continuous nodule-like warts), and lateral skin shaped like transverse wrinkles (versus covered by warts in *T. liuyangensis*); from *T. notialis* by a broader (versus narrower) head, longer (versus shorter) hind-limbs, and higher tail (versus thinner tail in *T. notialis*); from *T. panhai* by wider (versus shorter) distance between the eyes, presence (versus absence) of labial fold, and overall dorsal coloration mostly dark (versus with presence of characteristic dorsal colorful markings in *T. panhai*); from *T. pasmansi* sensu lato by a narrower (versus wider) head, slightly wider (versus slightly narrower) distance between the eyes, tips of fingers reaching nostril (versus eye) when foreleg laid forward, longer (versus shorter) humerus length, and slightly enlarged round-like rib nodules (versus slightly smaller, pointy to rounded rib nodules in *T. pasmansi* sensu lato); from *T. p. pasmansi* by a longer (versus shorter) length between eye and nostril and wider (versus narrower) vertebral ridge in *T. p. pasmansi*; from *T. pasmansi obsti* by a longer (versus shorter) femur length; from *T. vietnamensis* by a moderately stout (versus slender) habitus, presence (versus absence) of gular fold, and round (versus slightly flattened) rib nodules and high vertebral ridge (versus low vertebral ridge in *T. vietnamensis*); from *T. wenxianensis* by a truncate (versus more rounded) snout in dorsal view, wider (versus narrower) distance between the eyes, distinctly separated rib nodules (versus continuous nodule-like warts), smoother (versus extremely rough) skin on ventral side shaped like transverse wrinkles (versus rounded

shaped and uniform to dorsal side), and colored marking on ventral slit (versus black colored ventral slit in *T. wenxianensis*); from *T. ziegleri* by a head longer than wide (versus wider than long), rounded but smaller (versus enlarged knob-like) rib nodules, and distinctly segmented vertebral ridge (versus even more segmented vertebral ridge in *T. ziegleri*).

Distribution. Known only from the type locality in Lai Chau Province, northern Vietnam (Fig. 2).

Natural history. Specimens were found in water between 9:00 and 16:30 h in ponds. The surrounding habitat was secondary forest of large, medium and small hardwoods mixed with shrubs and vines. Air temperature at the sites was 23 to 27 °C and relative humidity was 80 to 85%. Based on remote sensing information, the species occurs at sites with an annual mean temperature of 19.3 °C, ranging from 11.6 to 26.1 °C during the year. Annual precipitation is about 1843.7 mm with yearly variations from 9.6 to 421.6 mm. Further bioclimatic information is provided in Table 6.

Discussion

Based on examples listed in Table 7, we argue that clear genetic and morphological differences help clarify the taxonomic status of the taxa in question. The genetic differences between *T. pasmansi* and its closest relative *T. asperrimus* (from 3.2 to 3.6 %), between *T. sparreboomi* and *T. asperrimus* (from 4.1 to 4.2 %), and between *T. pasmansi* and *T. sparreboomi* (from 3.6 to 4.5 %) are higher than other minimum genetic distances between species of the genus *Tylototriton* (see *T. shanjing* × *T. verrucosus* × *T. pulcherrimus* × *T. podichthys*, *T. anguliceps* × *T. pulcherrimus*, *T. broadoridgus* × *T. dabienicus*, *T. anhuiensis* × *T. broadoridgus*, and *T. ngarsuensis* × *T. shanorum*).

It becomes apparent that these genetic differences, accompanied by clear morphological disparities, warrant taxonomic revision. The shape of the head of the holotype of *T. asperrimus* (a female) is slightly longer than wide, but evidence from literature, likely based on males, supports a head morphology being (slightly) wider than long in this species (Nishikawa et al. 2013b; Sparreboom 2014; Hernandez 2016). In the diagnostic comparisons above, we followed the major consensus found in literature and used head shape as a diagnostic characteristic to separate *T. asperrimus*, *T. pasmansi*, and *T. sparreboomi*. Seglie et al. (2010) found differences between the head shape of males and females in *T. himalayanus*. In *T. asperrimus* it is currently not clear if this change of head proportions is an exceptional occurrence or a feature related to sexual dimorphism. Until this issue is clarified, the diagnostic feature should be employed with reservations. The dorsal coloration described herein (as it is usually the case within this subgenus) should also be used cautiously as a diagnostic characteristic. Additional work might uncover intra-specific color variations, as in *T. notialis* (Nishikawa et al. 2013b), and *T. ziegleri* (Hernandez 2016).

Two taxa, *T. p. pasmansi* and *T. pasmansi obsti*, are herein cautiously described as subspecies, since their genetic divergences are lower (from 2.5 to 3.1 %) and morpho-

logical differences are more subtle. In this case, additional surveys and genetic study (e.g., microsatellites, nuclear DNA analysis) should follow to provide a more complete taxonomic evaluation of these taxa. These two subspecies appear to be separated by the Da River [Black River] (see Fig. 2). Since the Da River is the largest river in northwestern Vietnam, it may serve as a physical barrier restricting the gene flow between populations. Recently, Hernandez et al. (2018) assessed the patterns of macro-ecological niche differentiation in Asian crocodile newts. The authors suggested that both niche conservatism as well as niche differentiation can be detected. Many species occupy forested habitats at higher elevations, which are characterized by cooler and moister micro-habitats compared to lowland and open areas. Although our low sample size prevents detailed niche assessments for the new taxa, the overall niche structure within the genus suggests that the taxa are restricted to micro-climatic pockets in mountainous areas. Hence, not only the river systems represent likely barriers for gene flow, but also unsuitable micro-climatic conditions might limit dispersals in the region.

Wang et al. (2018) hypothesized that *Tylototriton sensu lato* originated from the ancestral area consisting of northern Indochina Peninsula and southern Yunnan Province during the middle Miocene, approximately 15 MYA. This period coincided with the warming Miocene climate optimum (Zachos et al. 2001; Böhme 2003). It is also evident that the speciation rates of the group have slowed down significantly from the beginning of the Pleistocene, probably due to the global cooling during this epoch (Wang et al. 2018). However, an important period between just before the Pliocene, around 6 MYA, and the Pleistocene, approximately 2.5 MYA, when a majority of speciation events within the group occurred (see Fig. 4 in Wang et al. 2018), has not been discussed in previous studies. During the Pliocene, the global temperature was about 2–5 °C higher than that of the pre-industrial time (Zachos et al. 2001; Ravelo et al. 2004; Salzmann et al. 2011). Warmer climates, which have been shown to promote diversification rates in different animal groups, including ants, mammals, plethodontid salamanders, and softshell turtles, possibly through increased dispersal rates (Moreau et al. 2006; Smith et al. 2006; Vieites et al. 2007; Le et al. 2014), are also likely to influence the evolution of the Knobby Salamanders in Asia. Our study also suggests that the two new species emerged during this period, further supporting the higher rate of diversification of *Tylototriton* in the Pliocene.

Wang et al. (2018) and also Zaw et al. (2019) did not find support for the monophyly of *T. asperrimus*. Their phylogeny placed the population from Thuong Tien, Hoa Binh (*T. p. pasmansi*) as conspecific to the *T. asperrimus* form from China (identified together as *T. asperrimus* lineage 1 in both studies). These studies also misidentified the population from Xinyi County, Guangdong Province, China as *T. asperrimus* lineage 2, although this population forms a sister clade to the topotypic *T. hainanensis* from Hainan Island. The population from Baise, which according to Hernandez (2018) is distributed in Napo and Jingxi counties, China, was also recovered as a sister taxon to *T. hainanensis* in previous studies (Yuan et al. 2011; Phimmachak et al. 2015a; Hernandez 2016). Moreover, the studies by Wang et al. (2018) and Zaw et al. (2019) did not support the monophyly of both, *T. wenxianensis* and *T. dabienicus* species

Table 7. Examples of integrative taxonomy in other species of the genus *Tylototriton*. *partial 16S rRNA and COI, and complete tRNA Leu, ND1, ND2, tRNA Ile, tRNA Gln, tRNA Met, tRNA Trp, tRNA Ala, tRNA Asn, tRNA Cys, and tRNA Tyr.

Source	Gene used	Species at stake	Genetic var. (%)	Morphological variation and conclusions
Zhang et al. (2007)	partial cyt b	*T. shanjing* × *T. verrucosus*	mean 1.2; range 0.4–2.6	Morphology not discussed. Conspecificity. Stuart et al. (2010), Nishikawa et al. (2013a) and Nishikawa et al. (2015) point out that only a single, unvouchered sample of *T. verrucosus* was included, and cautiously defended the need for further examinations before taxonomic conclusions.
Khatiwada et al. (2015)	complete ND2 & partial cyt b	*T. shanjing* × *T. verrucosus*	1.9	Size; head proportions; grooves on tail base; coloration. "The topotypic *T. verrucosus* were deeply nested within *T. shanjing*."
Khatiwada et al. (2015)	complete ND2 & partial cyt b	*T. pulcherrimus* × *T. verrucosus*; *T. pulcherrimus* × *T. shanjing*	2.1; 2.8	Not further discussed. Treated as separated species.
Nishikawa et al. (2013a)	partial ND2, POMC & Rag 1	*T. shanjing* (Jingdong and Nu Jiang, Yunnan, China)	mean 1.4; range 0.2–2.1	Morphology not discussed. Treated as intraspecific variation.
Nishikawa et al. (2013a)	partial ND2, POMC & Rag 1	*T. shanjing* (from above) × *T. pulcherrimus*	mean 2.6; range 2.5–2.8	Morphology not discussed. Considered conspecific due to small genetic differences.
Nishikawa et al. (2015)	partial ND2	*T. yangi* × *T. daweishanensis*	mean 0.4; range 0.2–0.5	Coloration. Considered conspecific due to small genetic differences.
Khatiwada et al. (2015)	complete ND2 & partial cyt b	*T. yangi* × *T. daweishanensis*	mean 0.7	Not discussed. Treated as separate species.
Phimmachak et al. (2015a)	*	*T. anguliceps* × *T. pulcherrimus*	mean 3.1; range 2.8–3.4	Morphology not discussed. Treated as separate species and used as example for low genetic divergence within species of the genus.
Phimmachak et al. (2015a)	*	*T. podichthys* (description) × *T. pulcherrimus*	mean 2.9; range 2.5–3.4	Morphology not discussed. The new species formed a unique clade within an unresolved polytomy containing *T. verrucosus*, *T. shanjing*, and *T. pulcherrimus*.
Phimmachak et al. (2015a)	*	*T. podichthys* (description) × *T. shanjing*	mean 3.4; range 2.1–4.6	Ridge on midline of crown; coloration. Treated as separate species.
Le et al. (2015)	partial ND2	*T. podichthys* (Xam Neua, Laos) × *T. shanjing*	0.4	When the paper was published, *T. podichthys* was not yet described. The authors referred to this population as *T. verrucosus* from Laos, which formed a clade with *T. shanjing*, *T. pulcherrimus*, and *T. verrucosus* from the type locality.
Phimmachak et al. (2015a)	*	*T. podichthys* (description) × *T. verrucosus*	mean 3.1; range 2.1–4.4	Ridge on midline of crown; coloration; skin on cranial crest; orientation of parotoids. Separate species.
Shen et al. (2012)	complete ND2	*T. broadoridgus* (description) × *T. wenxianensis*	mean 3.9; range 3.8–4	Dorsal ridge; height of tail; presence of genital papillae; form of rib warts. Treated as separate species.

Source	Gene used	Species at stake	Genetic var. (%)	Morphological variation and conclusions
Shen et al. (2012)	complete ND2	*T. broadoridgus* (description) × *T. dabienicus*	mean 3.5; range 3.4–3.5	Inferred morphological differences. Separate species.
Nishikawa et al. (2013b)	partial ND2	*T. broadoridgus* × *T. dabienicus*	mean 3.3; range 3.3–3.4	Morphology not examined. Treated as separate species and used as example for low genetic divergence within species of the genus.
Nishikawa et al. (2013a)	partial ND2	*T. broadoridgus* × *T. dabienicus*	3.3	Morphology not examined. The authors suspect conspecificity.
Khatiwada et al. (2015)	complete ND2 & partial cyt b	*T. broadoridgus* × *T. dabienicus*	3.4	Not discussed. Treated as separate species.
Stuart et al. (2010)	* (except COI)	*T. notialis* (description) × *T. hainanensis*	range 3.7–3.8	Form of rib warts. Treated as separate species.
Nishikawa et al. (2013b)	partial ND2	*T. notialis* (type from Laos) × *T. notialis* (Nghe An, Vietnam)	2.8	Coloration. Considered conspecific.
Nishikawa et al. (2013b)	partial ND2	*T. ziegleri* (description)	mean 1.7; range 0.1–2.8	Treated as intraspecific variation.
Nishikawa et al. (2013b)	partial ND2	*T. asperrimus* (China) × *T. asperrimus* (Thuong Tien, Hoa Binh, Vietnam)	mean 2.7; range 0.1–3.4	Morphology not examined. Considered conspecific by Nishikawa et al. (2013b); separate species, Tylototriton pasmansi, this study.
Qian et al. (2017)	ND1, ND2 & cyt b	*T. ziegleri* x *T. vietnamensis*	2.3	Known morphological differences based on Nishikawa et al. (2013b): ridges on head; skin; vertebral ridge; form of rib warts; tail size and height. Treated as separate species.
Qian et al. (2017)	ND1, ND2 & cyt b	*T. anhuiensis* (description) × *T. broadoridgus*	3.2	Dorsal ridge width; head proportions. Treated as separate species.
Grismer et al. (2018)	ND2	*T. ngarsuensis* (description) × *T. shanorum*	range 3.0–3.4	Size; head length; rib nodules; dorsal ridge; parotoid position; coloration. Treated as separate species.

complexes. The *T. wenxianensis* complex appears to consist of at least two undescribed lineages, one in Libo county, Guizhou Province and the other in Wufeng county, Hubei Province, while in the *T. dabienicus* complex both studies apparently missed the description of *T. anhuiensis* by Qian et al. (2017), and as a result, continue to identify the population from Yuexi, Anhui as an unknown lineage sister to *T. dabienicus*.

The so far undescribed population from Lao Cai Province, Vietnam has been successively attributed to a number of species: *T.* cf. *vietnamensis* (Böhme et al. 2005), *T. asperrimus* (Nguyen et al. 2009), purportedly *T. ziegleri* (Nishikawa et al. 2013b), and *T.* cf. *asperrimus* "northern Vietnam" (Hernandez 2018). Phimmachak et al. (2015a), using a comprehensive phylogenetic sample, defended the conspecificity of the population from Lao Cai with the population from Lac Son, Hoa Binh Province, which we herein describe as *T. p. pasmansi*.

Based on these new developments we suspect *T. asperrimus* (type) to be endemic to Guangxi Province, in China. It is distributed in Jinxiu Yao Autonomous County in Mt. Dayao (including Dayaoshan Nature Reserve [Hernandez 2016] and in Bainiu locality [Hernandez 2018]) and in Mt. Xianglu (also Xianglushan) (Yang et al. 2014); in Longsheng County (Shen et al. 2012); Ziyuan County in Mt. Miao'er (Hernandez 2018); in Huanjiang County including the Mulun Nature Reserve (Qin et al. 2012); and in Tian'e County (Hernandez 2018). According to Hernandez (2016 and 2018) the species has a wide distribution in fragmented mountain areas from northern through central and southern Guangxi. The population from E'huangzhang Mts., Yangchun County, Guangdong is shown as a sister to topotypic *T. asperrimus* (Hernandez 2016 and Hernandez 2018), but still awaits proper taxonomic allocation.

Given the high demand of *Tylototriton* species in the international trade, and the persistent evidence of a high poaching rate (Gong and Mu 2008; Nishikawa et al. 2014; Phimmachak et al. 2015b; Rowley et al. 2016; Bernardes et al. 2017; Grismer et al. 2018) we decided to follow Hou et al. (2014) and cautiously omit the exact locations in this manuscript.

Outlook

This study increases the currently known number of *Tylototriton* species from northern Vietnam, from four (*T. anguliceps*, *T. notialis*, *T. vietnamensis*, and *T. ziegleri*) to six and one subspecies, by discovering *T. sparreboomi*, *T. p. pasmansi* and *T. pasmansi obsti*. It also further affirms that this region supports the highest diversity within this genus (Nishikawa et al. 2013b).

The taxonomic separation of a single widespread species into multiple small-ranged taxa in turn has important implications for the conservation status of the original species (Köhler et al. 2005; Stuart et al. 2006). We therefore recommend a re-assessment of the outdated Near Threatened status of *T. asperrimus sensu lato* (van Dijk et al. 2008) to reflect taxonomic revisions and increasingly severe threats from international trade and habitat loss, which have taken place over the last decade.

Acknowledgements

References

Bain RH, Truong NQ (2004) Herpetofaunal diversity of Ha Giang Province in northeastern Vietnam, with descriptions of two new species. American Museum Novitates 3453(2004): 1–42. https://doi.org/10.1206/0003-0082(2004)453%3C0001:HDOHGP%3E2.0.CO;2

Bernardes M, Pham CT, Nguyen TQ, Le MD, Bonkowski M, Ziegler T (2017) Comparative morphometrics and ecology of a newly discovered population of *Tylototriton vietnamensis* from northeastern Vietnam including remarks on species conservation. Salamandra 53(3): 451–457.

Böhme M (2003) The Miocene Climate Optimum: evidence from ectothermic vertebrates of Central Europe. Palaeogeography, Palaeoclimatology, Palaeoecology 195: 389–401. https://doi.org/10.1016/S0031-0182(03)00367-5

Böhme W, Schöttler T, Nguyen TQ, Köhler J (2005) A new species of salamander, genus *Tylototriton* (Urodela: Salamandridae) from northern Vietnam. Salamandra 41(4): 215–220.

Deblauwe V, Droissart V, Bose R, Sonké B, Blach-Overgaard A, Svenning JC, Wieringa JJ, Ramesh BR, Stévart T, Covereur TLP (2016) Remotely sensed temperature and precipitation data improve species distribution modelling in the tropics. Global Ecology and Biogeography 25(4): 443–454. https://doi.org/10.1111/geb.12426

Drummond AJ, Ho SYW, Phillips MJ, Rambaut A (2006) Relaxed phylogenetics and dating with confidence. PloS Biology 4(5): 699–710. https://doi.org/10.1371/journal.pbio.0040088

Drummond AJ, Rambaut A (2007) BEAST: Bayesian evolutionary analysis by sampling trees. BMC Evolutionary Biology 7(1): 214. https://doi.org/10.1186/1471-2148-7-214

Dubois A, Raffaëlli J (2009) A new ergotaxonomy of the family Salamandridae Goldfuss, 1820 (Amphibia, Urodela). Alytes 26(1–4): 1–85.

Fei L, Ye C, Yang R (1984) A new species and a new subspecies of the genus *Tylototriton* (Caudata: Salamandridae). Acta Zoologica Sinica 30(1): 85–91. [in Chinese]

Felsenstein (1985) Confidence limits on phylogenies: an approach using the bootstrap. Evolution 39(4): 783–791. https://doi.org/10.1111/j.1558-5646.1985.tb00420.x

Gong D-J, Mu M (2008) Behavioral observations and descriptions of the endangered knobby newt *Tylototriton wenxianensis* and their application in conservation. Asiatic Herpetological Research 11(2008): 31–38.

Grismer LL, Junior PLW, Quah ESH, Thura MK, Espinoza RE, Grismer MS, Murdoch ML, Lin A (2018) A new species of Crocodile Newt *Tylototriton* (Caudata: Salamandridae) from Shan State, Myanmar (Burma). Zootaxa 4500(4): 553–573. https://doi.org/10.11646/zootaxa.4500.4.5

Grismer LL, Wood PL, Quah ESH, Thura MK, Espinosa RE, Murdoch ML (2019) A new species of crocodile newt *Tylototriton* (Caudata: Salamandridae) from northern Myanmar (Burma). Journal of Natural History 53(7–8): 475–495. https://doi.org/10.1080/00222933.2019.1587534

Hernandez A (2016) Crocodile Newts, The Primitive Salamandridae from Asia (Genera *Echinotriton* and *Tylototriton*). Edition Chimaira, Frankfurt, 415 pp.

Hernandez A (2018) Ecological affinities of *Tylototriton asperrimus* Unterstein, 1930 (Amphibia, Caudata: Salamandridae) at Bainiu, Dayaoshan, Guangxi Province, China with an emphasis on its cryptic diversity. Bulletin de la Société Herpétologique de France 166(2018): 79–82.

Hernandez A, Escoriza D, Hou M (2018) Patterns of niche diversification in south-east Asian crocodile newts. Zoologischer Anzeiger 276(2018): 86–93. https://doi.org/10.1016/j.jcz.2018.06.001

Hernandez A, Escoriza D, Pomchote P, Mian H (2019) New localities for *Tylototriton uyenoi*, *T. panhai* and *T. anguliceps* in Thailand with remarks on the southernmost distribution of the genus. The Herpetological Bulletin 147(2019): 15–18. https://doi.org/10.33256/hb147.1518

Hillis DM, Bull JJ (1993) An empirical test of the bootstrap as a method for assessing confidence in phylogenetic analysis. Systematic Biology 42(2): 182–192. https://doi.org/10.1093/sysbio/42.2.182

Hou M, Wu Y, Yang K, Zheng S, Yuan Z, Li P (2014) A missing geographic link in the distribution of the genus *Echinotriton* (Caudata: Salamandridae) with description of a new species from Southern China. Zootaxa 3895(1): 89–102. https://doi.org/10.11646/zootaxa.3895.1.5

IUCN SSC Amphibian Specialist Group (2016) *Tylototriton vietnamensis*. The IUCN Red List of Threatened Species 2016: e.T135868A88920562. https://doi.org/10.2305/IUCN.UK.2016-3.RLTS.T135868A88920562.en

IUCN SSC Amphibian Specialist Group (2017) *Tylototriton ziegleri*. The IUCN Red List of Threatened Species 2017: e.T47144899A47144905. https://doi.org/10.2305/IUCN.UK.2017-2.RLTS.T47144899A47144905.en

Jiang Y, Wei Z, Han F, Ni Q, Yao Y, Xu H, Li Y, Rao D, Zhang M (2017) The complete mitogenome sequence of *Tylototriton ziegleri* (Amphibia: Caudata). Conservation Genetics Resources 9(3): 503–506. https://doi.org/10.1007/s12686-017-0710-8

Khatiwada JR, Wang B, Ghimire S, Vasudevan K, Paudel S, Jiang JP (2015) A new species of the genus *Tylototriton* (Amphibia: Urodela: Salamandridae) from eastern Himalaya. Asian Herpetological Research 6(4): 245–256.

Köhler J, Vieites DR, Bonett RM, García FH, Glaw F, Steinke D, Vences M (2005) New amphibians and global conservation: A boost in species discoveries in a highly endangered vertebrate group. Bioscience 55(8): 693–696. https://doi.org/10.1641/0006-3568(2005)055[0693:NAAGCA]2.0.CO;2

Laking AE, Ngo HN, Pasmans F, Martel A, Nguyen TT (2017) *Batrachochytrium salamandrivorans* is the predominant chytrid fungus in Vietnamese salamanders. Scientific Reports 7(44443): 1–5. https://doi.org/10.1038/srep44443

Le M, Duong HT, Dinh LD, Nguyen TQ, Pritchard PCH, McCormack T (2014) A phylogeny of softshell turtles (Testudines: Trionychidae) with reference to the taxonomic status of the critically endangered, giant softshell turtle, *Rafetus swinhoei*. Organisms, Diversity & Evolution 14(3): 279–293. https://doi.org/10.1007/s13127-014-0169-3

Le DT, Nguyen TT, Nishikawa K, Nguyen SLH, Pham AV, Matsui M, Bernardes M, Nguyen TQ (2015) A new species of *Tylototriton* Anderson, 1871 (Amphibia: Salamandridae) from Northern Indochina. Current Herpetology 34(1): 38–50. https://doi.org/10.5358/hsj.34.38

Luu VQ, Le CX, Do HQ, Hoang TT, Nguyen TT, Bonkowski M, Ziegler T (2014) New records of amphibians from Thuong Tien Nature Reserve, Hoa Binh Province, Vietnam. Herpetological Notes 7(2014): 51–58.

Moreau CS, Bell CD, Vila R, Archibald SB, Pierce NE (2006) Phylogeny of the ants: diversification in the age of angiosperms. Science 312(5770): 101–104. https://doi.org/10.1126/science.1124891

Nguyen TQ, Nguyen VS, Ho LT, Le QK, Nguyen TT (2009) Phylogenetic relationships and taxonomic review of the family Salamandridae (Amphibia: Caudata) from Vietnam (in Vietnamese). Vietnam Journal of Biotechnology 7(3): 325–333.

Nishikawa K, Khonsue W, Pomchote P, Matsui M (2013a) Two new species of *Tylototriton* from Thailand (Amphibia: Urodela: Salamandridae). Zootaxa 3737(3): 261–279. https://doi.org/10.11646/zootaxa.3737.3.5

Nishikawa K, Matsui M, Nguyen TT (2013b) A new species of *Tylototriton* from Northern Vietnam (Amphibia: Urodela: Salamandridae). Current Herpetology 32(1): 34–49. https://doi.org/10.5358/hsj.32.34

Nishikawa K, Matsui M, Rao D (2014) A new species of *Tylototriton* (Amphibia: Urodela: Salamandridae) from Central Myanmar. Natural History Bulletin of the Siam Society 60(1): 9–22.

Nishikawa K, Rao D, Matsui M, Eto K (2015) Taxonomic relationship between *Tylototriton daweishanensis* Zhao, Rao, Liu, Li & Yuan, 2012 and *T. yangi* Hou, Li & Lu, 2012. Current Herpetology 34 (1): 67–74. https://doi.org/10.5358/hsj.34.67

Oksanen J, Blanchet F, Kindt R, Legendre P, Minchin P, O'Hara R, Simpson G, Solymos P, Stevens M, Wagner H (2015) Vegan: community ecology. R package version 2.2-1. R Project for Statistical Computing, Vienna, Austria.

Orlov N, Murphy RW, Ananjeva NB, Ryabov SA, Cuc HT (2002) Herpetofauna of Vietnam, a checklist. Part I Amphibia. Russian Journal of Herpetology 9(2): 81–104.

Phimmachak S, Aowphol A, Stuart BL (2015a) Morphological and molecular variation in *Tylototriton* (Caudata: Salamandridae) in Laos, with description of a new species. Zootaxa 4006(2): 285–310. https://doi.org/10.11646/zootaxa.4006.2.3

Phimmachak S, Stuart BL, Aowphol A (2015b) Ecology and natural history of the knobby newt *Tylototriton podichthys* (Caudata: Salamandridae) in Laos. Raffles Bulletin of Zoology 63(2015): 389–400.

Posada D, Crandall KA (1998) Modeltest: testing the model of DNA substitution. Bioinformatics (Oxford, England) 14(9): 817–818. https://doi.org/10.1093/bioinformatics/14.9.817

Qian L, Sun X, Li J, Guo W, Pan T, Kang X, Jiang J, Wu J, Zhang B (2017) A new species of the genus *Tylototriton* (Amphibia: Urodela: Salamandridae) from the southern Dabie Mountains in Anhui Province. Asian Herpetological Research 8(3): 151–164.

Qin W, Tang X, Qin G, Wei L (2012) Preliminary survey of *Tylototriton asperrimus* habitat in Mulun Nature Reserve, Guangxi (in Chinese). Sichuan Journal of Zoology 31(2): 303–306.

Ravelo AC, Andreasen DH, Lyle M, Lyle AO, Wara MW (2004) Regional climate shifts caused by gradual global cooling in the Pliocene epoch. Nature 429(6989): 263–267. https://doi.org/10.1038/nature02567

Ronquist F, Teslenko M, van der Mark P, Ayres DL, Darling A, Höhna S, Larget B, Liu L, Suchard MA, Huelsenbeck JP (2012) MrBayes 3.2: efficient Bayesian phylogenetic inference and model choice across a large model space. Systematic Biology 61(3): 539–542. https://doi.org/10.1093/sysbio/sys029

Rowley JJL, Shepherd CR, Stuart BL, Nguyen TQ, Hoang HD, Cutajar TP, Wogan GOU, Phimmachak S (2016) Estimating the global trade in Southeast Asian newts. Biological Conservation 199(2016): 96–100. https://doi.org/10.1016/j.biocon.2016.05.001

Salzmann U, Williams M, Haywood AM, Johnson ALA, Kender S, Zalasiewicz J (2011) Climate and environment of a Pliocene warm world. Palaeogeography, Palaeoclimatology, Palaeocology 309(1–2): 1–8. https://doi.org/10.1016/j.palaeo.2011.05.044

Seglie D, Roy D, Giacoma C (2010) Sexual dimorphism and age structure in a population of *Tylototriton verrucosus* (Amphibia: Salamandridae) from the Himalayan Region. Copeia 2010(4): 600–608. https://doi.org/10.1643/CG-08-218

Shen Y, Jiang J, Mo X (2012) A new species of the genus *Tylototriton* (Amphibia, Salamandridae) from Hunan, China. Asian Herpetological Research 3(1): 21–30. https://doi.org/10.3724/SP.J.1245.2012.00021

Simmons JE (2002) Herpetological collecting and collections management. Revised edition. Society for the Study of Amphibians and Reptiles. Herpetological Circular 31: 153 pp.

Smith T, Rose KD, Gingerich PD (2006) Rapid Asia-Europe- North America geographic dispersal of earliest Eocene primate *Teilhardina* during the Paleocene-Eocene thermal maximum. Proceedings of the National Academy of Sciences 103(30): 11223–11227. https://doi.org/10.1073/pnas.0511296103

Sparreboom M (2014) Salamanders of the Old World: the salamanders of Europe, Asia and northern Africa. Knnv Publishing, Zeist, Netherlands, 385 pp. https://doi.org/10.1163/9789004285620

Stuart BL, Inger RF, Voris HK (2006) High level of cryptic species diversity revealed by sympatric lineages of Southeast Asian forest frogs. Biology Letters 2(3): 470–474. https://doi.org/10.1098/rsbl.2006.0505

Stuart BL, Phimmachak S, Sivongxay N, Robichaud WG (2010) A new species in the *Tylototriton asperrimus* group (Caudata: Salamandridae) from central Laos. Zootaxa 2650(2010): 19–32. https://doi.org/10.11646/zootaxa.2650.1.2

Sun S-J, Dai Q, Dai Z-X, Zhang H-M, Gong R-H, Du J-F, Zou H-S, Nie CA (2011) Population resource and habitat selection in summer of Black Knobby Newt (*Tylototriton asperrimus*) in surrounding areas of Houhe National Nature Reserve, Hubei Province, China (in Chinese). Chinese Journal of Ecology 30(11): 2534–2539.

Swofford DL (2003) PAUP*. Phylogenetic Analysis Using Parsimony (*and Other Methods), version 4.0 b10. Sinauer Associates, Sunderland, Massachusetts.

Thompson JD, Gibson TJ, Plewniak F, Jeanmougin F, Higgins DG (1997) The ClustalX windows interface: Flexible strategies for multiple sequence alignment aided by quality analysis tools. Nucleic Acids Research 25(24): 4876–4882. https://doi.org/10.1093/nar/25.24.4876

van Dijk PP, Nguyen TQ, Wai NLM, Ermi Z, Shunqing L (2008) *Tylototriton asperrimus*. The IUCN Red List of Threatened Species 2008: e.T59482A11932895. https://doi.org/10.2305/IUCN.UK.2008.RLTS.T59482A11932895.en

van Dijk PP, Wogan G, Lau MWN, Dutta S, Shrestha TK, Roy D, Truong NQ (2009) *Tylototriton verrucosus*. IUCN Red List Threatened Species 2009 e.T59487A11934912.

van Ende CN (2001) Repeated-measures analysis: growth and other time-dependent measures. In: Scheiner S, Gurevitch J (Eds) Design and analysis of ecological experiments. Chapman and Hall, New York, 134–157.

Vieites DR, Min M-S, Wake DB (2007) Rapid diversification and dispersal during periods of global warming by plethodontid salamanders. Proceedings of the National Academy of Sciences 104(50): 19903–19907. https://doi.org/10.1073/pnas.0705056104

Wang B, Nishikawa K, Matsui M, Nguyen TQ, Xie F, Li C, Khatiwada JR, Zhang B, Gong D, Mo Y, Wei G, Chen X, Shen Y, Yang D, Xiong R, Jiang J (2018) Phylogenetic surveys on the newt genus *Tylototriton sensu lato* (Salamandridae, Caudata) reveal cryptic diversity and novel diversification promoted by historical climatic shifts. PeerJ 6(2018): e4384. https://doi.org/10.7717/peerj.4384

Weisrock DW, Papenfuss TJ, Macey JR, Litvinchuk SN, Polymeni R, Ugurtas IH, Zhao E, Jowkar H, Larson A (2006) A molecular assessment of phylogenetic relationships and lineage accumulation rates within the family Salamandridae (Amphibia, Caudata). Molecular Phylogenetics and Evolution 41(2): 368–383. https://doi.org/10.1016/j.ympev.2006.05.008

Yang D, Jiang J, Shen Y, Fei D (2014) A new species of the genus *Tylototriton* (Urodela: Salamandridae) from northeastern Hunan Province, China. Asian Herpetological Research 5(1): 1–11. https://doi.org/10.3724/SP.J.1245.2014.00001

Yuan Z-Y, Jiang K, Lü S-Q, Yang J-X, Nguyen TQ, Nguyen TT, Jin J-Q, Che J (2011) A phylogeny of the *Tylototriton asperrimus* group (Caudata: Salamandridae) based on a mitochondrial study: suggestions for a taxonomic revision. Zoological Research 32(6): 577–84.

Zachos J, Pagani M, Sloan L, Thomas E, Billups K (2001) Trends, rhythms, and aberrations in global climate 65Ma to present. Science 292(5517): 686–693. https://doi.org/10.1126/science.1059412

Zaw T, Lay P, Pawangkhanant P, Gorin VA, Poyarkov Jr NA (2019) A new species of Crocodile Newt, genus *Tylototriton* (Amphibia, Caudata, Salamandridae) from the mountains of Kachin state, northern Myanmar. Zoological Research 40(3): 151–174. https://doi.org/10.24272/j.issn.2095-8137.2019.043

Zhang M-W, Rao D-Q, Yu G-H, Yang J-X (2007) The validity of red knobby newt (*Tylototriton shanjing*) species status based on mitochondrial Cyt b gene. Zoological Research 28(4): 430–436.

Supplementary material 1

Regression of each morphological character to its respective snout-vent length value for taxon 1 and taxon 2

Authors: Marta Bernardes, Minh Duc Le, Truong Quang Nguyen, Cuong The Pham, Anh Van Pham, Tao Thien Nguyen, Dennis Rödder, Michael Bonkowski, Thomas Ziegler

Data type: measurement

Link: https://doi.org/10.3897/zookeys.935.37138.suppl1

Supplementary material 2

Time-calibrated tree of *Tylototriton* based on ND2 sequences. The values indicate the split time (in million years ago) calculated by BEAST 1.8.0.

Authors: Marta Bernardes, Minh Duc Le, Truong Quang Nguyen, Cuong The Pham, Anh Van Pham, Tao Thien Nguyen, Dennis Rödder, Michael Bonkowski, Thomas Ziegler

Data type: measurement

Link: https://doi.org/10.3897/zookeys.935.37138.suppl2